

Effects of Perturbation-Based Balance Training and Transcutaneous Spinal Cord Stimulation on Postural  
Balance Control in Healthy Subjects

Isirame Omofuma

Submitted in partial fulfillment of the  
requirements for the degree of  
Doctor of Philosophy  
under the Executive Committee  
of the Graduate School of Arts and Sciences

COLUMBIA UNIVERSITY

2022

© 2022

Isirame Omofuma

All Rights Reserved

## **Abstract**

Effects of Perturbation-Based Balance Training and Transcutaneous Spinal Cord Stimulation on  
Postural Balance Control in Healthy Subjects

Isirame Omofuma

The purpose of this dissertation was to explore methods for generating neuroplastic changes in healthy individuals using transcutaneous spinal cord stimulation (TSCS) and perturbation-based training in order to improve balance performance. This was done to gain an understanding of their effects on healthy individuals, which could then be used in designing treatments for both healthy and motor-impaired subjects. Three studies were undertaken. First, we set out to show that the Robotic Upright Stand Trainer (RobUST) could generate improvements in balance after perturbation balance training (PBT). In this same study, we showed that the assist-as-needed support of RobUST generates postural control improvements. Balance performance metrics including (i) margin of stability (MOS), (ii) metrics based on the center of pressure (COP) and center of mass (COM) excursions, (iii) postural muscle activations, (iv) balance strategy selection (between ankle and hip strategies) were used in this study. Electromyographic data were also collected from 11 subjects who participated in this study. Subjects were split into a RobUST assisted group (FF) and a non-assisted group (NF). An analysis of variance (ANOVA) was carried out to identify the main effects of the two factors, i.e., training and grouping. We also studied the

interaction effects between the two factors in the performance variables. After training, the threshold of the forces that destabilize balance increased for all participants. In addition, the area within which they could withstand perturbations without falling also increased. Muscle activation decreased in most muscles for subjects in both groups indicating that subjects improved balance while demonstrating more energetically efficient strategies. The post-training behavior of the two groups differed in the following way: the NF group adapted towards faster reactions to perturbations, greater use of the hip strategy, and more use of the erector spinae muscle, while the FF group adapted towards slower responses and less MOS. These results show that although balance adaptations with RobUST-assisted PBT are not the same as without RobUST, it is still a platform capable of improving balance performance.

Second, the effect of TSCS as a means of boosting neuroplasticity and a replacement for epidural stimulation were tested. Eight subjects were given TSCS for 30 mins while lying supine, and their neurophysiological and balance performance measures were tested before and after the intervention. T-tests were used to assess the difference in performance, and it was found that TSCS caused hypopolarisation of the sensory neurons, which increased the synaptic efficacy of sensory afferent–motoneuron synapses. This change was evidenced by increased H-reflex recovery and a leftward shift of the H-reflex recruitment curve. No improvement in fall frequency was observed, although balance adjustments were made that reduced muscle activity. This experiment showed that TSCS could be used to modulate the excitability of the spinal cord in healthy subjects.

Third, TSCS was combined with a training intervention in order to study how these two sources of plasticity interact. TSCS was applied to eleven subjects while they underwent a training intervention in which they played a game in virtual reality (VR) while their balance was perturbed by forces applied by RobUST. Balance characteristics were measured both with and without

TSCS, before and after the intervention. It was found that TSCS initially caused an increase in muscle activity and an increase in fall frequency for perturbations in the forward direction. With more practice, though, muscle activity decreased. It was postulated that the CNS adjusted to the initial elevated levels of muscle activity caused by TSCS by suppressing muscle activity in order to ensure successful motor control. These results suggest that TSCS can be used to elevate the resting potential of neurons in the dorsal (close to the back of the body) root, making them more easily excited by cortical signals. These changes induced by TSCS can be beneficial to spinal cord injury patients.

# Table of Contents

List of Charts, Graphs, Illustrations.....	iii
List of Tables .....	viii
Acknowledgments .....	ix
Dedication.....	xi
Preface .....	xii
Chapter 1: Postural Balance Control .....	1
1.1 Sensing.....	3
1.2 The Nervous System as Controller .....	5
1.3 The Neuromuscular System.....	8
1.4 Body Dynamics.....	9
1.5 Improving Postural Balance Control .....	13
1.6 The Robotic Upright Stand Trainer (RobUST) .....	18
Chapter 2: Training Postural Balance Control with Pelvic Force Field at the Boundary of Stability.....	22
2.1 Introduction.....	22
2.2 Methods.....	24
2.3 Results.....	33
2.4 Discussion.....	36
Chapter 3: Spinal Stimulation and the Measurement of Neuronal Excitability .....	42
3.1 Introduction.....	42
3.2 The Nervous System:.....	42

3.3	Electrical Stimulation.....	50
3.4	Transcutaneous Spinal Cord Stimulation (TSCS) .....	52
3.5	Testing the Effect of TSCS.....	55
Chapter 4: Effect of Transcutaneous Spinal Stimulation Applied During Quiet Lying on Balance and Neurophysiological Characteristics.....		64
4.1	Introduction.....	64
4.2	Methods.....	66
4.3	Results.....	75
4.4	Discussion.....	81
Chapter 5: Effect of Transcutaneous Spinal Stimulation on Balance and Neurophysiological Characteristics.....		87
5.1	Introduction.....	87
5.2	Methods.....	88
5.3	Results.....	96
5.4	Discussion.....	106
Conclusion.....		116
6.1	Summary of Contributions.....	116
6.2	Challenges and Limitations.....	118
6.3	Future Work .....	119
References.....		123

## List of Charts, Graphs, Illustrations

Figure 1-1: The human sensorimotor system modeled as a closed-loop system. Red lines indicate disturbances introduced into the system. Modeled based on Rasman et al 2018 [9].....	2
Figure 1-2: Example movements for the different reactive balance strategies. Horak and Kuo 2000 [20].....	6
Figure 1-3: A - Workspace showing the relationship between ankle and hip angles and ankle and hip strategies. Top outline of shaded area identifies the limits of the pure ankle strategy and the bottom outline the pure hip strategy. The shaded area are feasible combinations of ankle and hip angle movements which in general are mixed strategies. Horak and Kuo 2000 [20] B – Limits of sway frequency (Hz) and center of gravity sway angle for which the ankle strategy can restore balance. C – Limits of sway frequency and center of gravity sway for which the hip strategy can restore balance. Nashner et al. 1989 [21].....	7
Figure 1-4: Relationship between moment arms as a subject oscillates about their ankle. ‘g’ in this figure represents the horizontal projection of the COM, represented by ‘x’ in the text. ‘p’ is the position of the COP, represented by ‘u’ in the text. Winter 1995 [33].....	11
Figure 1-5: KineAssist. Peshkin 2005 [68].....	15
Figure 1-6: Balance Assessment Robot (BAR). Shirota 2017 [69].....	16
Figure 1-7: A CAREN system in use. Reproduced from Collins 2015 [71] .....	17
Figure 1-8: The Robotic Upright Stand Trainer (RobUST).....	18
Figure 1-9: Flow diagram of architecture of Stand Trainer.....	19
Figure 1-10: Description of Stand Trainer force field. The star in the middle is the center of the force field. The solid arrows show the direction the device pulls the subject when they move past the solid circle. Force in the region between the solid circle and the dashed circle is only activated	

as the subject is being pulled to the center after they have moved past the solid circle. There is no force within the dashed circle ..... 20

Figure 2-1: Steps of the experimental protocol..... 24

Figure 2-2: View of VR game and subject. From top to bottom: Subject prepares to receive the ball, subject catches the ball, subject throws the ball, subject tries to recover balance after throwing the ball at target..... 26

Figure 2-3: Center of mass (COM) shown within base of support (BOS). Markers on the feet, RTOE – Right Toe, R5MT – Right Fifth Metatarsal, RH – Right Heel, LT – Left Toe, LM – Left Fifth Metatarsal, LH – Left Heel, form the BOS. Margin of Stability (MOS) is the minimum distance of the COM to the BOS. B: MOS calculated at several time points before and after perturbation onset. This study uses the minimum value observed during the time of interest. In steady standing the MOS may oscillate between a range depending on their posture and foot placement. The MOS is typically highest in steady standing. .... 28

Figure 2-4: Average correlation upper-body angle – lower body angle correlation of a subject. Blue – pretest correlation; red – posttest correlation. We see at perturbation onset. .... 30

Figure 2-5: Distribution of retrievable successful trials per subject ..... 32

Figure 2-6: Stability area for pre-test and post-test values in NF and FF groups. We can observe that RobUST, in combination with the VR, was enough to increase the area of postural stability in standing. .... 33

Figure 2-7: The plots show an increase in force thresholds between pre- and post-tests for FF and NF groups across the four directions. We can notice that both groups improved their tolerance to receive greater perturbation intensities ..... 33

Figure 3-1: A – Parts of the brain. Miall 2006 [95]. B - Control pathways in the brain. Shumway-Cook et al. 2014 [3].	43
Figure 3-2: Spinal cord section showing connections to dorsal and ventral roots Bican 2013 [118]	49
Figure 3-3: Innervation of the body [118]	54
Figure 3-4: : Sample EMG readings of the right (R) and left (L) soleus (SL), tibialis anterior (TA), lateral gastrocnemii (LG), rectus femorii (RF).	55
Figure 3-5: A - Artifact of electrical stimulus; B - M-wave; C - H-reflex	57
Figure 3-6: Sample H-reflex recruitment curve. * represents points H-reflex curve and * represents points on the M-wave curve.	59
Figure 3-7: Typical H-recruitment curve profile. Klimstra 2007 [129].	60
Figure 3-8: Paired pulse response of soleus.	61
Figure 4-1: RobUST with subject strapped in	66
Figure 4-2: Flow Diagram of the experimental procedure	68
Figure 4-3: Electrode placement for stimulating an H-reflex from the tibial nerve. Left: Cathode placed in the popliteal fossa; Right: anode placed above the knee cap	70
Figure 4-4: Electrode placement for eliciting posterior root muscle reflexes. Top: Cathode was placed on the back at the L2-L3 intervertebral space; Bottom: Anode was placed on the abdomen	71
Figure 4-5: Intervention was carried out while the subject lay supine	72
Figure 4-6: Sample H-reflex recruitment curve. Left: Individually recorded data points; --- Line passes through average of datapoints elicited by the same current level; Right: Boltzmann	

sigmoidal curve fit for H-reflex and M-wave. Only the ascending limb of the H-reflex curve is fit.  
..... 74

Figure 4-7: Mean group pre-test (blue) and post-test (orange) iEMG results. F – Forward, B – backward, R – right, L- left perturbations. LRF – Left rectus femoris, RRF – right rectus femoris, LBF – left bicep femoris, RBF – right bicep femoris, LTA – left tibialis anterior, RTA – right tibialis anterior, LLG – left lateral gastrocnemius, RLG – right lateral gastrocnemius, LSL – left soleus and RSL – right soleus. \* =  $p \leq .05$ ; \*\* =  $p \leq .01$ ..... 76

Figure 4-8: Mean muscle activity duration in pre-test (blue) and post-test (orange). F – Forward, B – backward, R – right, L- left perturbation direction. LRF – Left rectus femoris, RRF – right rectus femoris, LBF – left bicep femoris, RBF – right bicep femoris, LTA – left tibialis anterior, RTA – right tibialis anterior, LLG – left lateral gastrocnemius, RLG – right lateral gastrocnemius, LSL – left soleus and RSL – right soleus. \* =  $p \leq .05$ ; \*\* =  $p \leq .01$  ..... 78

Figure 4-9: Graph showing individual changes in subjects for HMax, MMax, HCurrent50 and MCurrent50. None of the group changes were significant. Number in plots are subject ID numbers.  
..... 79

Figure 4-10: Individual subject changes between pre-test and post-test when subjects which had changes in MMax greater than 10% were eliminated. \* =  $p \leq .05$  ..... 80

Figure 4-11: H-reflex recovery cycle. Pre-test and post-test ratios of H2:H1 at 80, 150, 250, 500, 1000 ms interstimulus intervals. \* =  $p \leq .05$ ..... 81

Figure 5-1: Flow chart of experimental procedure. Physiological tests were conducted at the beginning and end of the protocol. Balance tests T1 and T4 were conducted without TSCS (blue) and balance tests T2 and T2 (red) were conducted with TSCS ..... 89

Figure 5-2: Subject standing in RobUST..... 92

Figure 5-3: Plots comparing integrated EMG (iEMG) without TSCS, T1, (blue) and with TSCS, T2, (red) during trunk force perturbation in the anterior direction. Top row plots are of the right rectus-femoris (R-RF) muscle and bottom row are of the left rectus femoris (L-LF). Left column plots are from individual subjects showing muscle activity from 0.5s before perturbation, through perturbation onset (pert on the graph), and for four seconds after. Right plots are average iEMG for individual subjects in session1 (without TSCS) and session 2 (with TSCS)..... 97

Figure 5-4: Bar plots of iEMG of muscles monitored. Muscles are measured bilaterally. R – Right side of body, L-Left side of body. RF - rectus femoris, BF - biceps femoris TA - tibialis anterior, TA – tibialis anterior, LG – lateral gastrocnemius, SL – soleus. Mean and SD values are shown at T1, T2, T3 and T4 for perturbations in the forward (F), backward (B), right (R) and left (L) directions. \* =  $p \leq 0.05$ ; \*\* =  $p \leq 0.01$  ..... 98

Figure 5-5: Bar graphs of kinematic measures - COP-COM max velocity, margin of stability, max forward ground reaction force (GRF), and max backward GRF - showing mean and SD values at T1, T2, T3 and T4 for perturbations in the forward (F), backward (B), right (R) and left (L) directions. \* =  $p \leq 0.05$ ; \*\* =  $p \leq 0.01$  ..... 99

Figure 5-6: Bar plots of coactivation indices for muscle pairs. Mean and SD values are shown at T1, T2, T3 and T4 for perturbations in the forward (F), backward (B), right (R) and left (L) directions. \* =  $p \leq 0.05$ ; \*\* =  $p \leq 0.01$  ..... 99

Figure 5-7: Pretest and posttest values of posterior root muscle reflex thresholds in the pretest (P1) and posttest (P2). Numbers on the side are for subject identification ..... 103

Figure 5-8: H-reflex recovery cycle. H2/H1 ratios at 80, 150, 250, 500 and 1000ms interstimulus intervals. \*:  $p \leq .05$  ..... 104

Figure 5-9: Correlation coefficient of trunk rotation and shank rotation. Positive values above 0.3807 indicate Ankle strategy and negative values below -0.3807 indicate Hip strategy. Subjects 4, 5, 6, 8 and 9 have average correlation coefficient significantly lower than subjects 3,7,9,10 and 11 indicating that they use the hip strategy more often. .... 106

## **List of Tables**

Table 2.1: Results of correlation for different combinations of upper body and lower body rotations  
..... 29

## **Acknowledgments**

I would like to express my great appreciation to Dr. Sunil Agrawal for his invaluable advice, continuous support, and patience during my PhD study. His consistent guidance and mentorship have pushed this thesis to its successful completion. Throughout my years at Columbia University, I have been privileged to receive further mentorship from a number of researchers. I am grateful to Dr. Victor Santamaria for opening up to me questions in this research space worth pursuing. Similarly, Dr. Bushra Yasin was critical to making the use of transcutaneous spinal cord stimulation possible. I offer special thanks to Dr. Dario Martelli who trained me in a number of the data collection and analysis methods applied in my experiments and Dr. Moiz Khan who was critical in the construction of the exoskeleton platform used and Dr. Lauri Bishop with whom I ran my first patient study.

I would like to express my sincere gratitude to my many labmates at the Rehabilitation and Robotics Laboratory and my close collaborators there including Robert Carrera, whose input was critical to the success of the electrical stimulation experiments, Xupeng Ai, to the balance experiment, Tatiana Luna to the Stand Trainer exoskeleton, and Antonio Prado to the Virtual Reality Catch-and-Throw game. In addition, Jayson King-ori, an undergrad mentee was of immense help in completing my experiments, and Daniel Weiss, a master's student, in processing data. I am also deeply grateful to the many volunteer participants in the studies I conducted. This project would not have been possible without them.

I also would like to extend sincere thanks to those who I collaborated with through my PhD career. A great part of this dissertation was inspired by the ROAR Lab's collaboration with Dr.

Susan Harkema and Dr. Enrico Rejc. Other collaborators include Dr. Damiano Zanotto, Dr. Patrick Brown, Dr. Heidi Schambra, Dr. Jean Timmerberg, Dr. Katherine Dimitropoulou, Dr. Jacqueline Montes, Dr. Sylvie Goldman, Dr. Scott Barbutto, and Maleeha Naqvi. Lastly, I would like to thank my friends who proofread my thesis, Tess Murray, Isabel Velarde, Danielle Stramel and my sister, Omonefe Omofuma.

## **Dedication**

To God, in thanksgiving for the talents he has given and the grace to multiply them in His service.

To my parents Mr. Tony Omofuma and Mrs. Abiodun Omofuma. I will be forever grateful for the love with which they raised me and the strong virtues which they instilled in me. I am grateful for their continued support even now.

To my siblings Omonefe, Akome and Aluya Omofuma with whom I am running the race of life.

To all the researchers working to improve the quality of life of the motor impaired.

## Preface

This thesis details research on the interaction of perturbation balance training (PBT), transcutaneous spinal cord stimulation (TSCS), and postural balance control in healthy subjects. Knowledge gained from these studies would contribute to understanding how patients with spinal cord injury may recover motor function after injury or disease.

Chapter 1 introduces the concept of postural balance control. It discusses the systems in the human body that work together in performing this function and presents models used by researchers in assessing balance. The Robotic Upright Stand Trainer (RobUST) developed during the course of this thesis is also presented.

Chapter 2 treats the first of three balance studies conducted. This study discusses the effectiveness of PBT performed in RobUST and compares the training with assist-as-needed force support and training without force assistance.

Chapter 3 introduces electrical stimulation and TSCS in particular. We describe the human nervous system and how electrical current interacts with it. In addition, we present posterior root muscle (PRM) reflexes and the H-reflex as tools for assessing the excitability and efficacy of the nervous system circuitry.

Chapters 4 and 5 present experiments involving TSCS and PBT. Chapter 4 describes an experiment in which we studied the effects on balance, and neurophysiological measures of TSCS applied while the subject quietly lay supine. Chapter 5 describes another experiment in which we looked at the effect of TSCS applied while subjects performed a functional task.

## **Chapter 1: Postural Balance Control**

Postural balance control is the ability to direct one's body segments to take a desired position and orientation in order to carry out a functional task [1]–[3]. Our body segments form the basic instrument with which we interact with our environment; thus, our ability to control these is important. Postural control is the process that integrates acquired distributed sensory data and actuators within the body [4] to maintain a task-appropriate dynamic posture while resisting internal and external perturbations.

Good postural control and balance are foundational to successfully completing physical tasks. For example, during standing, a person coordinates the musculoskeletal structure to keep an upright position while resisting the inherent instability of a bipedal stance. In reaching, they coordinate balance while carrying out the task that induces disturbance due to changes in position and orientation of body segments during the process. In walking, they maintain upright balance while moving the entire body in the presence of disturbances due to body mechanics, foot placement, ground unevenness, and so on [5]. It is thus important to have the ability to control balance for successful completion of activities of daily living.

Loss of postural control has negative implications on quality of life. Poor postural control can result in falls, devastating injuries, and even death. The Center for Disease Control and Prevention (CDC) reports that one in four adults 65 years and older falls annually. In addition, approximately 800,000 individuals are hospitalized each year because of a fall injury and the total falls related medical costs during the year 2015 totaled more than \$50 billion [6]. The understanding of postural balance control thus has the potential to improve the quality of life of millions of individuals.

We would like to develop a framework for postural balance control. This framework will help visualize and simplify our analysis of the systems contributing to balance control. In this project,

we focus on upright-standing, its robust execution, and its use as a way to characterize the postural balance control system. The task in upright standing is to regulate the body in the inherently unstable bipedal upright position and maintain this position while resisting disturbances.

The postural control system can be modeled as a closed loop control system in which the input is an instruction to maintain an upright position, the nervous system is the controller, the neuromuscular system is the actuator, and the sensory system provides feedback on the configuration, Figure 1-1. The sensory system provides the position and orientation of the body to the brain, which then determines the appropriate corrective action to set the body's configuration to the desired position and sends signals to the musculo-skeletal system. From the literature, there is reason to believe that this corrective action is evaluated not only in the brain but depending on the needed speed of reaction, at the level of the spinal cord or even in the muscle spindles [3], [7]. The body executes the corrective action by activating the relevant muscles. In upright standing, this comes down to applying forces on the feet in order to move the body's position.

The bipedal upright position is said to be one in unstable equilibrium [8], a state in which a small disturbing force can move the center of gravity outside its base of support (BOS), causing

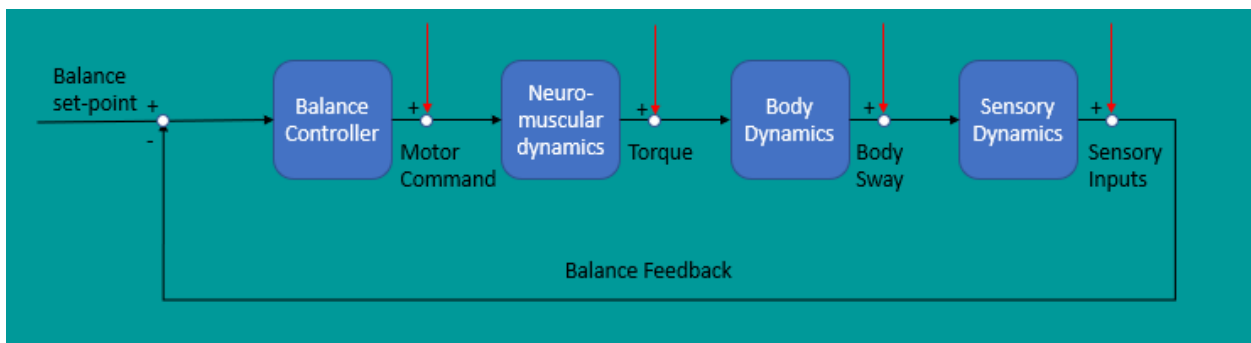


Figure 0-1: The human sensorimotor system modeled as a closed-loop system. Red lines indicate disturbances introduced into the system. Modeled based on Rasman et al 2018 [9]

toppling, as opposed to stable equilibrium where a body is able to resist a slight disturbance. Our description of the postural control system would not be complete without including disturbances.

The body is always having to correct for internal perturbations, e.g., movement of body organs or sensory loss due to a lapse in concentration, and external perturbations, e.g., movement of the support platform or a push. Sensing and correcting for these disturbances are the main tasks of the postural control system in upright standing.

## 1.1 Sensing

The sensory system is crucial to balance as it is the source of information on body position. Studies have shown that balance characteristics in general deteriorate when one or more sensory systems are removed, sometimes to the point of not being able to stand. The human body has a number of senses through which it sources balance information and it uses this information to balance robustly. There is the somatosensory system, the visual system, the vestibular system and the auditory system. The **somatosensory system** is a distributed network of receptors at the muscles, joints and the skin of the body that encode static and dynamic joint angle and/or muscle force. They can sense contact forces and the texture of surfaces [9]. Proprioception is a subset of somatosensation where humans sense the position of parts of their body in three-dimensional space [10]. It relies on Golgi tendon organs and sensory receptors located at the insertion of skeletal muscle fibers into the tendons of skeletal muscles and muscle spindles (muscle spindles - sensory receptors within the belly of a muscle that primarily detect changes in the muscle length). They convey information to the central nervous system (CNS), which translates this information to interpret the position and orientation of different body segments.

The importance of somatosensory receptors in standing is seen in patients with large fiber neuropathy [11], damage or dysfunction of nerves [12], where individuals lose the sense of joint position, vibration, and have sensory ataxia [13]. These patients lose all sense of proprioception and are unable to carry out many daily living tasks when also deprived of visual input [9], [11].

Another way we see the contribution of proprioception is in light touch experiments. Researchers have shown that postural sway reduces when subjects make light contact with an external reference despite the fact that the reference provides no real support [14], [15]. The somatosensory system is thus one of the ways humans get sensory information that contributes to postural stability.

The **vestibular system** encodes motion of the head in three translational and three rotational dimensions. It is well suited to transmit static and low frequency changes in head orientation associated with postural oscillations [16].

The effect of **vision** on balance is commonly assessed by quiet standing tasks in both eyes open and eyes closed conditions. The latter is widely used to increase the difficulty of a balance task because of elimination of vision input. Ordinarily, there is increased sway during standing balance task with eyes closed as opposed to eyes open [17]. The contribution of vision to stability in balance is thought to be limited to low frequency or slow disturbances but this is debated in literature. Scientists have set up experiments where other sensory inputs are mostly eliminated and the subjects attempt to balance using only vision signals. Nagata et al. showed that vision only reduced sway at oscillations below 0.4 Hz and they concluded that the processing of visual information was so slow that vision provided only a minor influence on the control of standing balance [18]. Rasman et al. [9] went on to show that although subjects showed 5-6 times larger sway variability when balancing with access only to visual cues, after 5 days of training this variability was reduced by 75% but it remained twice that observed when balancing with all sensory cues. This result not only shows that the body ordinarily depends on multiple senses and sensory integration, but that it can recalibrate its weighting of sensory input when deprived of some of its senses. Thus, a picture of the balance status of the body can be drawn from the sensory input collected.

## 1.2 The Nervous System as Controller

The brain does the job of assembling, processing, and interpreting all sensory information collected and determining an appropriate response. It selects the best strategies to achieve the balance target (standing upright) using the sensory information and generates the control signals to actuate the body. It comes up with postural strategies, which are high level plans formulated by the nervous system for achieving these goals [19]. There are many possible strategies the body can use but this dissertation focuses on strategies applied to modulate standing balance response. In literature, these strategies are grouped into ‘in-place’ strategies and ‘change-in-balance’ strategies. Ankle and hip strategies are among the in-place strategies, and the stepping strategy is a change-in-balance strategy.

Horak and Kuo explain that the ankle strategy is used to control anterior-posterior sway in quiet stance and in response to small and slow center of mass (COM) displacements while standing on a firm and flat surface. The ankle strategy controls the COM by exerting torques about the ankle joint while the knee and hip joints are held relatively straight and rigid. As the actuating force is generated at the ankles there is distal to proximal activation of muscles [20]. Nashner et al. go further and state that this strategy is effective for moving the COM within an arc of approximately 12 degrees; however, such movements are constrained to low frequencies because the body’s moment of inertia about the ankles is large [21].

The hip strategy also precludes lifting the feet off the support surface but involves more vigorous movement than the ankle strategy. It is used to respond to rapid or larger amplitude perturbations. It consists of simultaneous flexing of the trunk at the hip joints and counterrotating at the ankle and neck joints. It involves early activation of the hip/trunk flexors e.g., rectus

abdominis, gastrocnemius and soleus muscles, and is used when responding to large, fast perturbations.

The stepping strategy is used to respond to large and/or fast perturbations and is used when

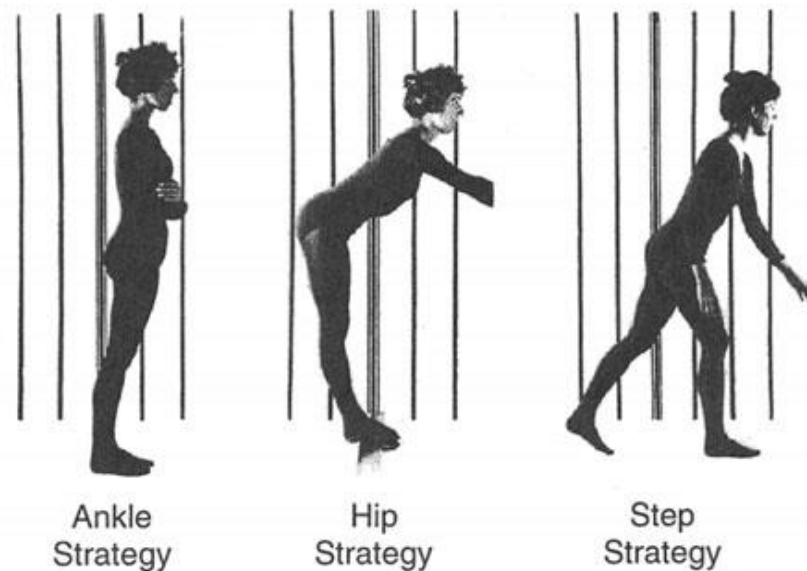


**Figure 0-2: Example movements for the different reactive balance strategies. Horak and Kuo 2000 [20]**

neither the ankle or hip strategies can generate enough restoring force. It involves changing the area of the BOS so that the COM falls within the new BOS area, restoring equilibrium. It is usually associated with an anticipatory lateral weight shift to unload the stepping leg.

These strategies are not exclusively expressed in practice but exist on a continuum [19]–[23] whereby an individual can apply a mix of strategies depending on their balance objectives, physical ability (ankle/knee/hip joint range of motion) and constraints (evenness and size of balance surface, stepping restriction and others). The ankle and hip strategies represent extremes of a response continuum [21].

In Figure 1-3 A, culled from Horak and Kuo [20], the shaded region represents all the possible combinations of ankle and hip angles a subject might assume when balancing. In Figure 1-3 B, the solid line shows combinations of angular displacement and sway frequencies for which the ankle

strategy restores balance successfully. The solid line on the plot denotes the limit of the torque the ankle can generate for a given sway frequency (see Section 1.4). As the speed of sway [21] increases, the restoring ankle torque reaches a limit and the maximum sway amplitude rapidly reduces [21]. Figure 1-3 C shows similar limits for the hip strategy, and we observe that this strategy can be used at higher frequencies of sway but allows for less range of movement of the COM. Nashner et al. note that the hip strategy can be combined with the ankle strategy to increase its limits of stability by up to 3 degrees because hip movements are equally effective with the body centered over feet, or leaning forward or backwards [21]. Hence, a subject can start responding to a perturbation with the ankle strategy but switch to the hip strategy once they sense they are likely

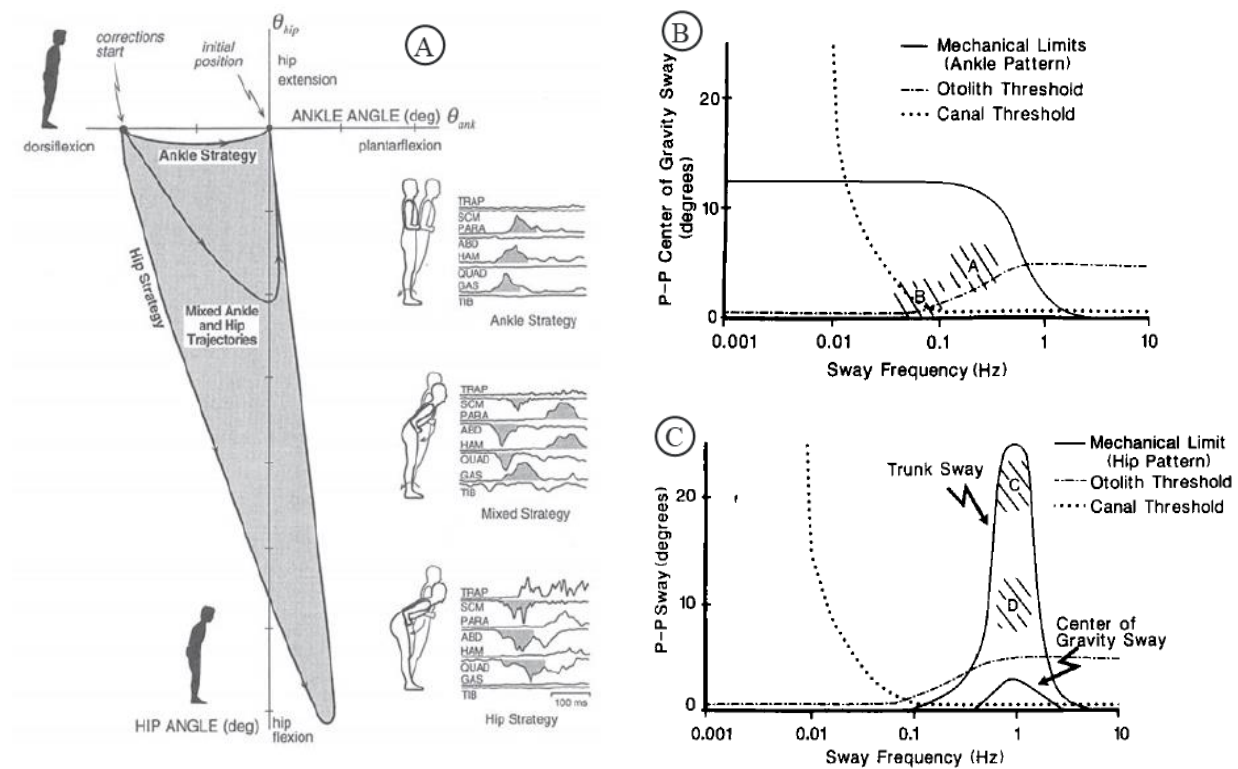


**Figure 0-3:** A - Workspace showing the relationship between ankle and hip angles and ankle and hip strategies. Top outline of shaded area identifies the limits of the pure ankle strategy and the bottom outline the pure hip strategy. The shaded area are feasible combinations of ankle and hip angle movements which in general are mixed strategies. Horak and Kuo 2000 [20] B – Limits of sway frequency (Hz) and center of gravity sway angle for which the ankle strategy can restore balance. C – Limits of sway frequency and center of gravity sway for which the hip strategy can restore balance. Nashner et al. 1989 [21]. to fall.

The fluidity with which strategies can be transitioned makes it difficult to identify which strategies are observed during experimentation. Since strategy selection is not a choice between discrete options but choices that lie on a continuum, we can rather evaluate how much of each strategy is observed in a balancing activity. This could be used to assess the degree to which the subject felt destabilized during the activity. Thus, observing how this distribution between ankle and hip strategy changes after a training protocol could be a way of assessing a training protocol.

Some ways of distinguishing the strategies that will be developed in subsequent chapters are

- i. Hip and ankle angle plots
- ii. Angular acceleration of the trunk (large angular accelerations point to hip strategy)
- iii. Cross-correlation of hip and ankle displacement

Blenkinsop et al. [24] identified strategies by calculating the correlation coefficient of ankle, knee, and hip torques in pairs over a one-second interval. Ankle strategies were identified with statistically significant positive correlations between all the torques, and the hip strategy with significant negative correlation of knee and hip torques. Joint torques were not measured in this project; thus, correlations between trunk and shank angular displacements were used (Section 2.1.3).

### **1.3 The Neuromuscular System**

Once a strategy is chosen it is up to the neuro-muscular system to execute it successfully. This includes the brain, spinal cord, peripheral nervous system, muscles and skeleton. The nervous system plays a role in the control and coordination of body movements and exerted forces [7] while the muscles and skeleton are the actuators and structures through which movements are executed.

Chapter 3 contains a detailed discussion of the nervous system but here we want to note that the muscles of the body are controlled through the afferent and efferent signals passed through the

nervous system. Muscles are the prime movers of the body and they are controlled by nerves that innervate them. There are approximately 700 muscle crossing over 300 joints [25] in the human body. In addition, each muscle is innervated by a number of neurons that control distinct motor units within the muscle. A muscle is composed of many motor units, and each motor unit contains many muscle fibers. A motor unit is a grouping of muscle fibers innervated by a single nerve cell/neuron [26]–[28]. The solution space for the number of ways the skeletal system can be actuated is much smaller than the ways nerves can activate the muscles to produce movement, i.e., there exists multiple or redundant movement solutions for achieving the same task [25]. Bernstein [29] was one of the first researchers to develop a framework to uncover the organizing principles of the human motor system and, along with other researchers, came up with the concept of muscle synergies as the means by which the motor control system makes this problem tractable.

A muscle synergy can be defined as “the coordinated recruitment of a group of muscles with specific activation patterns or specific activation waveforms” [30]. For example, in a walking task, the CNS is not activating each muscle involved in the task independently nor is it determining their activation levels. Rather, it is dealing with a problem with a much lower resolution, and activating sets of muscles known to be used to achieve the task in the right activation patterns for the task.

The neuromuscular system thus coordinates the muscles of the body to carry out the actions that preserve balance and in doing so moves the body against gravity in physical space. The next section explores some physical quantities used to assess segment body dynamics.

## **1.4 Body Dynamics**

In free-standing balance tests, for successful completion of the task, the only contact the subject has is with the support surface under their feet. Thus, if, for example, a subject is perturbed at the trunk and wants to apply a resistive force at the feet so as not to fall, that force has to be

channeled through their body to the support surface. The center of pressure (COP) is used to conceptualize foot action on the support surface at a single point of application such that it captures the sum total of forces and moments acting between the feet and support surface in that application [31], [32]. Thus, the CNS directs the muscles to exert forces through the legs onto the support surface to maintain balance.

In literature, the inverted pendulum model is well known for simplifying the force relationships in upright standing. Winter in [33] explains the model. In summary, imagine a person standing upright with weight  $W$  concentrated at their COM, reaction force,  $R$ , acting at the COP, swaying at angular velocity “ $\omega$ ,” and angular acceleration, “ $\alpha$ .” With the person swaying about their ankle,  $W$  has a moment arm of length “ $g$ ” and “ $R$ ” has a moment arm of  $p$ , and their moment of inertia is “ $I$ ,” Figure 1-4. In quasi-static equilibrium,  $W = R$ . For force and moment balance, we have:

$$\text{Force balance: } W = R$$

$$\text{Moment balance: } Wx - Rp = I\alpha$$

$$\rightarrow W(x - p) = I\alpha$$

These equations tell us that if  $g > p$  the forward moment of the weight overcomes the moment of the ground reaction and the body falls forward. In order to prevent a fall,  $p$  has to be greater than  $g$  so that there is a restoring moment. So, when the body sways anteriorly, in order to prevent a fall, the subject has to push his COP ahead of his COM so that  $p > g$  and that way he is able to generate enough restoring moment to sway himself backwards. With this scenario in mind, we see that  $p$  is limited by the foot length and so if ever  $g$  goes beyond the toes, nothing can be done to create enough restoring moment in this quasi-static condition [33].

The postural control task involves the control of the projection of the body COM inside the supporting surface area delineated by the feet, the base of support (BOS) [34]. That is, the COM is the controlled variable in balance control. Dietz [35] expresses this idea (COM within BOS) by saying that “the neuronal pattern evoked during a particular postural control task is always directed to hold the body’s center of mass over the base of support.”

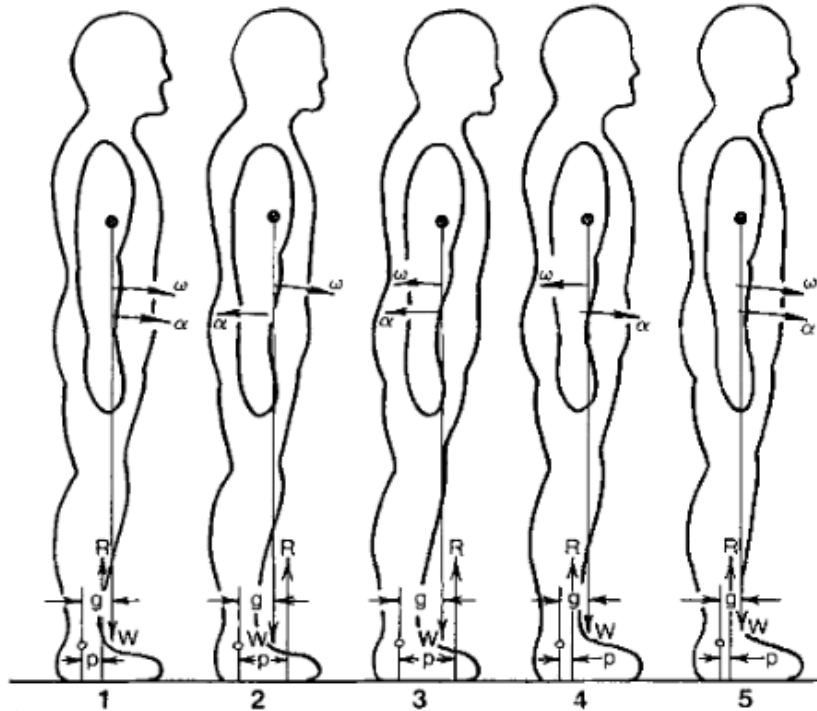


Figure 0-4: Relationship between moment arms as a subject oscillates about their ankle. ‘g’ in this figure represents the horizontal projection of the COM, represented by ‘x’ in the text. ‘p’ is the position of the COP, represented by ‘u’ in the text. Winter 1995 [33].

Although some doubt about the validity of the inverted pendulum model has been expressed in literature [36], studies have been undertaken to verify it [37], [38] and this dissertation will rely on its legitimacy.

We can include further considerations of how the body generates restoring moments in this model. First, in the anterior sway situation described previously, the subject can manipulate the position of his COM by moving his arms or bending at the joints. In this situation, they would add

the hip strategy to the ankle strategy. This manipulation does not destroy the validity of the inverted pendulum model since the interaction between the COM and COP is still intact even though the COM can be altered.

Hof et al. [39] included the effect of inertia, making the model no longer quasi-static but dynamic. He solves the dynamic equation thus:

$$\text{setting } I = ml^2; \alpha = \frac{\ddot{x}}{l}; W = ma_g$$

where  $l$  = height of COM above the fround;  $m$  = mass of subject;  $x$

= displacement of COM;  $a_g$  = acceleration due to gravity

$$ma_g(x - u) = ml^2 \frac{\ddot{x}}{l}$$

$$(x - u) = \frac{l}{a_g} \ddot{x}$$

For small angle displacements of the COM (less than 10°), a new term,  $\omega_o$ , the natural frequency of a pendulum is defined as  $\omega_o = \sqrt{g/l}$ . Figure 1-3C shows that that the mechanical limit of the COM displacement is less than 5 degrees, and the small angle approximation holds.

Setting initial velocity as  $\dot{x}_o$  and solving this differential equation, we get:

$$x(t) = u + (x_o - u) \cosh(\omega_o t) + \frac{\dot{x}_o}{\omega_o} \sinh(\omega_o t)$$

For the COM to not be greater than the COP,  $x \leq u \rightarrow x - u \leq 0$

$$(x - u) = (x_o - u) \cosh(\omega_o t) + \frac{\dot{x}_o}{\omega_o} \sinh(\omega_o t) \leq 0$$

$$(x_o - u) \cosh(\omega_o t) \leq -\frac{\dot{x}_o}{\omega_o} \sinh(\omega_o t)$$

$$(x_o - u) \leq -\frac{\dot{x}_o}{\omega_o} \tanh(\omega_o t)$$

$$(u - x_o) \geq \frac{\dot{x}_o}{\omega_o} \tanh(\omega_o t)$$

$$-1 < \tanh(\omega_o t) < 1$$

Hence, we have

$$x_o + \frac{\dot{x}_o}{\omega_o} \leq u$$

This equation tells us that the distance of the COP from the ankle needs to be greater than the sum of the distance of the COM from the ankle and  $\frac{\dot{x}_o}{\omega_o}$ . This additional term takes the momentum (and the implied inertia) of a body balancing into consideration and thus provides a more robust condition for balance.

In this chapter, we have outlined a framework for understanding postural balance control. We see that balance control is an integrative process involving many body systems. There are, therefore, many points at which this system can fail, and understanding these failure modes can help with the diagnosis and treatment of the different pathologies that arise from them.

## 1.5 Improving Postural Balance Control

The question of how to improve postural balance control can be addressed from many angles, but first, we would like to ask whether it is even possible. In literature, improvements in balance after training are seen in the elderly and in subjects with postural dysfunctions [40]–[42], e.g., in SCI, or stroke patients. Sometimes, it is difficult to see balance control improvements in healthy adults because of the ceiling effect where the subject's initial performance has a score close to the best possible score [7]. Small improvements may not be noticeable because of the limitations in the measurement scale or because the experiment is not challenging enough when performed in the natural setting. This underlines the difficulty in quantitatively capturing postural control improvements in healthy subjects.

In the model of the postural control system described so far, any one of the parts of the system could be a failure point. Vestibular problems are seen in Alzheimer's and Parkinson's disease patients [43]; problems with the visually challenged are self-evident; patients with problems in the controller (the brain) may have trouble with motor planning, like in Cerebellar Ataxia, or with sending the appropriate control signal like in individuals with spina bifida or cerebral palsy; patients may lose the capacity to actuate their muscle such as in stroke and spinal cord injury, and so on. There are many possible failure modes in this balance control system, but this thesis focuses on a holistic picture since experimentation was done on healthy people who have the different parts of the system working. Thus, we focus on their ability to respond to perturbations, integrate sensory signals, and examine their potential for improvement under a number of training regimes.

One of the ideas central to the human ability to improve on and learn new motor skills is neuroplasticity, the ability of the nervous system to change its activity in response to intrinsic or extrinsic stimuli by reorganizing its structure, functions, or connections [44]. Many researchers argue that this ability is an intrinsic property of the nervous system and we retain it throughout our lives [3], [45], [46]. With the ability of the brain to learn, researchers and physical therapists are able to design interventions for the rehabilitation or retraining of subjects. In this work, we hypothesize that neuroplasticity will enable subjects in our experiments to learn improved balancing patterns. Shumway-Cook and Woollacott [3] highlight an experiment with monkeys where after considerable training on a task, the area of the brain mapped to the middle fingers, which were being trained, was much larger [47]. This highlights the plasticity of the brain, and it also highlights the role training and repetition play. They go on to note that not all forms of training go on to induce this "cortical reorganization" as in Remple et al. [48].

The beneficial effects of balance training are well documented in literature [49]–[55]. Key to the benefits is the use of training principles that promote neuroplasticity. Kleim and Jones [56] outline 10 principles of experience-dependent neural plasticity that inform the therapy process. Our experimental design embraces these core training principles to induce changes in the postural control system of healthy adults.

In literature there are two kinds of balance training: conventional balance training (CBT) and reactive balance training (RBT). CBT includes strength training, training on wobble boards, sissles, soft mats [54], and balance balls. In RBT, an imbalance is induced by a perturbation which may come in different forms and thus it is also called perturbation-based balance training. Several studies have shown the effectiveness of perturbation balance training [57]–[60]. PBT creates the environment for subjects to work on balance control through repeated exposure to destabilizing perturbations. Balance training has served to improve motor reaction time, joint stability, and improve confidence during daily life interactions with the surroundings [61]–[64]. PBT has been implemented in several forms such as slip perturbations on treadmills [58], [59] or through waist pulls [65]–[67].



**Figure 0-5: KineAssist. Peshkin 2005 [68]**

In order to improve on the efficacy of conventional balance training devices, researchers have developed robotic devices for balance training. KineAssist (Figure 1-5) is an FDA approved robotic balance training device that provides partial body weight support and postural torques on the torso capable of “catching” a subject if they fall. The subject is strapped into the device at both the pelvis and trunk through fixtures that allow motion at the point of connection along many axes [68]. In the KineAssist, the subject can act out their regular

gait pattern while the device provides body weight support and can catch the subject in case of a fall. To challenge the subject, therapists can perturb them with pushes and the device allows the motions necessary to recover balance while keeping them within a safety zone. The device acts mostly as a support device that allows subjects the independence to try to recover from stumbles, perturbations or falls independently while preventing them from falling out of the safety zone but unlike our RobUST system, it does not have the ability to perturb subjects.



**Figure 0-6: Balance Assessment Robot (BAR). Shirota 2017 [69]**

The balance assessment robot (BAR) (Figure 1-6) developed at the University Rehabilitation Institute, Ljubljana, Slovenia [69], is a balance training device that actuates the pelvis. It has three actuated degrees of freedom, all in the transverse plane (anterior/posterior displacement, lateral displacement and rotation about the vertical axis), and three passive degrees of freedom. It can apply perturbations in the actuated directions as well as assistive forces. It is used in the assessment and training of balance during overground walking.

Several researchers utilize the idea of a moving platform for rehabilitation and evaluation of balance performance. The PROPRIO Reactive Balance System is a device that provides perturbations through the platform on which the subject stands. The platform is capable of tilting in both pitch and yaw rotations, and the amount, direction, and speed of tilt can be programmed to challenge the user so that both patients in the early stages of rehabilitation and world-class athletes benefit from the device [70].



Figure 0-7: A CAREN system in use. Reproduced from Collins 2015 [71]

The Computer Assisted Rehabilitation Environment (CAREN) (Figure 1-7) is an immersive virtual reality environment whose primary active feature is a 6-degree of freedom platform that can be used to perturb subjects [71] and test balance and locomotion. CAREN has a forceplate-instrumented

treadmill and optical motion capture for measuring motion kinematics. Its support surface sits on a Stewart platform which allows for quick, accurate perturbations.

Balance Quest [72] is a platform that is used for evaluation of postural balance which allows 6-DOF movement with limited translation. It is capable of simulating different scenarios to test balance, such as platform instability, and visual, vestibular and proprioceptive sensory suppression during the task. Perturbations may only be applied through the platform.

## 1.6 The Robotic Upright Stand Trainer (RobUST)

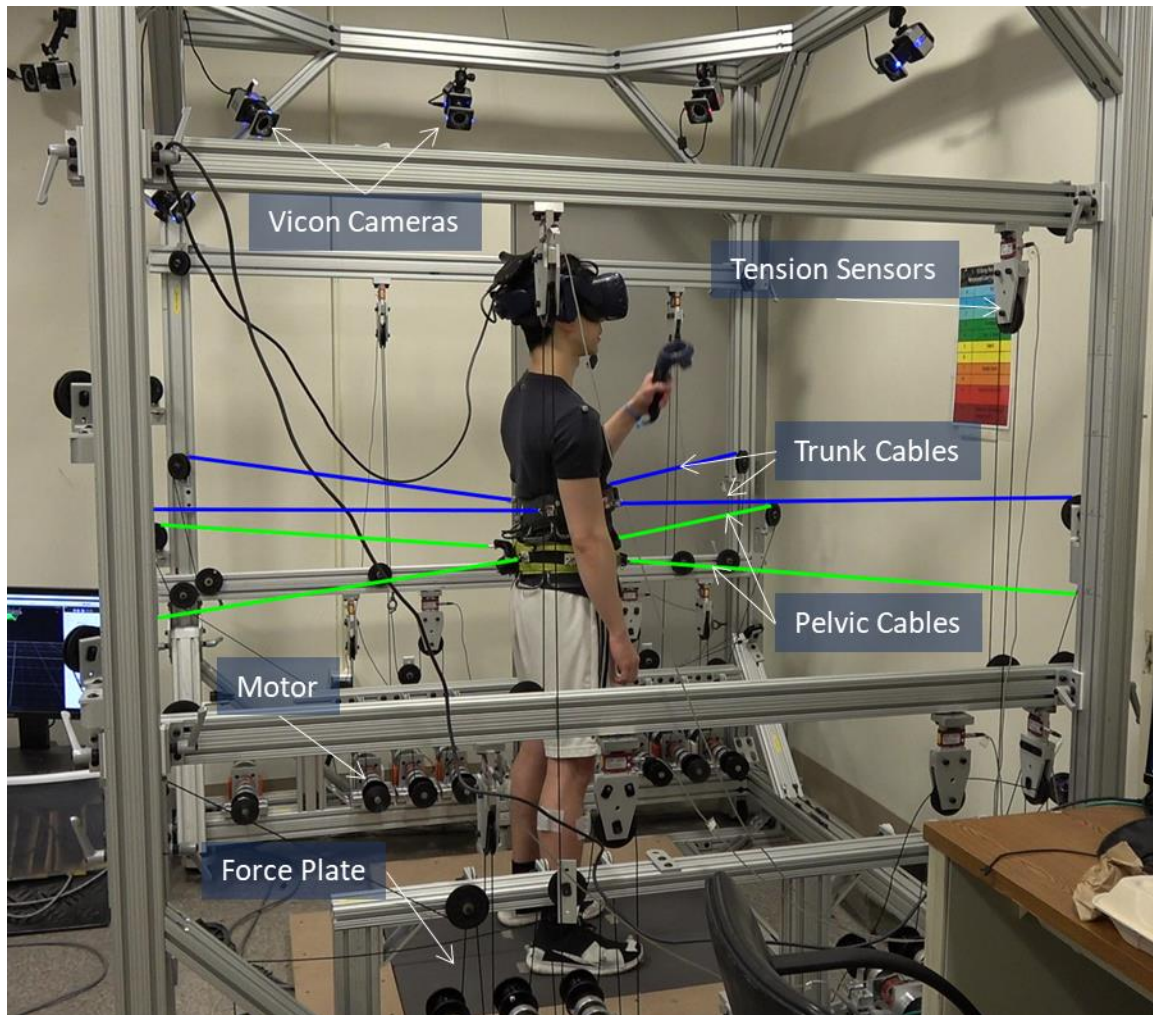


Figure 0-8: The Robotic Upright Stand Trainer (RobUST).

The ROAR Lab Robotic Upright Stand Trainer (RobUST) has several features that distinguish it from these similar devices.

**RobUST** is a cable-driven exoskeleton that applies forces on a subject's upper body via belts worn by the subject at the trunk and pelvis. Each belt has four cables attached to it, as shown in Figure 1-8, and each cable is routed to a motor, with the routing supported on a frame that encloses the subject. The cables are made of PVC-coated flexible steel, 1/16" in diameter, and can support a load up to 440N. Each cable has a load cell connected in series that can measure tension in the cable, up to 1334N. Position sensing of the human body is done using a nine camera Vicon Motion

Capture system. Two six-axis force plates (Berotec, Columbus, Ohio) are used to measure foot forces during the experiment. Control and integration of sensing and actuation is implemented with LabVIEW and a PXI real-time controller (National Instruments, Austin, TX). With this configuration of the stand trainer, forces can be applied in any direction in the horizontal plane at both trunk and pelvis levels.

The device has been described in more detail in publications [73], [74]. Figure 1-9 shows the overall -system architecture and its component functions. Control is implemented in two stages with a high-level and a low-level controller. The high-level controller prescribes the desired behavior of the belts. In this system, we have three modes of operation for each belt.

1. **Constant Force Mode:** in which the wire tensions keep the belt in place
2. **Perturbation Mode:** in which a force is applied in a chosen direction. The force is the form of a short impulse that pulls the subject.
3. **“Force Field” Mode:** This is our implementation of an assist-as-needed controller in the Stand Trainer. Here, assistance is provided to the subject as a restoring force when the subject travels outside a defined boundary. The assistance is in the form of a force that

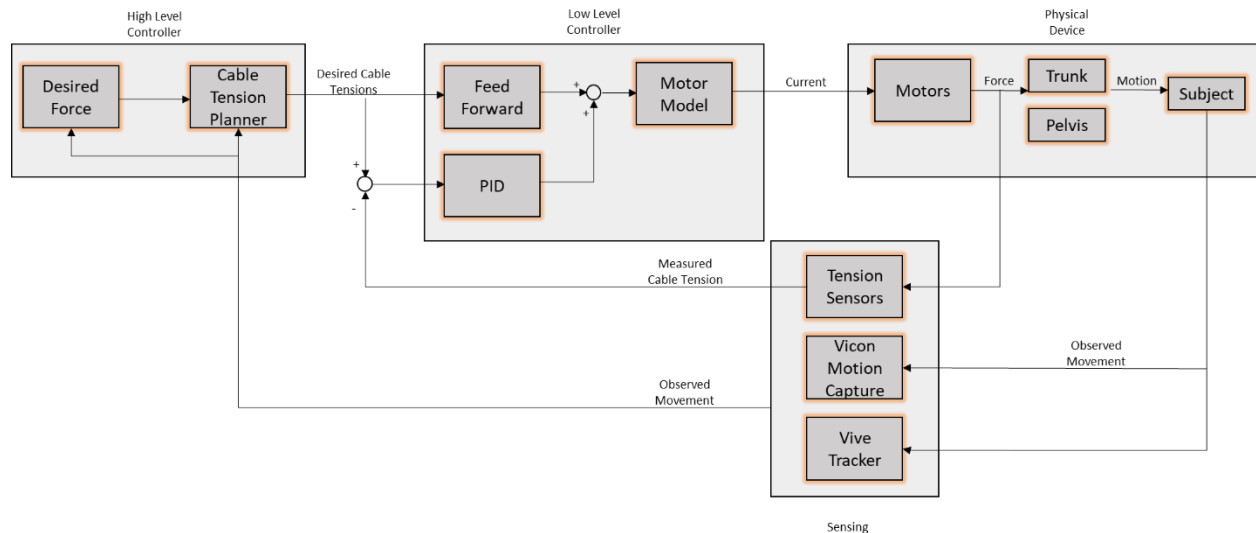
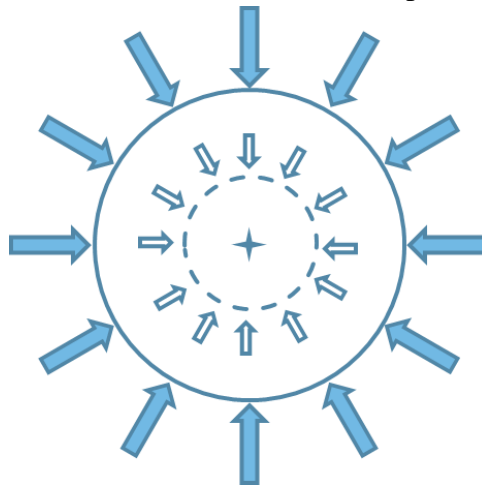


Figure 0-9: Flow diagram of architecture of Stand Trainer

pulls the subject back to the center of the defined boundary. Figure 1-10 shows a schematic

of how the force field works. The star at the middle of the figure signifies the center of the force field built around the subject. At the start, in the interior of the solid circle, there is no force assistance. Force assistance only begins once the subject drifts outside the solid circle. The force is directed towards the center of force field. The force assistance continues up until the subject is within the dashed circle which is set at a very small radius so that the subject is very close to the starting stable position.

The high-level controller outputs a tension command that is implemented by the low-level controller. A PID controller is implemented with current, velocity, tension limits and friction compensation. The low-level controller sends current inputs to the motors that maps to a desired



**Figure 0-10: Description of Stand Trainer force field. The star in the middle is the center of the force field. The solid arrows show the direction the device pulls the subject when they move past the solid circle. Force in the region between the solid circle and the dashed circle is only activated as the subject is being pulled to the center after they have moved past the solid circle. There is no force within the dashed circle**

tension in the cables. The loop is closed using a load cell that measures the tension in the cables. The motors apply forces on the subject. In some studies, we have added an HTC Vive Tracker for position sensing and control. HTC Vive is a virtual reality engine which immerses the subject in a virtual environment when carrying out the tasks. As we explain later, we have integrated the Vive into a training protocol.

RobUST improves on the devices highlighted previously with the following key features:

- i. The device does not encumber subjects' movement and they retain all their natural degrees of freedom. This allows for balance assessment in situations that are close to real world.
- ii. The only attachments to the body are belt straps to the trunk and pelvis and pulley cables. Inertia due to the device is thus small allowing for it to be highly transparent although there is some drag due to the slow speed of response of the motors.
- iii. The device is instrumented with force plates and optical motion tracking which allows for the collection of kinetic and kinematic data.
- iv. The subject can be immersed into a virtual reality world through its integration with the HTC Vive.
- v. RobUST can both provide support and perturb subjects at its two points of attachment.

## **Chapter 2: Training Postural Balance Control with Pelvic Force Field at the Boundary of Stability**

### **2.1 Introduction**

The previous chapter discussed how postural control is foundational to everyday functional tasks. This chapter explores the potential for improvement in postural control by training within an exoskeleton.

Technological development has seen the introduction of robotic devices as platforms for balance control training with many benefits, including high repeatability and scalability of treatments. Still, researchers have called their overall effectiveness into question. In rehabilitation robotics, a distinction must be made between replacing a function with a device and improving the function. Researchers argue that although the trained function improves while using some robotic devices, upon removal, there is limited improvement and, in some cases, reduced muscle use which could eventually lead to atrophy. At ROAR lab, we have recently designed and validated a robotic platform named the Robotic Upright Stand Trainer (RobUST) [73], [74] which offers unique advantages in the training of postural standing. It permits weight bearing and only intervenes when assistance is needed, thereby encouraging the improvement, not replacement, of body function. In the device, a subject can train in close to real-life situations.

An experiment to analyze the potential for improvement in postural balance control of healthy subjects given perturbation balance training (PBT) in RobUST is presented in this chapter. In addition, the difference in outcome between training with robotic assistance and without assistance was also assessed.

In assessing balance, we look for measurable parameters that tell how well a subject performs. In literature, a lot of these measures are based on the center of pressure (COP), the location at which the sum total of forces and moments acting between the feet and support surface would act

if these forces were considered to have a single point of action [31], [32]. In non-supported in-place balance tasks the COP captures all interaction a subject has with the world. Hof et al. show that in standing, the restoring moment on the COM generated by the vertical ground reaction force (GRF) is directly proportional to the distance between the COP and the projection of the COM to the horizontal plane [39], [75]. In addition, as the COP can only exist within the base of support (BOS), the ability to apply a restoring force is limited. Once the COM drifts outside the BOS, the toppling moment of the COM surpasses the restoring moment of the COP. As a result, the subject either loses balance or has to change their BOS. We thus begin to think of the distance of the COM from the perimeter of the BOS as a measure of how close a subject is to toppling. As explained in section 1.4, Hof et al. consider a dynamic model with the effects of COM velocity and angular momentum included and summed up these effects in a term called the extrapolated COM. A new term, the margin of stability (MOS), was defined using this extrapolated COM. It was defined as the distance from the perimeter of the BOS to the extrapolated COM.

This formulation of the MOS captures the condition for toppling in an inverted pendulum model where the subject only applies torque about the ankle when trying to restore balance. For a more general assessment of balance control, Hof [76], using a multi-segmental model, identified three mechanisms: (i) moving the COP described above, (ii) using internally generated moments, and (iii) applying an external force. Postural control with the hip strategy is identified with internally generated moments as the body rotates its segments in opposite directions to generate a net movement of the COM towards the interior of the BOS. We can thus assess balance responses to perturbations by studying a subject's preference for ankle or hip strategy, their COP, and the interaction of COP, COM, and the ground reaction forces.

## 2.2 Methods

### 2.2.1 Experiment

The study protocol and consent forms were approved by Columbia University (IRB-AAAR6780). All subjects consented to participate in the experiment. Data are presented from ten healthy adults (5 male, 7 right-handed, weight:  $M = 62.4 \pm SD = 8.34\text{kg}$ , and height:  $M = 1626 \pm SD = 65\text{mm}$ ). Subjects were randomly assigned to one of two groups: a group with assistive force field at the pelvis (FF) ( $n = 5$ ) and a second group without assistance (NF) ( $n = 5$ ).

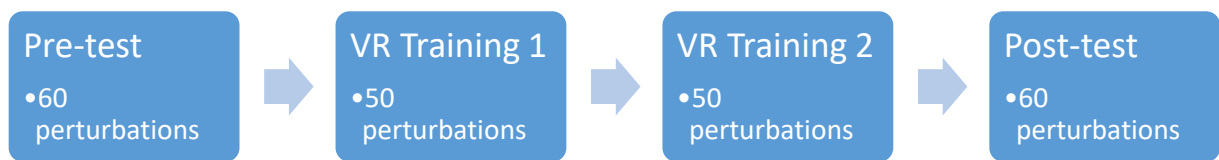


**Figure 0-1: Steps of the experimental protocol**

In this study, we used two of RobUST’s operational modes: (i) *Perturbation mode* - a force is applied on the trunk in one of the anterior, posterior, left, or right directions. (ii) *Force field mode* - an assist-as-needed restoring force, directed towards the neutral standing position, is applied to the pelvis when the pelvic center of the subject travels outside a predefined boundary.

The trunk belt was set to ‘perturbation mode’ for FF and NF groups. The pelvic belt was set to ‘force field mode’ for the FF group and left unused for the NF group.

Perturbations were given as a percentage of the subject’s body weight (BW) with a short trapezoidal profile having 150ms ramp up, 300ms at the set force, and 150ms decay time.

The experiment comprised four sessions: (i) Pre-test, (ii) Virtual reality training 1, (iii) Virtual reality training 2, and (iv) Post-test.

#### 2.2.1.1 Pre-Test:

The subjects’ pre-intervention balance was characterized in this session. They were blindfolded [77] and perturbed without pelvic assistance 15 times in each direction, starting at 40%

BW and using the 4-2-1 algorithm to progress the perturbation force. The primary outcomes measured were the force threshold and the stability area. The steps of the algorithm are as follows:

1. Increase perturbation force by 4% after each successful trial until the subject loses balance (an unsuccessful trial).
2. After the first time the subject loses balance, decrease perturbation force by 2% and keep decreasing until the next successful trial.
3. Once the subject has a successful trial again, increase perturbation force by 1%
4. Increase or decrease force by 1% in all subsequent successful or failed perturbation trials.

The average of the three highest force perturbations was taken as the force threshold for each direction.

The “stability region” of the pelvic center for trials in which a subject did not lose balance (i.e., a stepping reaction was not elicited) was measured. This region was calculated by collecting the points in space the subjects moved through when displaced from their starting position by a perturbation. An external boundary that enclosed these points was then computed. In summary, we determined a ‘force threshold’ in each direction and a ‘stability region’ for each subject during the pre-test. These two balance measures were used in subsequent sessions.

#### *2.2.1.2 Virtual Reality Training:*

We used a VR game developed in the ROAR Lab, run in Unity on an HTC Vive (HTC Corporation, Taoyuan City, Taiwan) VR headset, for the experiment (Figure 2-2). Subjects had to catch a ball projected at their sternum and then aim and throw it at a moving target to score points. The ball was programmed to reach the subject’s sternum chest in one second, and RobUST was set to randomly deliver trunk perturbations between 0 and 0.8s after the ball was tossed towards the participants. In this way, subjects were perturbed at some point during a catch. The force (%BW) of the perturbations delivered in each direction corresponded to the force threshold established during the pretest phase. The FF group received 15% BW restoring force from the

pelvic belt if they strayed outside their stability area when catching and throwing, while the NF group did not receive this assistance. At the beginning of each catch-throw sequence, the boundaries of the stability area found in the pre-test and beyond which force field assistance would kick in was centered around the pelvis position. The restoring force assisted the subject in returning to the neutral standing position. Before each perturbation, subjects were given enough time to reset to a neutral standing position, and the stability area was centered around this neutral standing position. The training session was divided into two sessions, and the catch-throw-perturbation sequence was repeated 50 times in each session.

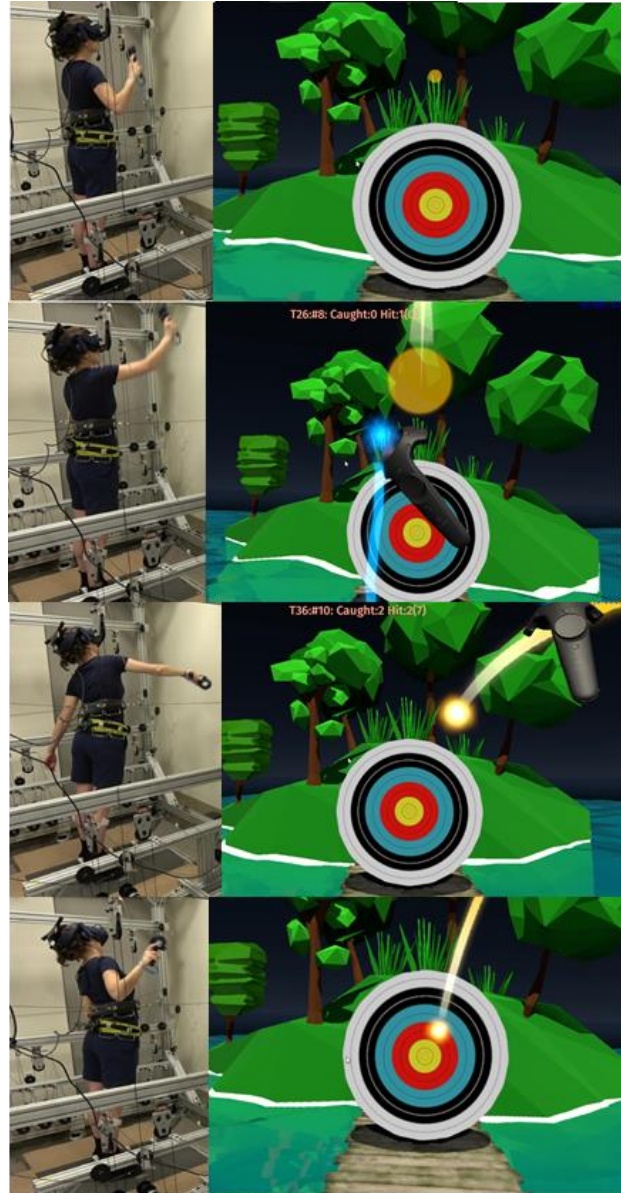


**Figure 0-2: View of VR game and subject. From top to bottom: Subject prepares to receive the ball, subject catches the ball, subject throws the ball, subject tries to recover balance after throwing the ball at target.**

### 2.2.1.3 Post-Test

The post-test was identical to the pretest in which the force threshold and stability area were measured, but subjects took a 5 min rest before beginning.

## 2.2.2 Data Collection

Kinematic data of the human body segments were collected using retroreflective markers with a motion capture system (Vicon, Denver) with nine cameras (Vicon Vero 2.2). Kinematics were

processed offline using Vicon Nexus software 2.10.0 and MATLAB R2019b (MATLAB, Natick). A biomechanical model was constructed based on reflective markers placed on the body. Markers were placed on the left and right shoulders, three on the trunk belt, and three on the pelvic belt. In addition, three markers were placed on each foot - on the nail of the big toe, the fifth metatarsophalangeal joint, and the heel.

Participants had a starting position with each foot on a six-axis force plate (Bertec, Columbus, Ohio). The force plate returned the ground reaction force data and the location of the combined and individual foot center of pressure. Data from the force plates were synchronized with Vicon Nexus software which provided the combined center of pressure of both feet. Electromyographic (EMG) data were also collected bilaterally using 14 channels of a Delsys Trigno Wireless System (Delsys Incorporated, Massachusetts) from the following muscles: tibialis anterior (TA), lateral gastrocnemius (LG), rectus femoris (RF), bicep femoris (BF), gluteus medius (GM), rectus abdominis (AB), and erector spinae (ES). Subsequently, in naming the muscles, we affix the side of the body to the muscle name on which the EMG sensor is placed, e.g., we refer to the left TA as L-TA and the right TA as R-TA.

### **2.2.3 Variables Measured**

There were three sets of data at the end of this experiment: (i) gross performance measures, (ii) kinematic and kinetic measures, and (iii) muscle activity measures.

**Gross Performance Measures:** Force thresholds and the stability area were calculated at the end of the balance tests (pre- and post-tests). During the virtual reality sessions, the trial success rate, the proportion of trials in which the subject did not lose balance, and the number of successful catches were also collected.

**Kinematic and Kinetic Measures:** These were calculated from the movement, force-plate, and EMG data over three seconds starting with each perturbation's initiation.

The minimum distance from extrapolated COM to BOS perimeter observed during a trial was recorded as the **margin of stability (MOS)** Figure 2-3 [39]. The COM was estimated by the position of an optical marker on the pelvis. Optical markers on both feet' big toe, fifth metatarsal, and heel were used to create the BOS outline.

As outlined earlier, in a free-standing setup, the COP is the point at which the subject applies a restoring force. The force applied is proportional to the distance between the COP and COM (**COPCOM**). The COP is thus the primary manipulative tool the subject has for restoring balance. Movement of the COP was assessed with the root mean square of the COP displacement during a trial (**ΔCOP**), its maximum (**ΔCOP MAX**), and the timing of this maximum (**COP MAXTIME**). In addition, we assess the time taken for COP movement to settle out (**COP-TS**) and the speed of this restorative force by measuring its maximum velocity and acceleration and the timing of both.

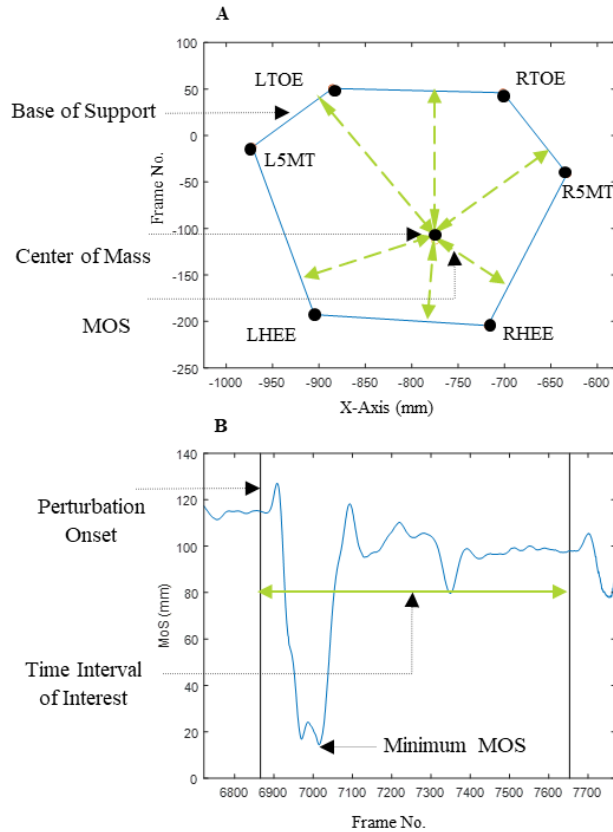


**Figure 0-3: Center of mass (COM) shown within base of support (BOS). Markers on the feet, RTOE – Right Toe, R5MT – Right Fifth Metatarsal, RH – Right Heel, LT – Left Toe, LM – Left Fifth Metatarsal, LH – Left Heel, form the BOS. Margin of Stability (MOS) is the minimum distance of the COM to the BOS. B: MOS calculated at several time points before and after perturbation onset. This study uses the minimum value observed during the time of interest. In steady standing the MOS may oscillate between a range depending on their posture and foot placement. The MOS is typically highest in steady standing.**

The maximum, the timing of the maximum, and the rms of the distance between the COP and COM ( $\Delta\text{COPCOM-MAX}$ ,  $\Delta\text{COPCOM-MAXTIME}$ ,  $\Delta\text{COPCOM}$ ) were measured. In addition, those of the ground reaction forces in the anterior-posterior (**GRF-AP**) and the mediolateral (**GRF-ML**) directions were also measured.

The balance strategy used was determined for each time point using the method in [78] with modifications. In this study, we divided the body into an upper body trunk segment and a lower body segment (thighs, shank, and feet) and examined correlations between the upper body angle in the sagittal plane and the lower body angle. The ankle strategy was identified by positive correlations between the upper and lower body, while negative correlations between these segments identified the hip strategy. This gives us the following classification for upper and lower body rotations.

**Table 2.1: Results of correlation for different combinations of upper body and lower body rotations**

	Anterior Perturbation	Posterior Perturbation
Ankle Strategy	Trunk forward rotation – Lower body forward rotation	Trunk backward rotation – Lower body backward rotation
Hip Strategy	Trunk forward rotation – Lower body backward rotation	Trunk backward rotation – Lower body forward rotation

Strategies were identified at each time point by finding the correlation coefficient of a 250ms centered window between the upper and lower body rotation angles. The critical value for correlations with 25 data points (position data was recorded at 100Hz) at 0.05 significance level is .3807. Therefore, correlations above .3807 were identified with the ankle strategy and below -.3807 with the hip strategy. The percentage of time spent using the ankle and hip strategy was calculated for each trial as **ankstrat** and **hipstrat**, Figure 2-4.

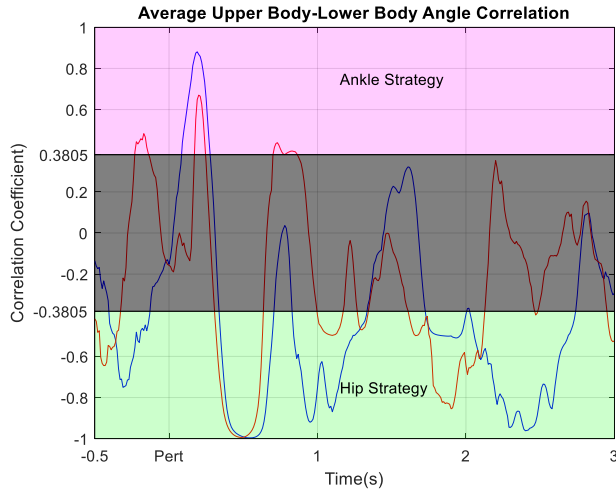


**Figure 0-4: Average correlation upper-body angle – lower body angle correlation of a subject. Blue – pretest correlation; red – posttest correlation. We see at perturbation onset.**

**Internally generated moments, MT**, in the anteroposterior (AP) and mediolateral (ML) directions were calculated using equations from [76] and assuming there was no external force applied to the subject, which was the case after the 600ms period during which the perturbation force was applied. This variable was thus calculated from 0.6 -3s after perturbation initiation. Internally generated moments were calculated as:

$$(x_{COP} - x_{COM})GRF_z + 1.1 (l \times GRF_x) = MT_{AP}$$

$$(y_{COP} - y_{COM})GRF_z + 1.1 (l \times GRF_y) = -MT_{ML}$$

Where  $(x_{COP}, y_{COP})$  and  $(x_{COM}, y_{COM})$  are the positions of the COP and COM respectively,  $(GRF_x, GRF_y, GRF_z)$  the ground reaction force measured by the force plate,  $(MT_{ML}, MT_{AP})$ , internally generated moments and  $l$ , the vertical height of the COM.

**Muscle Activity Data:** EMG signals were detrended, band-pass filtered between 20 and 300 Hz, full-wave rectified, and low-pass filtered at 20 Hz. The following EMG metrics were examined for each perturbation trial: integrated electromyography (**iEMG**), maximum EMG amplitude (**MAX**), EMG activity duration (**DUR**), and EMG coactivation index (**CIdx**).

iEMG is the summation of muscle activity over a period of interest, and it was calculated and normalized using the formula:

$$iEMG = \frac{\sum_{onset}^{onset+t} EMG - \sum_t EMG_{baseline}}{t \times \max(EMG_{global})}$$

where  $\sum_{onset}^{onset+t} EMG$  is the summation of the EMG signal from perturbation onset over a  $t = 3$ s time window and;  $\sum_t EMG_{baseline}$  is the summation of baseline EMG signal while the subject is in quiet standing over 3 secs.  $max(EMG_{global})$  is the maximum observed EMG value per subject.

**EMG MAX** is calculated as:

$$EMG\ MAX = \max\left(\frac{EMG_{trial}}{\max(EMG_{global})}\right)$$

$EMG_{trial}$  is the EMG signal in a trial for a muscle, i.e., the signal from perturbation onset to 3s after onset;  $max(EMG_{global})$  is the maximum observed EMG value for the subject being assessed.

EMG activation was calculated from detrended EMG data passed through the Teager-Kaiser energy operator (TKEO) [79], rectified and low-pass filtered at 50 Hz. The activation threshold was set to the baseline tkeo mean plus 3 standard deviations. A muscle was considered active when its signal rose above this activation threshold for more than 50ms and inactive when the muscle signal fell below the threshold for more than 50ms after being previously active. Activity duration was the sum of all intervals between muscle activation and deactivation.

Coactivation indices were calculated using the following formula:

$$CI = \frac{2 \times \sum \min[EMG_{agonist} + EMG_{antagonist}]}{\sum EMG_{agonist} + \sum EMG_{antagonist}}$$

$EMG_{agonist}$  is EMG voltage of the agonist muscle when the muscle was deemed to be activated,  $EMG_{antagonist}$  is EMG voltage of antagonist muscle when that muscle was deemed to be activated.  $\min()$  returns zero at time points when either  $EMG_{agonist}$  or  $EMG_{antagonist}$  is not activated.

## 2.2.4 Statistical Analysis

Statistical tests to detect the effect of training in virtual reality on the subjects and the difference between training in the NF group and the FF group were setup using SPSS (IBM, version 26, 2019). Only successful trials were used in this analysis. Tests to detect main effect of training, training type and the interaction effect between the two were set up and described in what follows.

**Gross Performance Measures** and **Kinematic, Kinetic, and Muscle Activity Data** were averaged by subject and test phase (i.e., pretest/posttest). First, these data were tested for normality, after which a mixed analysis of variance (ANOVA) with a repeated measures factor (time: pre- and post-training) and a between-subjects factor (training type: FF or NF) was applied. In case of a significant ANOVA model, *post-hoc* analyses were carried out using Bonferroni's inequality procedure to correct for multiple comparisons. Interaction effects were prioritized to distinguish any relevant postural effects in the group that received the assistive force field. However, if interaction effects were absent, the main effects were interpreted.

To examine the frequency of stepping (or not stepping) during the VR training session, we applied a non-parametric Mann-Whitney U test to this data as it was not normally distributed.

Since the use of force field was hypothesized to have only a positive effect, the statistical test was one-tailed. The statistical variables examined were the median, minimum, and maximum stepping frequencies of the NF and FF groups.

The range of perturbation forces differed between pretest and posttest, as seen

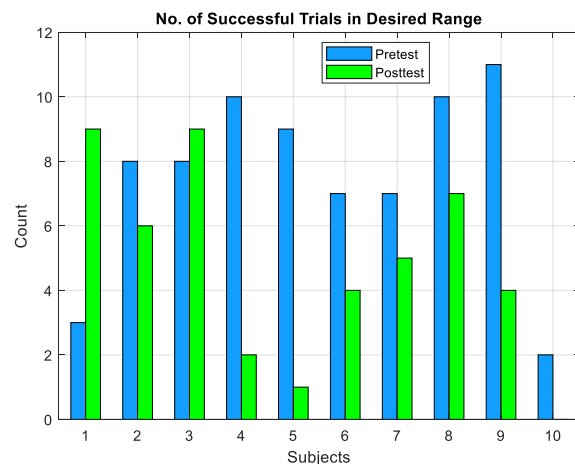


**Figure 0-5: Distribution of retrievable successful trials per subject**

by the change in perturbation force threshold values. To compare metrics within the same range, metrics calculated for perturbation forces above 50% BW and below the pretest force threshold were used in our analysis. Fig 2-5 shows the number of valid trials for each subject used to calculate the results.

## 2.3 Results

### 2.3.1 Gross Performance Measures:

#### 2.3.1.1 Force Thresholds and Stability Area

The force thresholds, across all four directions significantly improved in the FF and NF groups: posterior ( $F(1,8) = 6.51; p = .03$ ), anterior ( $F(1,8) = 6.37; p = 0.04$ ), left ( $F(1,8) = 19.82; p = 0.02$ ), and right ( $F(1,8) = 18.14; p = 0.003$ ), Figure 2-6. The same was true for the postural stability area in standing ( $F(1,8) = 13.63; p = 0.006$ ) (Fig. 2-7). Our data shows that assistive force fields did not impact either perturbation force threshold or postural stability area ( $p < 0.05$ ).

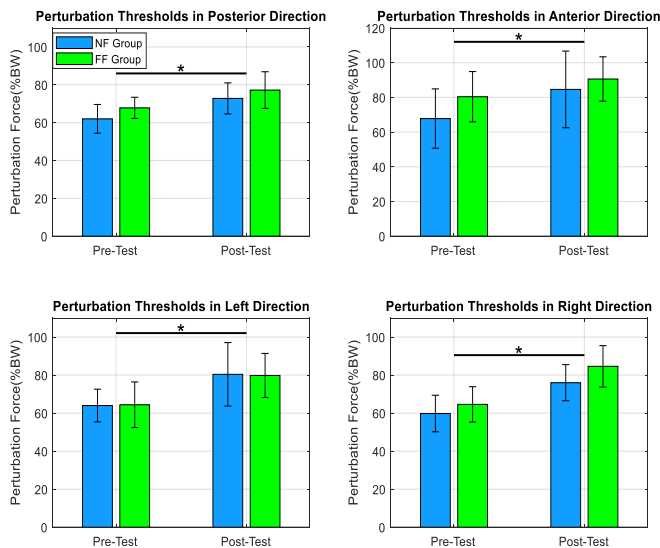


Figure 0-7: The plots show an increase in force thresholds between pre- and post-tests for FF and NF groups across the four directions. We can notice that both groups improved their tolerance to receive greater perturbation intensities

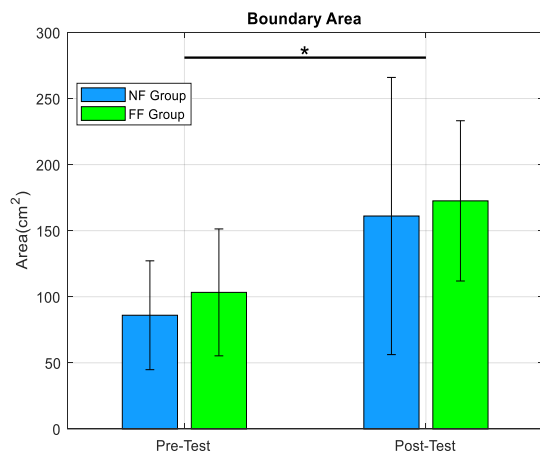
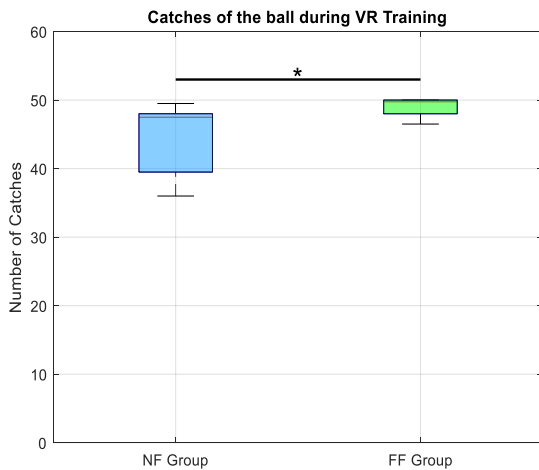


Figure 0-6: Stability area for pre-test and post-test values in NF and FF groups. We can observe that RobUST, in combination with the VR, was enough to increase the area of postural stability in standing.

### 2.3.1.2 Virtual Reality Training

Differences in motor performance between the NF and FF groups were also observed during the training session. The number of times a subject caught the ball (i.e., number of catches) and the number of times they lost balance (i.e., number of steps) were recorded. Figures 2.8 and 2-9 depicts group performance during the VR training sessions. The number of successful catches in the FF group (median = 50) was significantly higher than that in the NF group (median = 48) ( $U = 6.5; p = .03$ ), and although not significantly higher, subjects in the NF groups lost balance more often than subjects in the FF group ( $U = 3.0$ , NF group median = 8 and FF group median = 1,  $p = 0.1$ ).



**Figure 2-8: Average number of times each group is able to catch the ball. Subjects in NF group are significantly less successful at catching**

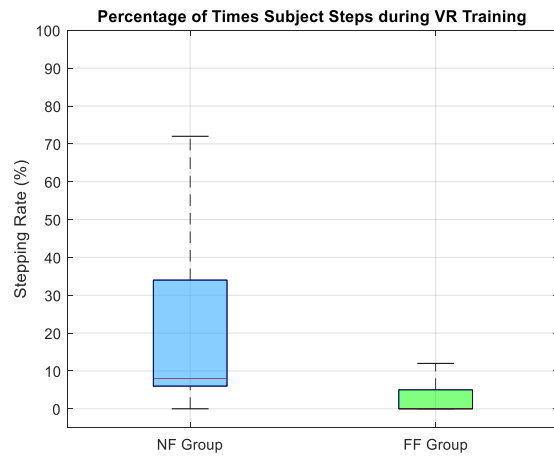


**Figure 2-9: Stepping rate of subjects. Although not statistically significant we see a trend towards more stepping in the NF group**

### 2.3.1.3 Kinematic, Kinetic, and EMG Measures:

**Posterior Perturbations:** There were statistically significant interactions between the effects of training and training group on the following metrics: **MOS** ( $F(1,6) = 8.815, p = .025$ ), FF decreased ( $p = .028$ ) and NF did not change significantly ( $p = .300$ ); **Ankstrat** ( $F(1,7) = 8.813, p = .021$ ), FF had no significant change ( $p = .133$ ) but NF decreased ( $p = .001$ ); **Ankle-Vel MAX**

( $F(1,7) = 5.704, p = .048$ ), FF decreased ( $p = .002$ ) and NF did not change significantly ( $p = .322$ ); **Ankle-Accl MAX** ( $F(1,7) = 7.129, p = .032$ ), FF decreased ( $p = .004$ ) and NF did not change significantly ( $p = .876$ ); **GRF-AP MAXIdx** ( $F(1,7) = 5.649, p = .049$ ), FF peaked later ( $p = .049$ ) but NF did not change significantly ( $p = .091$ ) **R-RF MAXIdx** ( $F(1,7) = 8.987, p = .002$ ), FF did not change significantly ( $p = .645$ ) but NF peaked earlier ( $p < .041$ ) and **L-TA/LG CIdx** ( $F(1,7) = 10.00, p = 0.016$ ), FF decreased significantly ( $p < .001$ ) but NF did not ( $p = .058$ ).

Simple main effects analysis showed that training did not have a statistical effect on **MOS** ( $p = .384$ ) but did have significant group training effects that resulted in increases in **Hipstrat** ( $p = .017$ ), **R-LG DUR** ( $p = .038$ ), and **L-RF MAXTIME** ( $p = 0.007$ ), and decreases in **L-AB iEMG** ( $p = .030$ ), **L-TA iEMG** ( $p = .024$ ), **L-BF iEMG** ( $p = .043$ ), **R-TA iEMG** ( $p = 0.007$ ), **L-TA MAX** ( $p = .022$ ), **R-TA MAX** ( $p = 0.017$ ), **L-GM MAX** ( $p = .002$ ), and **R-TA/LG CI** ( $p = .047$ ).

**Anterior Perturbations:** There were statistically significant interaction effects in the anterior direction in the following: **L-ES iEMG** ( $F(1,6) = 13.41, p = .011$ ), FF had no significant change ( $p = .077$ ) but NF increased significantly ( $p = .025$ ); **L-ES MAX** ( $F(1,6) = 9.874, p = .020$ ), FF had no significant change ( $p = .077$ ) and NF increased ( $p = .016$ ).

Simple main effects analysis showed that training had statistically significant effects that resulted in decreases in **MT-AP** ( $p = .035$ ), **R-LG DUR** ( $p = .049$ ), **L-RF DUR** ( $p = .024$ ), **R-RF DUR** ( $p = .027$ ), **L-TA iEMG** ( $p = .045$ ), **R-LG iEMG** ( $p = .005$ ), **R-RF iEMG** ( $p = .022$ ); **R-TA/LG CI** ( $p = .024$ ), and **R-RF/BF CI** ( $p = .007$ ).

**Right Perturbations:** There were statistically significant interactions between the effects of training and training group on the **L-TA DUR** for ( $F(1,5) = 20.824, p = .006$ ) and **L-TA iEMG** ( $F(1,5) = 7.132, p = .044$ ). Simple main effects analysis showed that training had a statistically

significant effect resulting in decreases in **R-RF iEMG** ( $p = .020$ ), **R-GM iEMG** ( $p = .028$ ), **R-RF MAX** ( $p = 0.020$ ), **L-GM MAX** ( $p = 0.034$ ).

**Left Perturbations:** There were statistically significant interactions in the left direction in the following: **COP MAXTIME** ( $F(1,7) = 8.632, p = .022$ ), FF increased significantly ( $p = .016$ ) and NF had no significant change ( $p = .412$ ); **GRF-ML MAXTIME** ( $F(1,7) = 15.369, p = .006$ ) FF had no significant change ( $p = .092$ ) but NF decreased significantly ( $p = .008$ ); and **R-RF/BF CI** ( $F(1,4) = 25.546, p = .007$ ), FF had no significant change ( $p = .296$ ) but NF decreased significantly ( $p = .006$ ).

Training had a statistically significant main effect resulting in decreases in **COP excursion** ( $p = .016$ ), **COPCOM-ML** ( $p = .024$ ), **GRF-ML** ( $p = .008$ ) **R-TA DUR** ( $p = 0.050$ ), **R-LG DUR** ( $p = 0.046$ ), **L-TA iEMG** ( $p = 0.023$ ), **L-LG** ( $p = 0.017$ ), **R-LG** ( $p = .012$ ), **L-BF iEMG** ( $p = .046$ ), **L-GM iEMG** ( $p = .027$ ), **R-GM iEMG** ( $p = .030$ ), **L-TA MAX** ( $p = .045$ ), **R-LG MAX** ( $p = .015$ ), **L-BF MAX** ( $p = .014$ ), **R-BF MAX** ( $p = .048$ ), **L-GM MAX** ( $p = .015$ ).

## 2.4 Discussion

This study examined the effects of a robot-mediated PBT with RobUST on two groups of healthy adults: one assisted and the other unassisted. The PBT training, either with or without force field assistance, led to significant improvement in balance performance, as indicated by the improvements in the ability to resist trunk perturbations in both groups. The two groups displayed muscle activity adjustments that suggest greater movement control and muscle coordination. Nevertheless, we also show differences between the adjustments made by the NF group and the FF group.

Primary evidence of improvement in both groups was the increase in force thresholds in all perturbation directions and stability area between the pretest and the posttest, Fig 2-6 and 2-7.

Reduction in muscle activity in multiple muscles as measured by iEMG, muscle activity duration and max amplitude for the different directions are suggestive of muscle coordination adjustments that improve efficiency. We saw evidence of differences in adaptation between NF and FF groups primarily for posterior perturbations, where the MOS of FF subjects after training was lower and NF subjects used the ankle strategy less often. In this paper, we have provided measurement variables that show the effect of PBT and the differences in training modes.

### **2.4.1 Balance Strategies**

Our assessment of balance strategies plays a crucial role in understanding the postural adjustments made in the presence and absence of assistive force fields. We identified a pattern of postural behaviors that belonged to either ankle or hip strategies. Perturbations were enacted as a pull on the trunk lasting 600ms. During this time, subjects' COM was forcibly moved in the direction of the force, leaving them closer to the edge of their BOS after the force was applied. They are left in a position where the COP-COM distance was already minimal, and thus the ability of subjects to generate any restoring torque using the ankle strategy was minimal. In the first 100 milliseconds, most subjects tried to use the ankle strategy but quickly changed to the hip strategy once they had been substantially displaced. Once they moved their COM within their BOS, they used the hip strategy less Fig 2-4. This difference between the early and later responses was quantified. In the first 500ms of reaction, across all conditions and subjects, the average ratio of hip strategy to ankle strategy was 2.4:1, and in the following 500ms, it was 1.4:1.

Observing the subjects individually, we noticed variation in their responses. Posterior perturbations force trunk extension uniformly in all subjects, but subjects varied in the timing and direction of movement of their lower body. Some subjects started flexion of their lower body very early and for lower forces, while others only attempted hip flexion when exposed to stronger forces. This difference could be because some had the required flexibility to flex the hips during

trunk extension and others did not. An additional mechanism used by subjects is the fast dorsiflexion of the feet. This dorsiflexion comprised part of what was classified as the hip strategy in which internally generated moments were used to move the COM. To dorsiflex about the ankles, a moment was applied to the feet, resulting in an equal and opposite moment being applied to the rest of the body. This moment rotated the body forward to a more stable position. Anterior perturbations, on the other hand, forced trunk flexion. In the first few hundred milliseconds, the subjects complied with the perturbation, rotating forward, but eventually, they reacted with an extension. At higher anterior forces, they also plantarflexed, rising to their toes. This served a similar purpose to dorsiflexion in posterior perturbations so that the forward rotation of the ankle provided an equal and opposite moment about the hips, moving it backwards towards stability.

#### **2.4.2 Effect of Perturbation Training**

Subjects in our study completed a single training session and improved their tolerance to perturbative force thresholds in all perturbation directions. Sturnieks et al 2013 [66], using observations from their waist-pull experiment, showed that the value of the force threshold is a strong indicator of the robustness of postural balance control in older adults. The authors also showed that exposing adults to repeated perturbations could improve balance control.

Subjects increased their stability area, and thus the region within which they maintained balance while being perturbed. The stability area measured the extent to which the COM could be pulled away from its neutral starting position without the subjects failing to maintain balance. It differs from postural sway during steady standing [80]–[87]. In this study, COM movement was induced by trunk perturbations. Previous studies have highlighted a positive relationship between steady postural sway in standing and an increased risk of falls. Our results indicate that the stability area was significantly larger in the posttest. This finding indicates that subjects withstood larger perturbation forces without needing to step after completing a session with the robotic PBT and

VR with RobUST. As noted in Nagy et al. 2007 [88], where older adults were subjected to an 8-week training program that included combinations of strength and flexibility, static and dynamic balance exercises, an increase in mediolateral sway resulted in an improvement in dynamic functional postural tasks, such as the Timed Up & Go Test. In this study, the participants learned to control their balance through a greater range of motion and with a greater degree of freedom, which translated to an expanded standing workspace in dynamic balance. Accordingly, we can hypothesize that the observed increase in stability area in our experiment would translate to an improvement in the ability of the subjects to maintain balance.

Reductions in muscle activity were observed along with this increased level of performance. There is evidence in the literature that repeated exposure to perturbations results in more efficient and effective postural strategies in which individuals change from a more vigorous to a less vigorous response, with fewer or different muscles recruited [89]. Specific observations support this. For example, in the posterior direction, coactivation of the L-TA/LG reduced; in the left direction, R-TA, R-LG activation duration reduced, as well as iEMG of L-TA, L-LG, L-BF, and R-LG, and the max amplitude of L-TA, R-LG, L-BF, and R-BF. Similar reductions were observed in the anterior and right directions.

Differences in the effect of training on thresholds were not observed between the NF and FF groups. This may be due to a ceiling effect, i.e., the threshold and stability area measures were at maximum levels after PBT of healthy subjects.

### **2.4.3 Effect of Perturbation Training with RobUST Force Field**

As stated above, from the literature, we expect muscle activity to decrease after repeated practice except when there is a change in strategy. Even though a number of the adjustments made by both groups were similar, there were a number of metrics in which they differed. The greatest differences were observed in the posterior direction. First, the MOS of the FF group decreased

while that of the NF group increased. MOS measures how close the body is to being in an unstable configuration thus, this result suggests that the NF group became more stable than the FF. We hypothesize that this difference results from the FF subjects learning to rely on pelvic support provided by RobUST during the training sessions. As a result, expecting the forcefield to kick in, they drift further before finally applying forces to restore balance. On the other hand, NF subjects learn to react quicker, resulting in less drift. This theory is supported by the fact that the GRF-AP MAX timing occurs earlier in the NF group after training, but is delayed in the FF group.

In this posterior direction, there was also a modification of balance strategy. Both groups spent less time using the ankle strategy after training, but there was a significantly greater decrease in NF than in FF. Furthermore, both groups used the hip strategy more after training, but this increase was primarily in the NF group, Table 2. This change in strategy use was reflected in muscle activation by a significantly greater reduction in iEMG of the R-TA in the NF group – the hip strategy activates the R-TA less [90]. From these discrepancies between the adjustments made by the NF and FF groups we can surmise that pelvic assistance by RobUST reduced the trend towards greater hip strategy use after training.

In addition, the speed of foot dorsiflexion was reduced for both subject groups, suggesting that the restoring moment generated by this movement was also reduced. This reduction was more prominent in the FF group, again pointing to reliance on RobUST support.

Across the anterior, left, and right directions, the same trend of muscle activity reduction was observed. However, this trend was not observed across as many muscles as was for posterior perturbations, and so a conclusion of more efficient muscle activity could not be made.

In summary, in the posterior direction, the percentage of time spent using the ankle strategy decreased significantly more in the NF group than in FF. The timing of the ground reaction force

maximum in the backward direction was earlier in the NF, while it was delayed in FF. Overall, our results suggest that PBT combined with a VR reaching task enhanced balance control, but the addition of an assistive force field was associated with the reduced effect of the training – less hip strategy and delayed reactions. Postural muscle adjustments were also specific and modulated after RobUST-mediated PBT, especially in the posterior direction.

In this experiment, we tested the sensorimotor adaptation of the postural control system. We found that subjects improved balance after training postural control in a VR game in the two experimental conditions tested - training with RobUST force field and training without force field. Even though both groups improved balance, differences were observed in MOS and ankle strategy parameters suggesting that the two groups adapted differently. FF group applied a balancing strategy with less MOS than the NF group and thus is likely to be the more unstable group.

The primary limitation of this study was the low amount of valid data used in the comparison between groups. This was due to the fact that the range of perturbations tolerated by subjects varied so only a narrow common range for all subjects and conditions could be found. There was also data loss because of the malfunction of recording devices. We have not tested the long-term effects of our robotic-VR training in this current study, but we hope to explore this aspect in future studies.

## **Chapter 3: Spinal Stimulation and the Measurement of Neuronal Excitability**

### **3.1 Introduction**

In the next phase of this work, we explore the effect of transcutaneous spinal cord stimulation (TSCS) on the spinal excitability of healthy, uninjured adults and the translation of these effects to postural balance control. Information is propagated through the central nervous system (CNS) by electrical signals [91], [92], and so it is plausible that external electrical stimuli can affect the system as well. Epidural stimulation has been shown to be effective at restoring functional performance but electrode implantation comes with risks and expenses of invasive surgery, and the risk of infection after surgery. TSCS being transcutaneously applied precludes these risks and therefore makes electrical stimulation treatments more accessible. We would like to explore its potential for restoring motor control in this thesis. To understand how this may happen, we will briefly summarize the workings of the CNS and introduce some of the neurophysiological tools used in our studies.

### **3.2 The Nervous System:**

The nervous system performs an enormous number of functions [93]. It can be thought of as the processing center of the human being that controls almost every body function. It organizes the body's motor control, which is our focus in this study. The nervous system is organized into two anatomically separate but functionally interdependent parts: the central and the peripheral nervous systems (CNS and PNS). Both play a role in motor control. The CNS consists of the brain and the spinal cord. These play the critical role of processing sensory input, coordinating responses, and directing motor output. The PNS consists of the network of nerves outside the brain and spinal cord that serve somatic, autonomic, and enteric functions. Of these, somatic functions are most critical to motor control. The somatic division has neurons that innervate the skin,

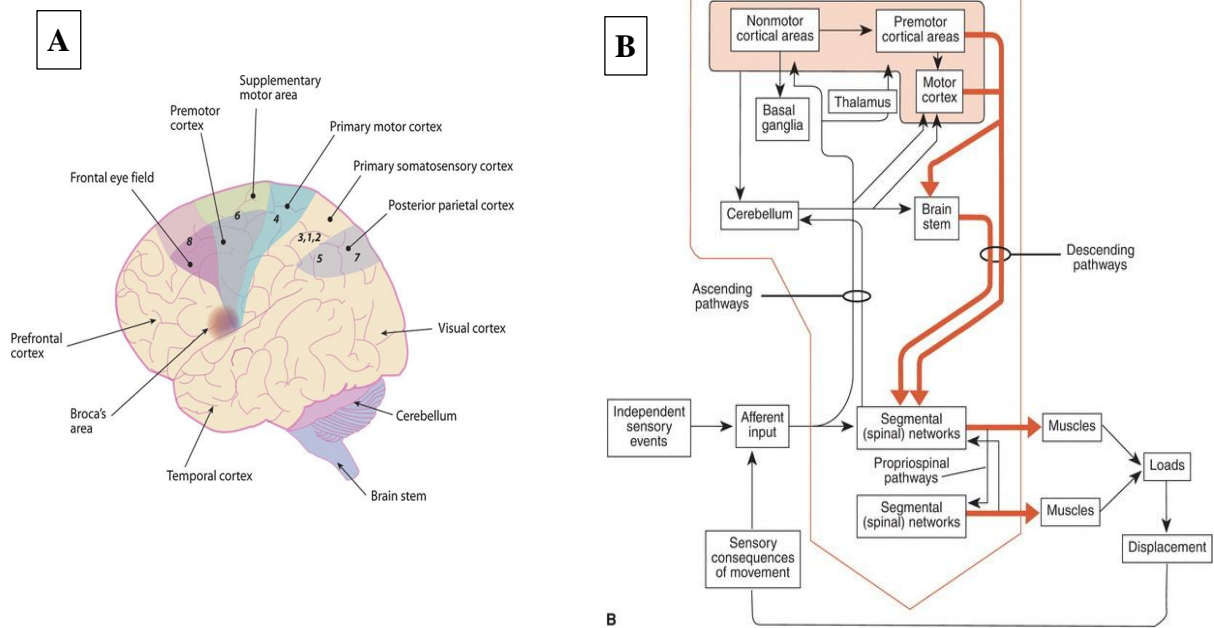


**Figure 0-1: A – Parts of the brain. Miall 2006 [95]. B - Control pathways in the brain. Shumway-Cook et al. 2014 [3].**

muscles, and joints, providing inputs such as temperature, touch, and vibratory sensation and outputs such as motor commands. From these, the body develops a sense of its physical state in space (proprioception).

### 3.2.1 The Brain and the Spinal Cord:

The nervous system (NS) is a complex system, and it is the means by which humans control their body and carry out intended actions. The system is so complex that many processes regulated by it do not rise to the conscious/voluntary control of the human actor. The motor system consists of the complex interplay of many components (nerves, neurons, synapses) and processes (inhibitory and excitatory processes). These components and processes are organized in the nervous system in a hierarchy [3], where each successive level exercises control over the level below it, and the control signals move through descending and ascending pathways. The brain is at the top of this hierarchy and, specifically within the brain, with regard to motor control, the premotor cortical areas, where motion planning and body coordination are done. Afferent and

efferent nerves that actuate and sense at the periphery are at the bottom of the hierarchy. The motor cortex, cerebellum, basal ganglia, thalamus, and brain stem all contribute to motor function. In this study, the functions of the various brain regions are not differentiated, and the resulting signals are generally referred to as supraspinal/cortical signals. Outputs from the brain descend through a pathway from the brain to the spinal cord, known as the corticospinal tract, to make synaptic connections in the spinal cord with motoneurons which innervate muscles and control voluntary movement [3], [94]. Figure 3-1A, culled from [95], shows the regions of the brain, and Figure 3-1B, from [3], is an abstraction of the nervous system showing how signals travel. Aspects of the control system model described in Chapter 1 can be seen. A controller, the motor cortex in the brain, sends outputs, e.g., movement commands, through **descending pathways** to the spinal cord, an intermediate controller. Then the spinal cord sends signals along **efferent** neurons to activate the muscles (the plant) and generate movement. Finally, sensing is achieved through **afferent** neurons.

The body has sensory organs through which it collects information about its state, such as limb position, joint position, and movement velocity, known as proprioception. This information is relayed to the brain through **ascending pathways**. Thus, the sensory system detects the consequences of muscle activation and movement and sends this information as input through **afferent** neurons both to the spinal cord and to the brain, closing the loop.

At each level of the nervous system there is an interplay between perception and action such that the brain and spinal cord process and react to input signals. Figure 3-1B illustrates how the same input stimulus is transmitted to the spinal cord and the brain, and how different parts of the brain perform their processing action on the stimulus. The spinal cord is the lowest level of the perception/action hierarchy. Supraspinal control from the brain does not control individual

muscles directly but movement patterns which are then encoded into muscle contraction signals by neurons in the spinal cord. The spinal cord also can autonomously react to stimuli by way of reflexes. Thus, the nervous system is organized both in parallel and hierarchically (in series). This organization allows the overlap of functions so that segments lower in the hierarchy take over when environmental and task conditions require [3].

Control lower in the hierarchy is typically achieved through reflexes. Reflexes are stereotyped responses to sensory stimuli, i.e., simple stimulus-action protocols saved in the spinal cord. A typical example is the knee jerk reflex which is activated by a tap on the patellar tendon. The tap on the knee activates stretch receptors which generate afferent signals that synapse in the spinal cord and then (i) homosynaptically and monosynaptically with a motoneuron that contracts the rectus femoris and (ii) heterosynaptically with a motoneuron that stretches the biceps femoris. This sequence of activations extends the lower leg quickly. [Homosynaptic connections are synaptic connections between sensory and motoneurons of the same name while heterosynaptic connections are those between synapses of different names. Monosynaptic connections are synaptic connections involving only one sensory neuron and one motoneuron.]

The “reflex arc” described, that is, the pathway in the nervous system that generates this response, is made of three kinds of neurons: a sensory neuron in the knee which is stimulated by the tendon stretch and through which the stimulus travels to the spinal cord; an interneuron, which passes the signal to a non-homonymous motoneuron (a motoneuron from a different muscle); and the motoneuron, which moves the leg through coordinated flexion and extension of various muscle groups [96]. In this sequence, although information about the stimulus and the spinal cord’s response to it is sent to the brain, the brain has no initial input to the body’s response. Thus, even at the spinal cord level, there is control of body function.

Spinal reflexes thus enable the body to respond to stimuli more quickly than when relying solely on the brain. This is because the time taken for a signal to travel from a peripheral sensor along the ascending pathways to the brain and then back down the descending pathways to the reacting muscle is longer than the time it takes to travel to the spinal cord and back. This difference is captured in the concepts of short-latency reflexes (SLR) and long-latency reflexes (LLR). Kurtzer (2015) writes that SLRs occur within 20-45ms of a sudden limb displacement and are exclusively generated by spinal networks. LLRs, which occur around 50-100ms, are believed to be mediated through spinal and supraspinal circuits [97].

Reflexes can be more sophisticated to the point of involving a network of neurons that coordinate complex rhythmic movements like swimming, walking, and hopping [98]. These low-level coordinated movements are facilitated by so-called central pattern generators organized in the spinal cord and do not necessarily rely on supraspinal input but are activated by sensory cues such as weight-bearing during walking. Some authors claim that CPGs need not be activated by sensory cues or any input at all, although they can be modulated by descending pathways [99]. Gerasimenko et al. [100], [101] demonstrated the existence of these CPGs by generating walking patterns in people with SCI lying on their sides with spinal stimulation.

Again, in this project, we are not concerned with the details of this process but operate with the understanding that movement arises from the interplay of complex neural networks which are subject to neuromodulation by certain interventions and for which the spinal cord is an important center.

### **3.2.2 Neurons**

Neurons, another name for nerve cells, are the lowest functional unit of the nervous system. The CNS and PNS together contain over 100 billion neurons of different forms suited to their individual function. Neurons are the cells responsible for sensation, transmission, and

transformation of inputs and outputs in the nervous system. Neurons have three basic parts: the cell body (soma), and two extensions, an axon and a dendrite [102]. The cell body contains organelles and is the center in which inputs are integrated. Dendrites receive inputs from axons of other neurons, and a neuron may have many dendrites. An axon is a long, thin structure that transmits the neuron's signal across a distance to other neurons. An axon can extend for up to a meter.

A characteristic attribute of a neuron that enables it to play its role is that it has a negative electrical charge at rest of  $-70$  mV. This is called its resting potential and it is caused by an unequal concentration of sodium and potassium ions ( $\text{Na}^+$  and  $\text{K}^+$ ) on the inside versus the outside of the cell. The primary function of a neuron is to pass along electrical impulses, but they don't just act as simple conducting wires. A neuron passes along electrical signals in pulses called action potentials (APs) and it only releases these APs if it receives a strong enough electrical pulse to cause the depolarization of its resting potential. The neuron only releases an action potential when the received stimulus is above a threshold. The action potential lasts only a few milliseconds, and the neuron quickly repolarizes [103]. This process is called thresholding.

Neurons receive signals from many other neurons and these received signals are integrated in the cell body. The sum total of the dendritic input to the neuron determines whether that neuron itself fires an action potential [104] and when it does, the action potential generated travels from the cell body to the end of the axon and causes the release of neurotransmitters into the synapse. A synapse is a cleft between an axon terminal of one neuron and a dendrite of another neuron. The first neuron releases neurotransmitters (chemicals) into the synapse, which causes an excitatory post-synaptic potential (EPSP) in the latter neuron once the potential in the synapse is high enough to depolarize the neuron [105].

Neurons can also be depolarized by electrical signals imposed from outside the body because their function is based on the interaction of electrical pulses. This makes them amenable to manipulation by electrical stimulation methods and are thus a critical component used in understanding the effect of electrical stimulation on motor control.

As stated previously, reflexes are used to react quickly to external stimuli. For example, they are important for responding rapidly to unexpected balance perturbations and avoiding falls. The speed, efficacy, and coordination of reflexes are therefore of interest in assessing balance control. Understanding reflexes requires knowledge of how the peripheral nervous system integrates with the spinal cord. We will consider five parts of the reflex process: sensing, transmission to the spinal cord, synapsing, transmission from the spinal cord, and muscle activation.

**Sensing:** Muscle spindles and Golgi tendon organs are two sensory receptors important to proprioception. Muscle spindles are located in the muscle belly, and through group Ia and group II afferent endings within them, relay information about the length of a muscle and its rate of change [106], [107]. On the other hand, Golgi tendons are located in series between the muscle and the tendon. They signal information about the load or force applied to the muscle and are innervated by Group Ib fibers.

**Transmission to the spinal cord:** Neurons that transmit signals from the periphery to the CNS are called afferent neurons. Among them are the Group Ia, II and Ib neurons already mentioned. These neurons can span up to one meter and enter the spinal cord through dorsal roots Figure 3-2. Afferent neurons enter the spinal cord dorsally (towards the back), which has implications for transcutaneous stimulation: being closest to the skin, they are the most easily stimulated.

**Synapsing:** Afferent neurons carrying stimuli to the spinal cord may synapse directly with a motoneuron which, if activated, sends an action potential (AP) to a muscle and causes it to contract. This is called a monosynaptic connection. They may also synapse with an interneuron, which as the name suggests, is a bridge connecting sensory and motoneurons. Interneurons perform a number of functions, including connecting to heteronymous neurons and changing the sign of the signal from excitation to inhibition. Synapsing in the spinal cord is the means by which signals can be redirected to several different action centers.

**Transmission from the spinal cord:** Motoneurons leave the spinal cord through ventral (on the side of the abdomen) roots, Figure 3-2, on their way to peripheral muscles. Activated motoneurons transmit signals along the axon body to the muscle they innervate. They are not merely transmission lines, but as they have highly branched, elaborate dendritic trees can integrate inputs from large numbers of other neurons to calculate an appropriate response to stimuli being experienced. A single muscle may be innervated by several motoneurons, which, grouped together, form a motoneuron pool.

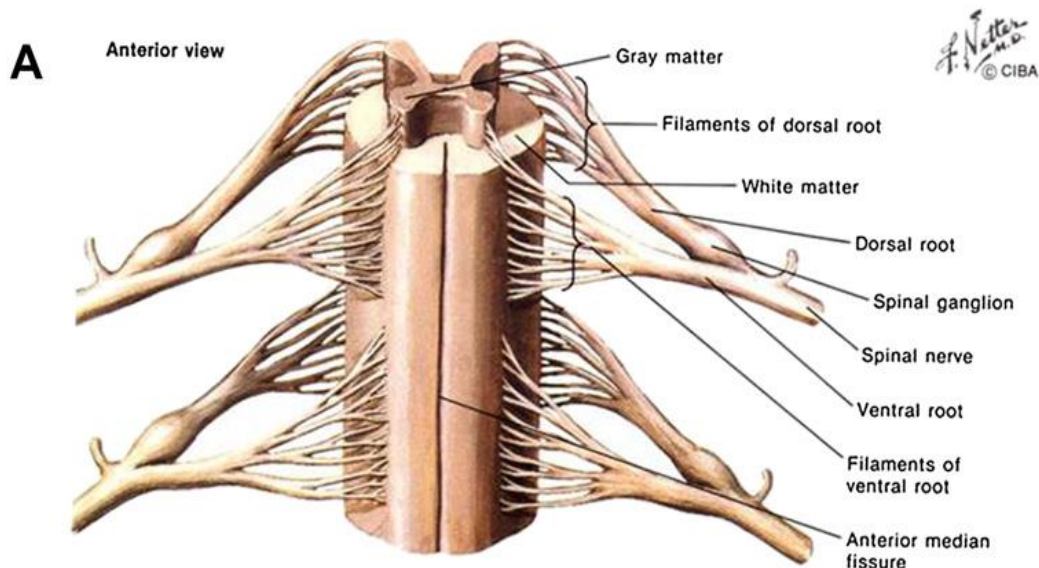


Figure 0-2: Spinal cord section showing connections to dorsal and ventral roots Bican 2013 [118]

**Muscle activation:** At the neuromuscular junction (where neurons meet the muscle) motoneurons release neurotransmitters which cause an action potential to propagate through muscle fibers and cause the muscle to contract. One motoneuron innervates a number of muscle fibers which, grouped together, are called a motor unit.

The interconnectedness of neurons permits the quick triggering of actions in various parts of the body which allow for some interesting phenomena that will be important for this project.

### **3.3 Electrical Stimulation**

As we have discussed so far, the nervous system operates through the conduction of electricity. Thus, it is logical that the imposition of an electrical charge from an external source will affect its operation. Electrical stimulation of the body has been directed to beneficial use in hearing aids, cardiac pacemakers, motor control, nerve regeneration, electro-anesthesia, and many other applications. Most promising of all for motor control is the use of electrical stimulation to delay muscle degeneration, promote nerve cell regeneration [108], promote the generation of new spinal pathways [101], promote functional recovery, reduce spasticity, ameliorate movement disorders like bradykinesia or dyskinesia and many more applications. Electrical stimulation has been used specifically to restore mobility in impaired individuals. For example, rehabilitation with one 30 min session of TSCS was shown to enhance walking speed and endurance in patients with multiple sclerosis [109]. In another study, refined, task-specific movement was restored after having no volitional muscle activation in a chronic motor complete paraplegic patient after 3.7 years of activity-based intervention using spinal cord epidural stimulation [110]. These and many other works prove the effectiveness of electrical stimulation.

In the field of motor learning, electrical stimulation aims to induce the body into a neuroplastic state in which there can be neuromotor learning. Spinal cord injury is one condition in which this

property of the human body can be used to improve the condition of the patient. In SCI, there is a disruption of the descending signals from the cortical centers as they travel to the actuating muscles with ventral roots below the injury. These patients thus lose volitional control below the lesion, and rehabilitation aims to restore some of the lost control. Scientists have therefore experimented with using epidurally placed electrodes to stimulate afferents to drive voluntary and autonomically controlled motor responses and have shown benefits in promoting functional recovery [111], [112].

In epidural spinal cord stimulation, electrodes are surgically implanted in the epidural space. When an electric pulse is applied, the electrodes excite large to medium-diameter afferent fibers in the area which engage spinal circuits. The result is the recruitment of these posterior (dorsal) root fibers, sensory fibers, which trans-synaptically activate motoneurons in the spinal cord [113], [114]. When the stimulus is strong enough, activation of the motoneurons results in compound muscle action potentials in the muscles innervated by the nerves stimulated and may cause muscle twitches. These are called posterior root muscle (PRM) reflexes as they are reflexes generated by stimulating afferents in the posterior root.

But epidural stimulation has many drawbacks. Implantation of the electrodes requires an invasive and risky surgery, and the connecting cables that run out of the body are fertile ground for infection. It has subsequently been found that electrodes placed paravertebrally on the skin could elicit these root-evoked spinal reflexes. This approach is called transcutaneous spinal cord stimulation (TSCS) and in it, one electrode is placed paravertebrally, and the complementary electrode is placed on the abdomen. TSCS is noninvasive, eliminating the significant risk involved in surgical implantation, and it is safe, opening up electrical stimulation studies to less severely impaired and even healthy individuals. In the literature, it has been shown that TSCS has similar

neuromodulatory effects as epidural stimulation, although their electric field distributions differ. In TSCS, current is conducted through layers of muscle and skin; therefore, its distribution is widespread but is still effective at exciting posterior roots [113].

TSCS also excites spinal interneurons (neurons within the spinal cord that connect to other cells in the spinal cord), which have been identified as a center of plasticity in SCI recovery [115]. Although these are located further interior to the body than posterior root afferents [100], they are made more excitable by TSCS, allowing action potentials to be triggered more easily by descending cortical signals. This is especially useful in SCI where only low levels of the cortical signals arrive below the lesion.

The desired effect of TSCS's excitatory actions is to induce spinal cord neuroplasticity. Although the mechanism by which this happens is not fully understood [100], [113], plasticity has been observed as the reconfiguration of neural networks, the recruitment of rhythmogenic sources (e.g. central pattern generators that trigger walking patterns on receiving certain sensory input), the exploitation of silent or newly sprouted connections [100], and in SCI, as the coaxing of cortical and subcortical axons across the lesion, and the rewiring or strengthening of spared connections [115]. In addition, spinal interneurons contribute to plasticity by forming novel neuronal pathways, synapse remodeling, or strengthening existing pathways [115].

### **3.4 Transcutaneous Spinal Cord Stimulation (TSCS)**

TSCS is a non-invasive analog to epidural stimulation in which paravertebral electrodes stimulate posterior root afferents and spinal interneurons, which can trigger PRM reflexes. Prolonged exposure to TSCS has the potential to induce neuroplastic changes, which can be harnessed for the treatment of patients with neuromotor disorders. In this work, we attempt to characterize the effect of TSCS in healthy subjects in a number of settings in order to lay a

foundation for future work with SCI patients. Although the nervous systems of the two populations differ greatly (e.g. loss of sensory signals, loss of motor control, spasticity in SCI patients), knowledge gained from the control of the uninjured system can be used for the injured one [100].

When the intensity of a spinal pulse in TSCS is high enough, it is capable of causing muscle twitches. The aim of this work is not so much to use stimulation to cause muscle movement but to raise the baseline excitability of the networks generating sensorimotor functions closer to the motor movement threshold. If this is achieved, it is theorized that the repeated performance of motor tasks in this state could lead to extensive sensorimotor learning in the networks that become engaged, which may cause improvements in the presence of neuromodulation to persist [100]. Sub-movement-threshold stimulation is thus used during interventions with TSCS. Although weak, the electric field causes small depolarizations in the afferent neurons, making them more easily triggered by supraspinal inputs. In addition, this stimulation is able to cause enough depolarization in the neurons to affect their biophysical properties and modulate synaptic transmission.

The amplitude, pulse width, and frequency of TSCS stimuli determine the amount of charge delivered and must be monitored to ensure that stimuli are tolerable to a subject. This work used a pulse width of  $500\mu\text{s}$  with monophasic pulse profile for all transspinal stimulation. Motor responses were produced using currents between 30mA and 70mA for most subjects. These super-threshold stimuli were given as individual pulses. Continuous TSCS current given during the intervention was between 5 and 10mA and at a frequency of 30Hz, just enough to cause paresthesia in the subjects. This frequency has been used in a number of studies when the intention was to boost motor response, while a frequency of around 60Hz is prescribed for treating spasticity [116], [117].

Since the profile delivered was monophasic, only one of the electrodes became polarized while the other was the ground. The polarized electrode, the anode, was a single electrode and it was placed longitudinally over the L2-L3 intervertebral space. The cathode was placed on the abdomen. Most studies place the electrode between T11-T12; however, initial testing demonstrated that it was challenging to evoke motor responses at that level but much easier at the L2-L3 level.

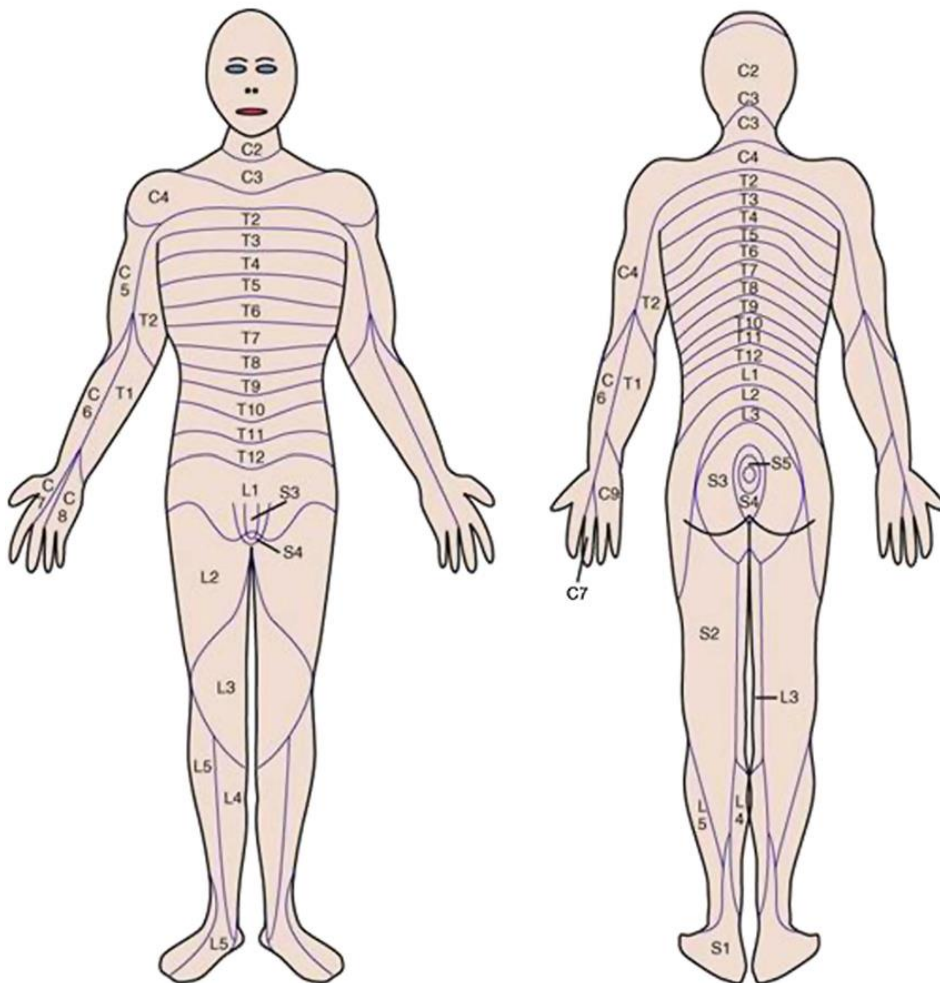


Figure 0-3: Innervation of the body [118]

Dermatome figures [118], [119] (Figure 3-3) show the segments of the body innervated by the bundles of spinal nerves and the segments of the spinal column from which the nerves emanate. The electric field generated with TSCS is widely dispersed and even though electrodes are placed

between L2 and L3, spinal nerves from many segments are stimulated by the field. PRM reflexes were generated in the left and right tibialis anterior, lateral gastrocnemius, rectus femoris, bicep femoris, and soleus muscles from this position in the experiments we conducted, Figure 3-4.

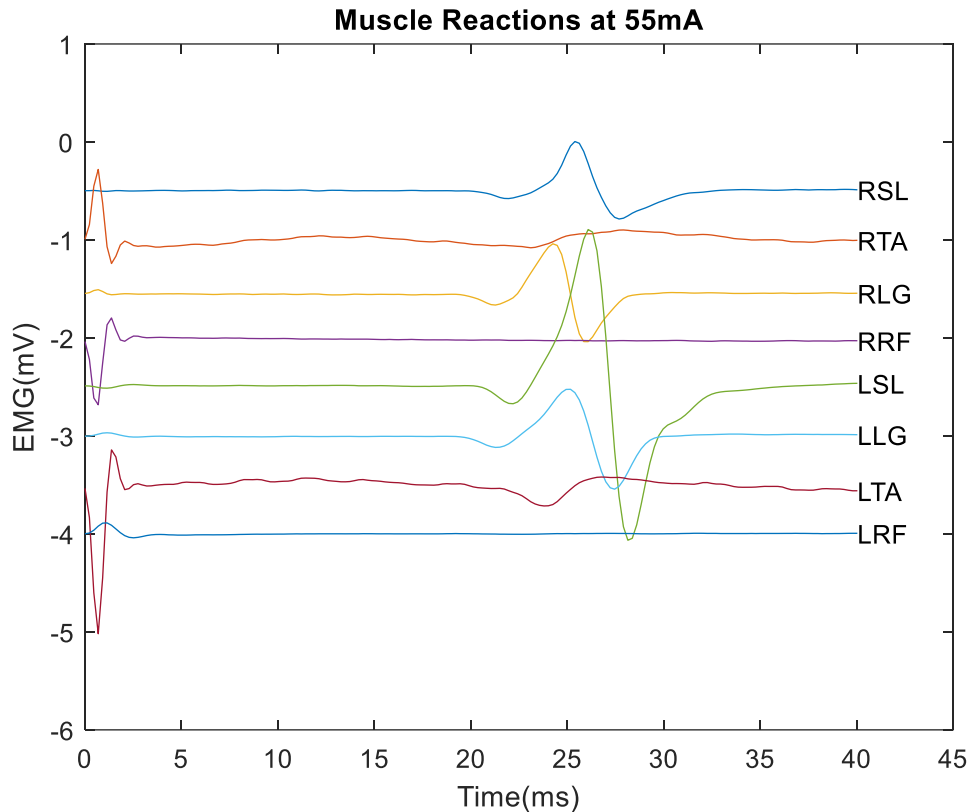


Figure 0-4: : Sample EMG readings of the right (R) and left (L) soleus (SL), tibialis anterior (TA), lateral gastrocnemii (LG), rectus femorii (RF).

### 3.5 Testing the Effect of TSCS

Neurophysiological tests have been developed to detect changes to the functioning of the spinal circuits caused by electrical stimulation or exercise. The tests used in this study assess the excitability of various stages of the neural conduction pathways. They are discussed below:

#### 3.5.1 PRM Reflex Thresholds

Posterior root muscle reflexes are evoked by stimulating afferents that enter the posterior root. In the literature, the threshold current of a muscle is the current that generates an evoked potential peak-to-peak amplitude of 100  $\mu$ V [113]. Thus, we can establish this threshold as a property of a

subject that describes the amount of stimuli required to excite a PRM reflex in that particular subject.

Several neural processes contribute to the generation of a PRM reflex, so an observed change cannot easily be ascribed to a cause without further investigation. TSCS, by nature, has a dispersed electric field and can stimulate multiple afferent fibers from various lower extremity nerves. Stimulation of an afferent fiber is expected to induce a response in the homonymous motor efferent fibers, but there are also heteronymous monosynaptic connections that excite PRM reflexes in a muscle. That is to say, for example, that stimulating the spinal nerve at L2 could heteronymously evoke motor potentials in the efferent nerve at L3. Therefore, changes to the PRM reflex threshold could change the motoneuron pool excitability of various posterior roots [120], [121], making the exact change location difficult to pin down.

### **3.5.2 H-Reflex**

H-reflexes are physiologic processes in which muscle contractions are induced by electrical stimulation of a sensory nerve at a point farther away from the spine than PRMs and closer to the innervated muscle. They were first clearly described by Hoffmann in 1918, hence the name. This study focuses on H-reflexes generated in the soleus muscle, but the literature describes H-reflex generation in as many as 20 other muscles [122]. In general, H-reflexes can be stimulated in muscles innervated by relatively superficial nerves.

An H-reflex is generated in the soleus muscle by stimulating the tibial nerve at the popliteal fossa of the knee. The tibial nerve is a compound nerve containing both sensory and motor neurons. Electrical stimulation of sufficient charge excites the sensory afferents of the tibial nerve, bypassing the muscle spindle. This signal is routed to the spinal cord and projected back onto the motoneurons of the same tibial nerve, exciting the soleus muscle. The excitation may be detected on electromyographic (EMG) recordings, with or without grossly visible muscle contraction. This

“long” latency signal (~ 30ms) [123] is the H-reflex. Electrical stimulation at the popliteal fossa also directly stimulates the motoneurons of the tibial nerve. This motoneuron stimulation shows up as a “short” latency (~10ms) [123], [124] burst on an EMG recording and is called the M-wave for motor response. Therefore, the overall response of the tibial nerve consists of both the M-wave and the H-reflex, Figure 3-5.

The H-reflex can be considered a tool to measure the excitability of the neural components of

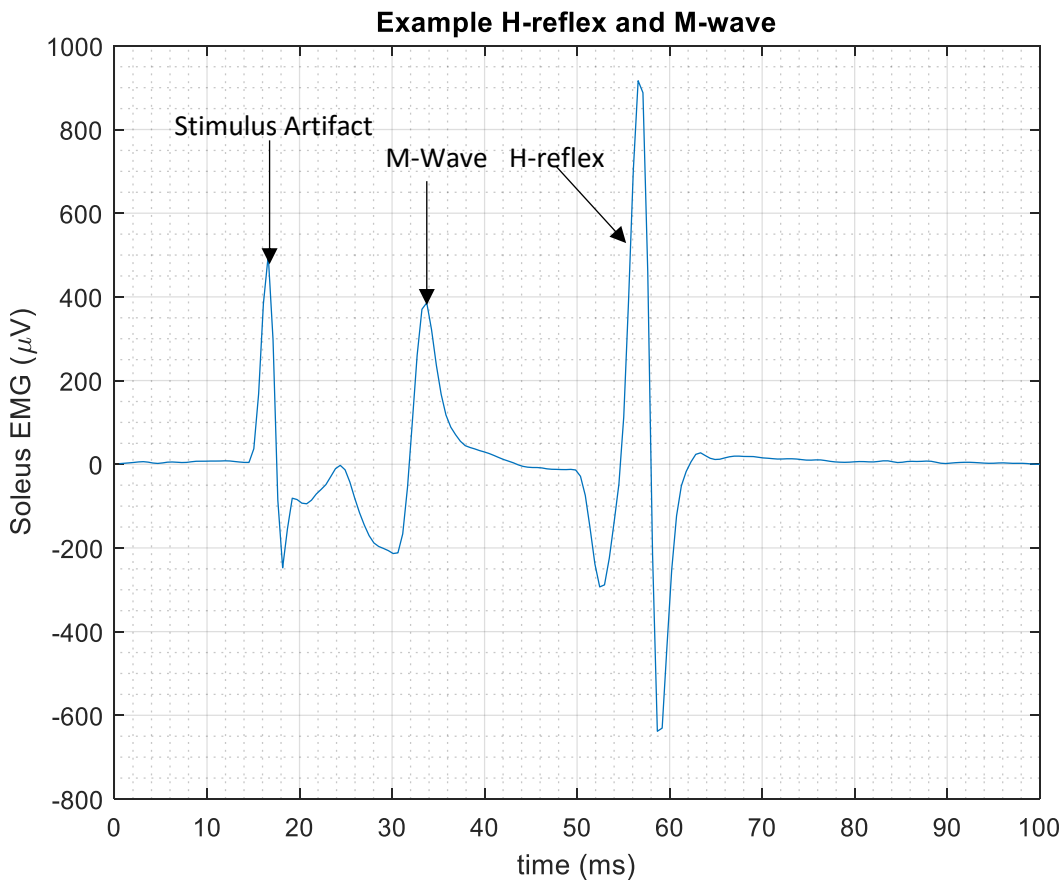


**Figure 0-5: A - Artifact of electrical stimulus; B - M-wave; C - H-reflex**

the arc through which it excites [122]. It is thought that the reflex is predominantly made up of monosynaptic projections of group Ia afferents on the homonymous motoneurons, and so the reflex can be summarized as having the following steps: conduction of an electric stimulus by sensory neurons; monosynaptic transmission across the spinal cord; and excitation of motoneurons. In this

simple model, changes in the H-reflex would be ascribed to changes in one of these steps. Nevertheless, it is known that the H-reflex includes oligosynaptic (“oligo” meaning more than one) contributions from other large-diameter afferents. This makes it difficult to interpret changes in the H-reflex [122], [125], [126], similar to the previously described difficulty with interpreting changes in PRMs. In addition to the contribution of other afferents, other processes that affect the size of an H-reflex include presynaptic inhibition, homosynaptic depression (treated in the next section), and antidromic collision. In the literature, an enhanced H-reflex after an intervention is interpreted as an enhancement in motoneuron excitability and/or reduced presynaptic inhibition [122], [124], where motoneuron excitability refers to the excitability of the entire pathway. Other processes contribute less as, for example, the effect of homosynaptic depression occurs only after an initial conditioning stimulus and that of antidromic collision is not subject to change [126]. The H-reflex can thus assess motor excitability changes due to training and/or stimulation.

#### *3.5.2.1 Generation of the Tibial Nerve H-reflex Recruitment Curve*

A plot of the amplitude in Volts of the H-reflex response against a range of stimulating currents is called an H-reflex recruitment curve. The accompanying m-wave response is also usually plotted. An H-reflex is generated by stimulating the tibial nerve at the popliteal fossa, and the amplitude measure is read off the Soleus EMG.

The electrical pulse depolarizes sensory nerves at low currents without depolarizing the motoneurons because motoneuron fibers are thicker than the group Ia sensory neurons. The pulse generates an EPSP in the sensory neuron that is transmitted to the spinal cord. It synapses there and generates an AP in the motoneuron that is picked up in the muscle. As noted earlier, this long latency reflex is recorded as the H-reflex. This can be seen in Figure 3-6 where low currents (above

5mA and below 15mA) only generate an H-reflex and no M-wave. Once the stimulating current is beyond the depolarization threshold of the efferent fibers, an m-wave can be generated.

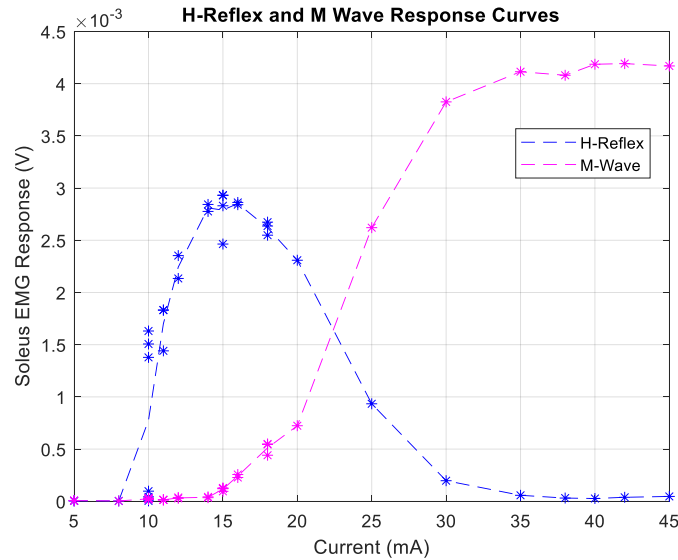


**Figure 0-6: Sample H-reflex recruitment curve. \* represents points H-reflex curve and \* represents points on the M-wave curve**

Higher currents directly stimulate both sensory and motor neurons, generating an H-reflex as with low currents. Alongside this, orthodromic (signal propagation in a neuron in the correct direction) and antidromic pulses are generated in the motoneuron. The orthodromic signal travels to the muscle and is picked up on EMG recordings as the M-wave, while the antidromic signal travels towards the spinal cord and collides with the reflexive signal generated by the sensory afferents. This collision cancels out a portion of the reflexive signal, and the resultant sum proceeds to the muscle and is recorded on the EMG as the H-reflex. Hence as stronger and stronger m-waves are generated, the antidromic signal increases in magnitude and cancels out a larger portion of the H-reflex and so the amplitude of the H-reflex plateaus and diminishes [123], [127].

The m-wave increases with increasing stimulation current until it reaches a maximal value and plateaus at Mmax. Mmax is said to represent maximum muscle activation engendered by the activation of the entire motoneuron pool [123].

The H-reflex recruitment curve is usually reported as a ratio of Mmax, i.e., it is normalized by Mmax. Mmax is the m-wave response when the entire motoneuron pool is activated, and therefore it is a value that can be attained with some repeatability and is thus a good benchmark for normalization as experimental inconsistencies like the variation in placement of electrodes and their reduction in conductivity may be eliminated. If there are actual changes to the motoneuron pool and therefore, neuromodulatory changes in the Mmax value, the H-reflex will also excite the same motoneuron pool so such changes will also be reflected in the H-reflex. In this scenario, normalizing by Mmax would make the H-reflex a measure of the excitability of the arc, excluding the motoneuron pool.

To compare changes in the H-reflex recruitment curve between test conditions, it is parameterized by fitting it to a sigmoid function [128], [129]. Klimstra and Zehr [129] show that a sigmoid function is the most reliable estimate for the ascending limb of the recruitment curve. It also emulates the threshold activation and saturation pattern of a neuron. Both the H-reflex and M-wave are fit and assessed with a sigmoid of the form:

$$R(s) = \frac{R_{max}}{1 + e^{R_{slp}(s_{50}-s)}}$$

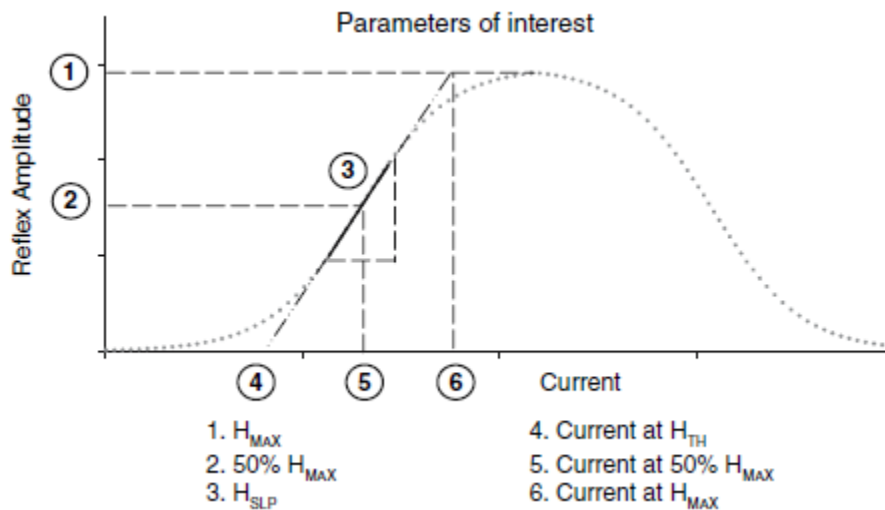


Figure 0-7: Typical H-recruitment curve profile. Klimstra 2007 [129]

$R(s)$  is the H or M response amplitude which is a function of  $s$ , the current;  $R_{max}$  is the  $H_{max}$  or  $M_{max}$ ;  $R_{slp}$  is the slope of the ascending limb at 50%  $R_{max}$ , and  $s_{50}$  is the current at 50%  $R_{max}$ . Figure 3-7 marks some of these important features on the H-reflex recruitment curve.

In this study, experimental data are fitted to this function using the MATLAB ‘fit’ function. If fitting was successful, the function gave  $R_{max}$ ,  $R_{slp}$ , and  $s_{50}$ . These parameters characterize the recruitment curve and can be used to compare recruitment curves across conditions.

### 3.5.3 H-Reflex Recovery Cycle

Presynaptic inhibition and homosynaptic depression are phenomena that reduce the amplitude of an H-reflex response when a nerve is stimulated multiple times in quick succession. Various authors term this reduction “low-frequency depression,” others “homosynaptic depression,” and still others “post-activation depression (PAD)” (Clair 2011). This work will refer to the phenomena simply as depression while reserving homosynaptic depression for a more specific aspect of this

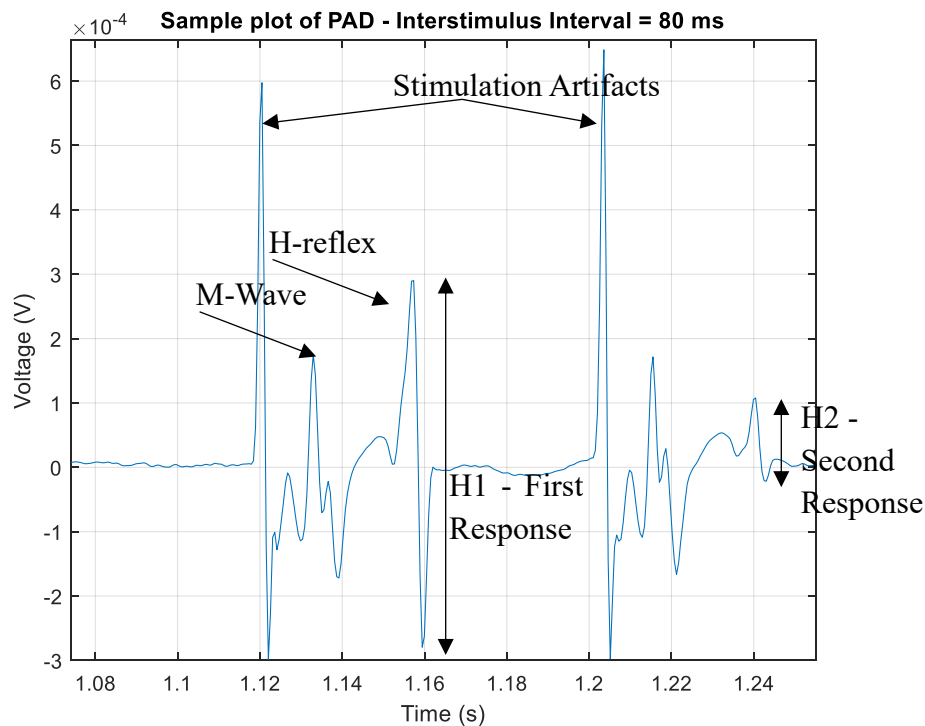


Figure 0-8: Paired pulse response of soleus.

effect. H-reflex depression is noticed in humans when the frequency of stimulation is above 0.1Hz (Clair 2011) –when a second stimulus is enacted within 10s of an initial one, Figure 3-8.

Several studies have attempted to characterize H-reflex depression and its time variation in plots called the H-reflex recovery cycle [130]–[133]. Researchers have suggested several mechanisms that cause facilitation and inhibition at certain time intervals, but there is no consensus among them. The H-reflex recovery cycle is characterized by a period of facilitation in the first 10ms, strong presynaptic inhibition at 25-75ms, a period of facilitation and incomplete recovery between 75 and 300ms, peaking around 250ms, and slow recovery to the level of the first stimulus for the next 10-15s [130]–[132].

This attenuation of the H-reflex is helpful because, at any given time, many sensory stimuli are crashing against the body. The body has to manage this and focus on the most important ones. The CNS uses presynaptic inhibition to limit the amount of incoming information, and this process has been observed in various situations and from multiple sources. For example, during passive movements of one limb, there is inhibition of the H-reflex in the other limb [126]. Inhibition also happens during body position changes, while tonic contraction is retained in a muscle, or while thinking of a movement [122]. It is used to suppress afferent inflow of background stimuli so that the CNS can concentrate on relevant afferent input [134]. Presynaptic inhibition in the nervous system is achieved through inhibitory neurons which suppress the sensory afferent signal before it is transmitted across the synapse. Thus, the post-synaptic neuron only receives a lower signal than experienced by the sensory neuron. The strength of presynaptic inhibition starts to wane at 75ms, and it runs its course within 400ms [132], [135]

The persistent depression observed after the effect of presynaptic inhibition is over is attributed to the depletion of neurotransmitters such that the probability of neurotransmitter release

from a previously active Ia afferent terminal is decreased [120], [135]. This reduced firing probability is called homosynaptic depression and is attributed to H-reflex depression beyond 250ms.

Because there are many sources of presynaptic inhibition and the role of homosynaptic depression is poorly understood [126], it can be difficult to interpret changes in the H-reflex recovery cycle. Nevertheless, improvements in balance control have been associated with more presynaptic inhibition [136]. Nielsen and Hultborn showed that well-trained ballet dancers have more presynaptic inhibition than non-ballet dancers [137], indicating, reasonably, that presynaptic inhibition is used to eliminate unwanted reflex responses so that muscles can be more steadily controlled. As shown in monkeys, presynaptic inhibition is amenable to plastic changes that lead to better task performance [125].

Changes in homosynaptic depression, on the other hand, could be interpreted as changes in the neuron's ability to release neurotransmitters. Homosynaptic depression is situation-dependent, as it has been observed to disappear during running. Additionally, when a subject is exposed to continuous stimulation, homosynaptic depression is eventually eliminated. This points to a certain priming effect and perhaps can be interpreted as the body meeting the demands of the task at hand.

In this chapter, we have treated the background necessary for understanding electrical stimulation, particularly TSCS, and its potential effects on the human body. We have also discussed tools that are used to detect changes to the human body's neurophysiology, which can indicate plasticity generated by stimulation. The following chapters treat two experimental studies carried out on healthy subjects that aimed at achieving a greater understanding of the effect of TSCS on the neurophysiological and balance characteristics of the subjects in two scenarios.

# **Chapter 4: Effect of Transcutaneous Spinal Stimulation Applied During Quiet Lying on Balance and Neurophysiological Characteristics**

## **4.1 Introduction**

Transcutaneous spinal cord stimulation (TSCS) and its effects were discussed in the previous chapter. TSCS has potential applications in treating several pathologies, but in the literature, it has been used primarily for improving sensorimotor function in spinal cord injury (SCI) patients [138]. It functions by exciting sensory afferents in the dorsal roots (posterior roots) so that when the current is high enough, it causes depolarization of the neuron, generating excitatory postsynaptic potentials (EPSPs) that homosynaptically and heterosynaptically generate action potentials in motoneurons that cause muscle contraction [139]. The action potentials transmitted to the motoneurons are called posterior root muscle (PRM) reflexes as they are reflexes activated across synapses generated by stimulating sensory afferents [120], [121] in the posterior root. Prolonged exposure to TSCS has been shown to lead to plastic changes in the nervous system [117], [140]. These changes include increases in motoneuron excitability, reassignment of neural pathways, strengthening of synaptic connections, and the modulation of presynaptic inhibition. These potentially beneficial effects of TSCS have been used by researchers to generate walking patterns in humans [101], and to facilitate loaded walking with exoskeletons [141] in SCI patients, among other applications. The mechanisms that lead to plastic changes and that translate these changes to sensorimotor improvements are complex [100]. However, understanding them is vital to designing training programs that boost recovery in SCI, stroke, and other pathologies and that improve the performance of athletes and dancers.

This chapter details an attempt to understand the effect of TSCS on the neurophysiological and balance characteristics of neurologically intact healthy subjects. A number of studies have

looked at particular aspects of the effect of TSCS on healthy subjects. For example, Hofstoetter et al. and Kawaishi et al. studied the recovery cycles of the posterior root muscle reflex [120], [136], and Inanici and Meyer studied its use in enhancing motor control [109], [142], [143]. But to this author's knowledge, none have characterized the effect of TSCS on balance in healthy subjects. Awosika et al., among others, studied the effect of transcutaneous spinal direct current stimulation (TSDCS) and balance training and showed that this combination could improve walking speed when walking backward [144]. This study examines the effect of TSCS on balance.

The intervention in this study was a sole 30min session with continuous TSCS applied to a supinated subject. Balance and neurophysiological measures were taken before and after the intervention and compared. Balance tests were carried out as in Chapter 2, with perturbations and balance measures taken similarly. The neurophysiological measures used are the parameters of the H-reflex recruitment curve, H-reflex recovery at different interstimulus intervals (ISI) and the PRM threshold described in Chapter 3.

We hypothesized that TSCS would lead to increased motoneuron excitability which in turn would cause an increased H-reflex response and a lower PRM threshold. We also hypothesized that these increases would be retained by the subjects and lead to increased muscle activity during the balance tests and better balance performance.

The hypotheses are justified by studies that have shown that electrical stimulation can selectively activate spinal locomotor networks [145], increases the H/M ratio (ratio of maximum H-reflex to maximum M-wave amplitude) [124], and induces plastic effects in the spinal cord [100], [101]. There is the potential that these plastic changes lead to sensorimotor improvements. We also explored the possibility that this induced, heightened neuroplasticity could lead to balance improvements.

## 4.2 Methods

### 4.2.1 Devices

#### 4.2.1.1 Robotic Upright Stand Trainer, RobUST

We conducted the experiments in RobUST, the Robotic Upright Stand Trainer. RobUST's design and operation were described in Chapter 2, and we used its trunk perturbation



Figure 0-1: RobUST with subject strapped in

mode for this experiment. We collected motion capture data using a nine-camera Vicon motion capture system (Vicon, Denver). Retro-reflective markers were placed bilaterally on the big toe, fifth metatarsal, lateral malleolus, heel, lateral femoral epicondyle, ASIS, PSIS, acromion, elbow and wrist. This marker set was used to generate the subject's center of mass (COM) based on the method in [146] and the anthropometric measurements of de Leva in [147]. Ground reaction forces were collected with two six-axis force plates (Bertec, Columbus, Ohio), one for each foot. The data from these two force plates were used to compute the combined foot center of pressure location. Both marker position and center of pressure data were smoothed with a 0.1s moving average window. EMG data were collected bilaterally from 10 muscles: soleus (SL), lateral gastrocnemius (LG), tibialis anterior (TA), bicep femoris (BF), and rectus femoris (RF).

## 4.2.2 Digitimer Stimulator

The Digitimer DS7A Constant Current Stimulator was used to pass electrical stimuli to subjects. This instrument can generate pulsed stimuli of up to 100mA current, with pulse widths of 50, 100, 200, 500, 1000, and 2000 $\mu$ s. This study used the 1000 $\mu$ s pulse width when stimulating the tibial nerve to generate H-reflexes and the 500 $\mu$ s pulse width when stimulating the spine. The device can be triggered externally and can also be set to produce trains of pulses at several frequencies. During continuous stimulation, a DG2A trigger generator (Digitimer, North America, Florida) was used to send pulses at 30Hz to the subject.

### 4.2.2.1 Stimulator App

Synchronization between the Digitimer DS7A stimulator and the recording EMGs was achieved through a custom MATLAB application (The MathWorks Inc., 2020) and a Particle Photon microprocessor. This app-photon setup sends single digital triggers to the DS7A stimulator that instructs it to send a stimulating pulse to the subject. The app then records the EMG activity from the muscles being monitored. In addition, the app allowed us the flexibility of having many recording modes tailored to particular protocols. This streamlined the data collection process. Some implemented modes were:

**H-Reflex Recruitment Curve:** To build an H-Reflex recruitment curve, we needed to collect stimulation responses over a range of current values, measure the peak-to-peak amplitudes of the H-reflex and M-wave responses and plot them on a current vs. amplitude graph. For each current, the app triggered a single pulse which stimulated the subject. 300ms of the response from the soleus muscle was recorded, and the app displayed this data. We manually identified the M-wave and H-reflex sections of the response and measured, recorded, and plotted their peak-to-peak height allowing us to detect peak H-reflex M-wave responses in real time and use them as event markers.

**H-reflex Recovery Cycle:** The recovery cycle was assessed by applying paired pulses to subjects. The app generated these paired pulses at set inter-stimulus intervals (ISI). The initiation of paired pulses also triggered the recording of EMG data so that the response was captured.

**Posterior Root Muscle Reflexes:** With PRMs, the aim was to find the current which generated muscle activity above 50  $\mu\text{V}$  in the LSL or RSL. The app triggered the stimulator, recorded activity from all the lower body EMGs, and displayed the record. The magnitude of the response was then measured after each stimulation pulse by selecting the region in which the response appeared on one muscle. This region was approximately the same as in all the other muscles recorded. The peak-to-peak height of the responses were measured, and a determination was made on the next step in the protocol.

### 4.2.3 Subjects

Study protocols and consent forms were approved by Columbia University (IRB-AAAR6780). Eight healthy subjects, five males (Mean  $\pm$ SD) age: 25.6 $\pm$ 4.5 years; weight: 70.78 $\pm$ 3.03 kg; height: 1.72 $\pm$ 4.92 m and three females (age: 30.7 $\pm$ 1.2 years; weight: 69.75 $\pm$ 7.63 kg; height: 1.67 $\pm$ 9.9 m) participated in this experiment.

### 4.2.4 Experimental Protocol – Study Design

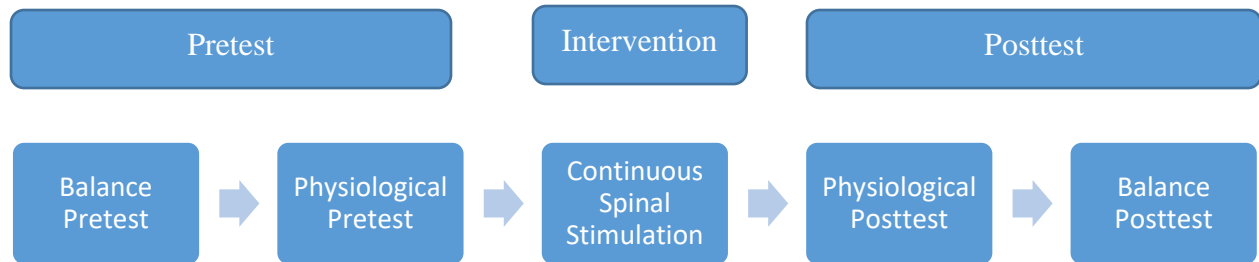


Figure 0-2: Flow Diagram of the experimental procedure

To measure the effect of stimulation on muscle activation and balance characteristics we structured our experiment as shown in Figure. 4-2. We assessed both kinematic and EMG balance measures before the intervention and assessed those same properties after the intervention.

#### **4.2.5 Balance Tests**

Balance was assessed by perturbing the subjects. Subjects were perturbed in RobUST at the trunk in the four cardinal directions – anterior, posterior, right and left - without any support at the pelvis. They were perturbed three times each at five perturbation force levels which ranged from 30% to 50% body weight (BW) in the anterior direction, and 40% to 60% in the posterior, right, and left directions in steps of 5%. The perturbation profile was a short trapezoid with a 150ms ramp up, 300ms at the set force and 150ms decay time. Perturbations forces were progressed from lowest to highest but perturbation direction was randomized. Both balance pretest and posttest were conducted in this same way.

Motion capture, force plate, and EMG data were collected during the experiment and analyzed offline. A record of whether the perturbation trial was successful or not was kept for each perturbation. A successful trial was one in which the subject did not lose balance, raise a foot or slide their foot to expand their base of support after being perturbed.

#### **4.2.6 Neurophysiological Tests**

H-Reflex, post activation depression, and posterior root muscle reflex assessments were carried out.

#### 4.2.6.1 Procedure for H-Reflex:

The H-Reflex is a tool for assessing spinal circuits. Its properties have been described in section 3.4.2. H-Reflex was assessed by generating a subject's H-reflex recruitment curve, a current vs response amplitude plot. An H-reflex was generated by stimulating the tibial nerve with 1000 $\mu$ s monophasic pulses. Natus disposable tab adhesive electrodes connected to the DS7A stimulator were used to stimulate the nerve with the cathode placed in the popliteal fossa, and the anode just above the knee cap, Figure 4-3. The area on which the

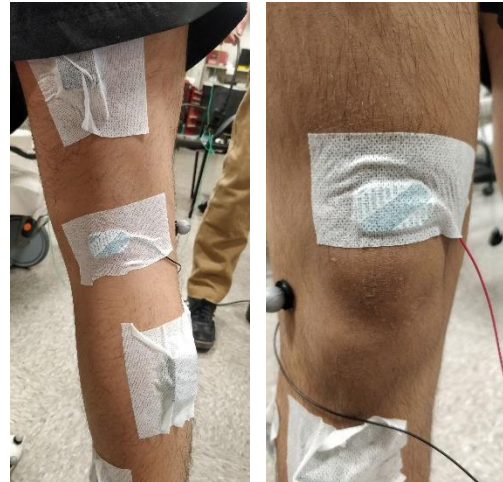


**Figure 0-3: Electrode placement for stimulating an H-reflex from the tibial nerve. Left: Cathode placed in the popliteal fossa; Right: anode placed above the knee cap**

electrodes were placed was cleaned with rubbing alcohol and then with Nuprep Skin Prep Gel (Weaver and Company, Aurora, CO) before the electrodes were placed. To generate the recruitment curve, we followed the steps below:

1. Start stimulating current at 5mA, increase in steps of 5mA, and record each stimulus's H-reflex and M-wave magnitude.
2. After the H-reflex amplitude reaches its peak and starts to decrease, start stimulating again from 5mA but this time stimulate twice at each current and increase current in steps of 2mA. This was done to record enough data points for fitting the ascending limb of the H-reflex recruitment curve to a sigmoid function.
3. Once intermediate data points on the ascending limb have been filled, continue with the descending limb of the H-reflex in steps of 5mA, stimulating once each time, until the maximum M-wave amplitude,  $M_{max}$ , is reached.  $M_{max}$  is reached when three consecutive stimulus responses are within 10% of each other.

Through all these steps, subjects lay supine on a bed in a comfortable position. Data collected here was used to generate the recruitment curve and determine the current for generating the H-reflex recovery cycle.

#### 4.2.6.2 Procedure for H-reflex Recovery Cycle

The H-reflex recovery cycle was generated by stimulating the tibial nerve with paired pulses, using the same electrode placement used to elicit single H-reflexes. The paired pulse's current was chosen as that current that would generate approximately 30% of Hmax on the ascending limb of the recruitment curve. Subjects were positioned similarly on a bed. 80, 150, 250, 500, and 1000ms inter-stimulus intervals (ISI) were assessed, and each ISI was tested five times.

#### 4.2.6.3 Procedure for Posterior Root Muscle Reflexes

When eliciting PRMs, the cathode was placed between the L2-L3 vertebrae and the anode para-umbilically on the lower abdomen, Figure 4-4. The anode was a 40mm x 50mm surface area Natus disposable electrode, SKU: 019-409100 (Natus Medical Incorporated, San Carlos, CA), and the cathode was a 2" x 4" surface area disposable electrode, SKU: 019-422200. 500 $\mu$ s monophasic pulses were used. All lower limb EMGs were monitored and the subjects lay on a bed in the supine position. Stimulation currents were progressed according to the following protocol in order to find a threshold of activation:

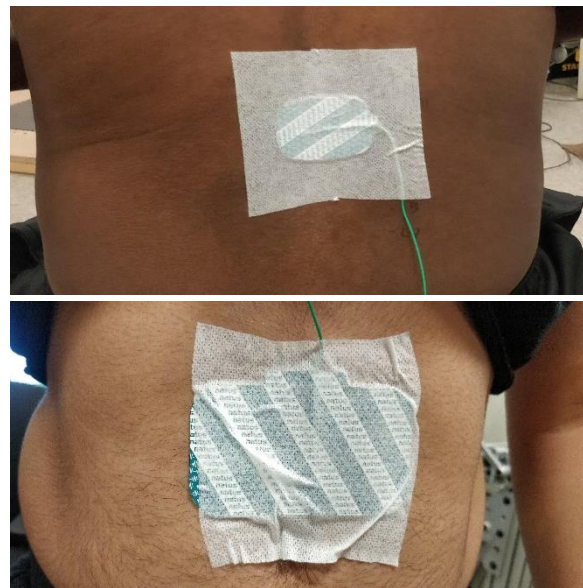


**Figure 0-4: Electrode placement for eliciting posterior root muscle reflexes. Top: Cathode was placed on the back at the L2-L3 intervertebral space; Bottom: Anode was placed on the abdomen**

1. Start stimulation at 30mA and increase current in steps of 5mA

2. After each stimulus, measure the amplitude of the response on the right or left soleus muscle
3. The first current at which the response exceeds  $50\mu\text{V}$  was taken as the threshold.

#### 4.2.6.4 Intervention - Transcutaneous Electrical Stimulation

The intervention in this study was thirty minutes of TSCS applied while subjects lay supine on a bed without carrying out any additional activity, Figure 4-5. Subjects were stimulated with  $500\mu\text{s}$  monophasic pulses at 30Hz at either 5, 7.5 or 10mA current. After trialing each current level, they were allowed to choose the current level they felt most comfortable receiving for the thirty minutes of the intervention.

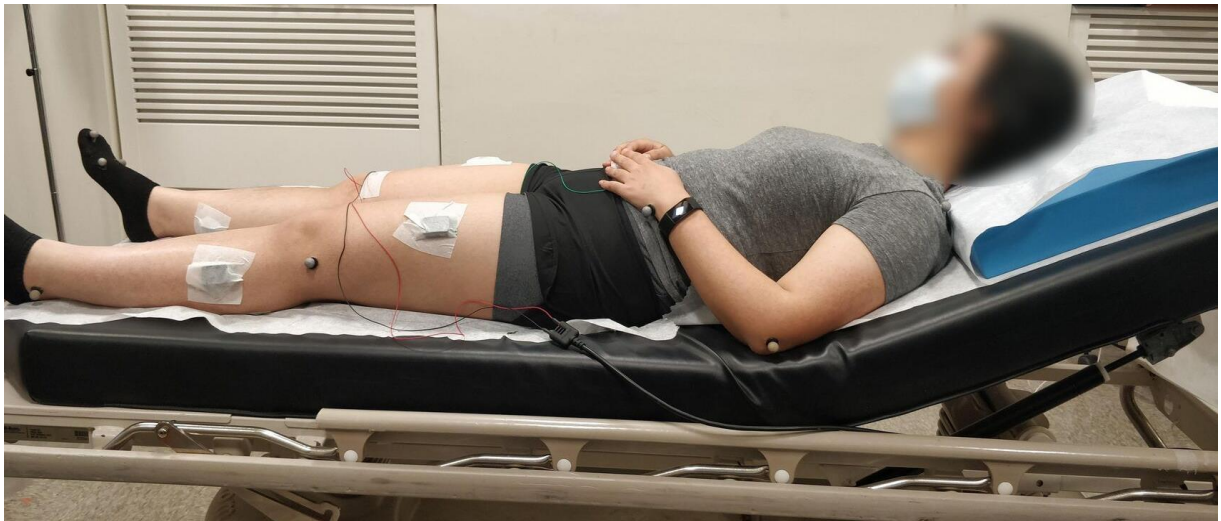


Figure 0-5: Intervention was carried out while the subject lay supine

#### 4.2.6.5 Posttests

Posttests were begun immediately after the intervention to avoid missing the window within which the stimulus effects were still present. Both physiological and balance pretests and posttests were conducted in the same way.

#### 4.2.7 Calculation of Metrics

Subject performance was assessed using performance variables calculated from the measurements carried out in the balance tests. Each perturbation trial was considered to last three seconds from perturbation onset, and all balance parameters were calculated over this period.

We recorded the COM position of each time point from motion capture data and the COP from the force plate data. The extrapolated center of mass (COM) was calculated as in [39] and used to calculate the margin of stability (MOS). The base of support (BOS) was bounded in the anterior-posterior direction by markers on the big toe and heel, and in the lateral direction by markers on the right and left fifth metatarsals. MOS was calculated as the distance from the COM to the boundary of the BOS. The difference between COP and COM (COP-COM) was also established as a variable to be assessed. COMExcursion and COPExcursion were calculated as the length of the COM and COP travel path during a perturbation trial, respectively. The maximum (MAX), root mean square (RMS), and timing (Idx) relative to perturbation onset of the maximum of each of these variables and their first and second derivatives were calculated.

Joint angles of the hip, right knee, and right ankle were calculated in the sagittal plane eliminating the lateral axis of the body from the optical marker data. The timing and value of the maximum and minimum of these angles and their first and second derivatives were calculated and their range.

EMG data was band-pass filtered between 20 and 300Hz, with a 250ms moving window, and used to calculate the area under the curve (iEMG) for each muscle, along with the maximum observed amplitude and the timing of the maximum. All EMG amplitude measurements were normalized to each subject's observed maximum. The duration of EMG activity was calculated using the Taiger-Kaiser energy operator method in [79], [148] to determine muscle activity onset and cessation. Muscle coactivation was measured with TA and SOL, TA and LG, and RF and BF agonist-antagonist pairs. The coactivation index was defined using the formula:

$$Cidx = \frac{2 \times \sum \min[EMG_{agonist} + EMG_{antagonist}]}{\sum EMG_{agonist} + \sum EMG_{antagonist}}$$

$EMG_{agonist}$  is the EMG voltage of the agonist muscle when the muscle is deemed to be activated;  $EMG_{antagonist}$  is the EMG voltage of antagonist muscle when that muscle is deemed to be activated.  $Min()$  returns zero at time points when either  $EMG_{agonist}$  or  $EMG_{antagonist}$  is not activated.

#### 4.2.8 Assessing the H-Reflex Recruitment Curve

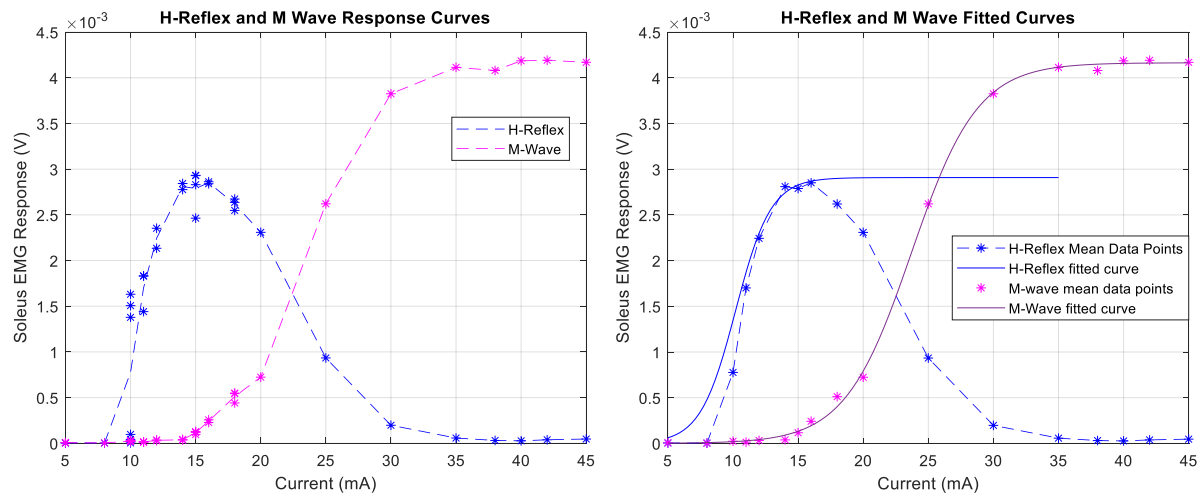


**Figure 0-6: Sample H-reflex recruitment curve. Left: Individually recorded data points; --- Line passes through average of datapoints elicited by the same current level; Right: Boltzmann sigmoidal curve fit for H-reflex and M-wave. Only the ascending limb of the H-reflex curve is fit.**

At the end of the data collection exercise for the H-reflex recruitment curve we had a set of current, H-reflex response, and M-wave response data points. To assess the H-reflex its recruitment curve was characterized using the method described in section 3.4.2. Figure 4-6. The MATLAB curve fitting function “fit” was used to fit the data points of the ascending limb of the H-reflex recruitment curve to the Boltzmann sigmoidal function by the Levenberg-Marquard non-linear least means -square algorithm [149], [150]:

$$H(s) = \frac{Hmax}{1 + e^{Hslope(Hcurrent50-current)}}$$

The MATLAB ‘fit’ function returns estimates for Hmax, Hslope, and Hcurrent50. This same curve fitting method was applied to the M-wave curve, which only has an ascending limb, and Mmax, Mslope and Mcurrent50 were realized.

#### **4.2.9 Assessing the H-reflex Recovery Cycle**

H-reflex recovery was assessed over five ISIs. The parameter calculated was the ratio of the amplitude of the H-reflex response to the second stimulus to that of the response to the first. This ratio was found for each trial and then averaged for each ISI.

#### **4.2.10 Statistical Analysis**

Paired t-tests comparing the pretest and posttest were used to compare the parameters evaluated during the balance and neurophysiological tests. All trials for each subject were averaged together regardless of perturbation force level, but trials in different perturbation directions were averaged separately. Only successful perturbation trials were included in the analysis.

Correlations were evaluated between the variables from the physiological measurements with significant changes and the balance measures with significant changes. For example, the change from pre-test to post-test of the conditioned H-reflex at 80ms ISI was assessed against the change in MOS between pre-test and post-test.

No correction for multiple comparisons was used because of the small sample size. The significance level for all statistical tests was set to 0.05.

### **4.3 Results**

#### **4.3.1 Kinematic and EMG Results**

Performance during the balance tests was analyzed for each direction. The results are shown in Figure 4-7 and 4-8.

**Anterior Perturbations:** There were not many changes in the results of the kinematic

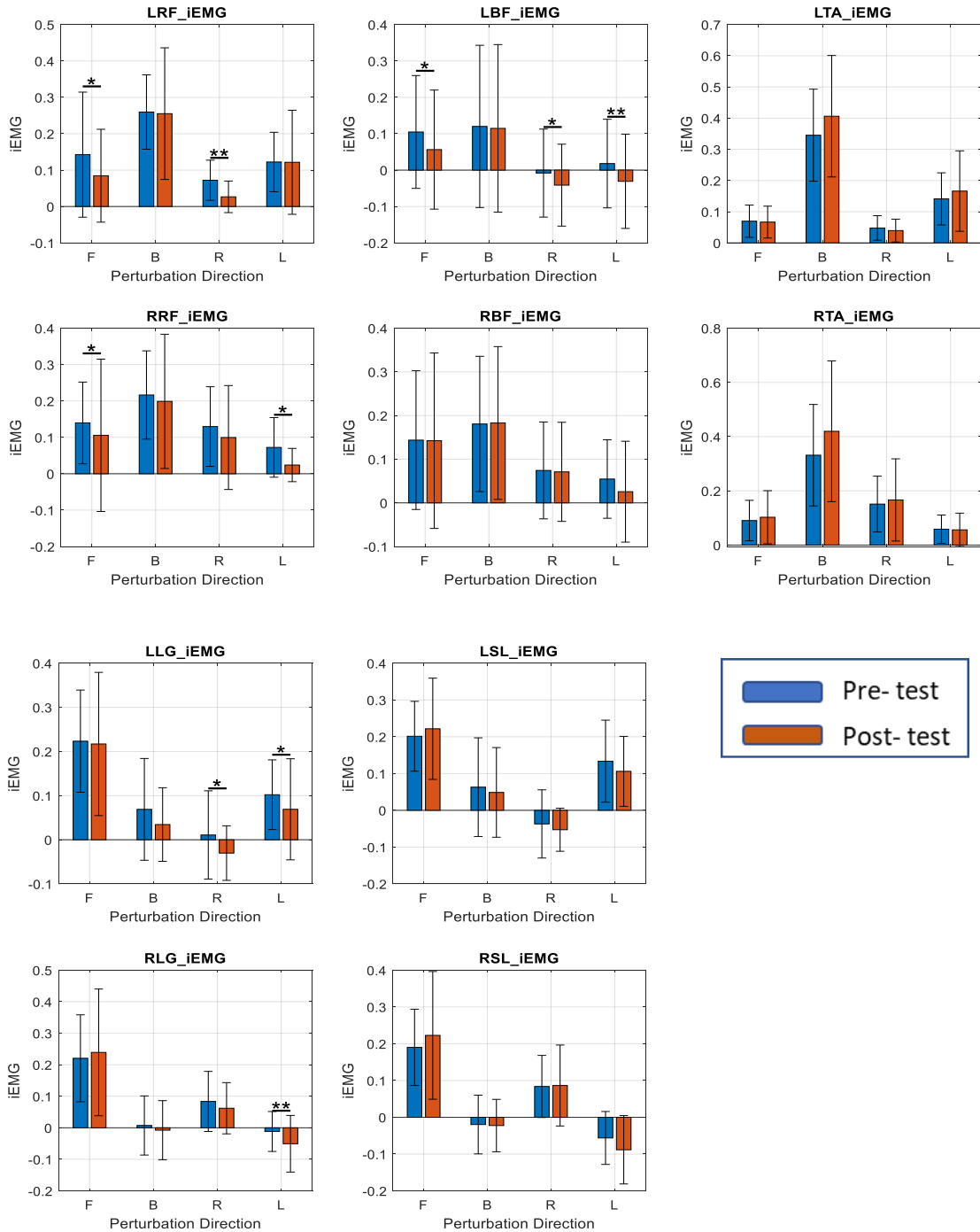


**Figure 0-7: Mean group pre-test (blue) and post-test (orange) iEMG results. F – Forward, B – backward, R – right, L- left perturbations. LRF – Left rectus femoris, RRF – right rectus femoris, LBF – left bicep femoris, RBF – right bicep femoris, LTA – left tibialis anterior, RTA – right tibialis anterior, LLG – left lateral gastrocnemius, RLG – right lateral gastrocnemius, LSL – left soleus and RSL – right soleus. \* =  $p \leq .05$ ; \*\* =  $p \leq .01$**

variables of the balance test, and critically there was no change in perturbation success rate ( $t(7)=-0.4827, p = .644$ ). One change that did occur was a statistically significant increase in the COPCOMmax ( $t(7) = -2.534, p = .039$ ). Statistically significant decreases in muscle activity were observed in the transfemoral muscles. LBF-iEMG ( $t(7)=2.630; p = .034$ ), LRF-iEMG ( $t(7)=3.392; p = .012$ ), RRF-iEMG ( $t(7)=3.217, p = .015$ ) all decreased, and LRF-Dur ( $t(7)=3.602, p = .009$ ), RRF-Dur ( $t(7)=3.621, p = .009$ ) decreased.

We observe that both the iEMG and activity duration of the LRF and RRF muscles decrease. In addition, there are decreases in LRF-LBF Cidx ( $t(7)=3.032, p = .019$ ), and RRF-RBF Cidx ( $t(7)=3.218, p = .015$ ).

**Posterior Perturbations:** Perturbation success rate did not change significantly ( $t(7)=1.623, p = .149$ ) but a decrease was observed in MeanMOS ( $t(7)=2.667, p = .032$ ). There were also statistically significant decreases in muscle activation time in RRF-Dur ( $t(7)=3.33, p = .013$ ) and LRF-Dur ( $t(7)=2.373, p = .049$ ).

**Right Perturbations:** Perturbation success rate did not change significantly ( $t(7)=-0.667, p = .525$ ) but there were decreases in MeanMOS ( $t(7)=3.720, p = .007$ ) and COPCOMmax ( $t(7)=2.410, p = .047$ ). Statistically significant decreases were observed again in the transfemoral muscles, in their activity duration RRF-Dur ( $t(7)=3.331, p = .009$ ), LRF-Dur ( $t(7)=4.375, p = .003$ ), LBF-iEMG ( $t(7)=3.104, p = .017$ ), and in iEMG, LRF-iEMG ( $t(7)=4.373, p = .003$ ). In addition, decreases were observed in one transtibial muscle, LLG-iEMG ( $t(7)=2.538, p = .039$ ), notably the on the perturbation direction. Lastly, there was a reduction RRF-RBF CIdx ( $t(7)=3.264, p = .014$ ).

**Left Perturbations:** Perturbation success rate did not change significantly ( $t(7)=-2.043, p = .080$ ) but a decrease in COPExcursion ( $t(7)=2.903, p = .023$ ) was observed. Statistically significant

decreases were observed in activity duration, RRF-Dur ( $t(7)=3.878, p = .006$ ) and in iEMGs, LBF-

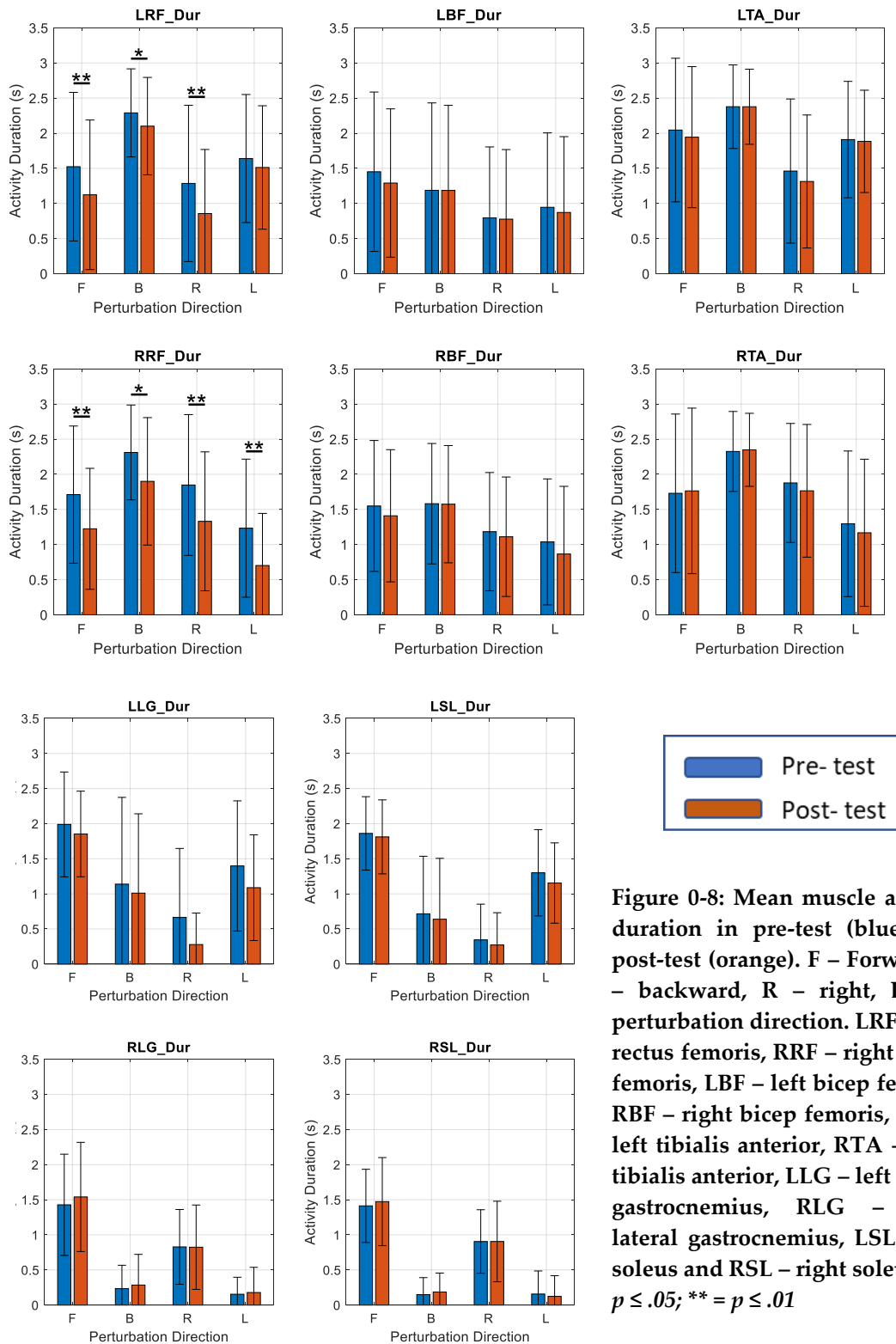


Figure 0-8: Mean muscle activity duration in pre-test (blue) and post-test (orange). F – Forward, B – backward, R – right, L- left perturbation direction. LRF – Left rectus femoris, RRF – right rectus femoris, LBF – left bicep femoris, RBF – right bicep femoris, LTA – left tibialis anterior, RTA – right tibialis anterior, LLG – left lateral gastrocnemius, RLG – right lateral gastrocnemius, LSL – left soleus and RSL – right soleus. \* =  $p \leq .05$ ; \*\* =  $p \leq .01$

iEMG(t(7)=4.571,  $p = .003$ ), RRF-iEMG(t(7)=2.750,  $p = .028$ ). Decreases were observed in RLG-iEMG(t(7)=3.502,  $p = .010$ ) and LLG-iEMG(t(7)=2.591,  $p = .036$ ), transtibial muscles. Coactivation index decreases were observed in RRF-RBF CIdx(t(7)=3.037,  $p = .019$ ) and LTA-LLG PCIdx(t(7)=2.696,  $p = .031$ ).

### 4.3.2 Neurophysiological Results

**H-Reflex:** Of the eight subjects enrolled in the study, data for one subject did not conform to the sigmoid curve. The fitting function converged to a solution for all other subjects with average R-Square correlation coefficient of  $95.43 \pm 2.07\%$ . No significant changes were observed in the H-reflex parameters between pretest and posttest for any of the parameters, Figure 4-9. HMax(t(6) = 2.281,  $p = .063$ ), MMax (t(6) = 0.558,  $p = .597$ ), HCurrent50 (t(6) = 1.058,  $p = .331$ ), MCurrent50 (t(6) = -0.922,  $p = .392$ ) and HSlope (t(6) = 0.496,  $p = .638$ ), and MSlope (t(6) = 0.602,  $p = .569$ ).

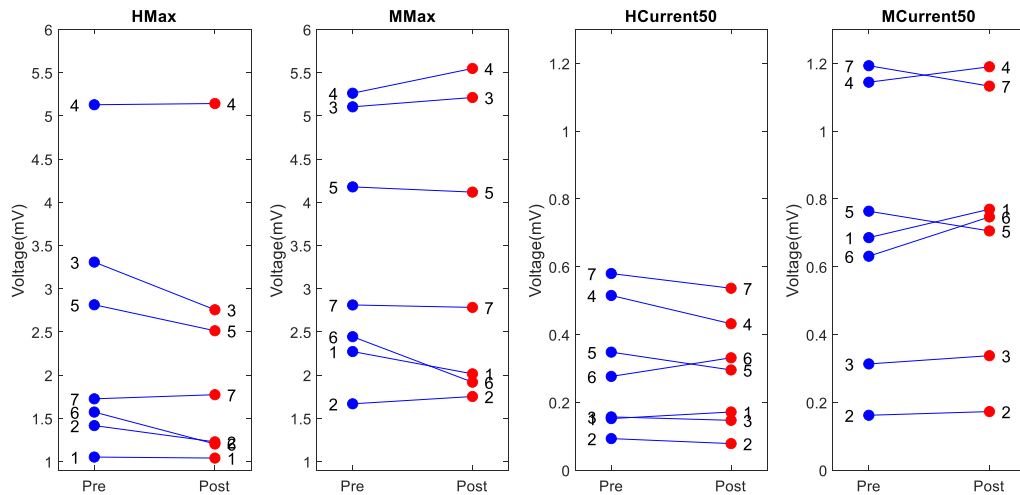
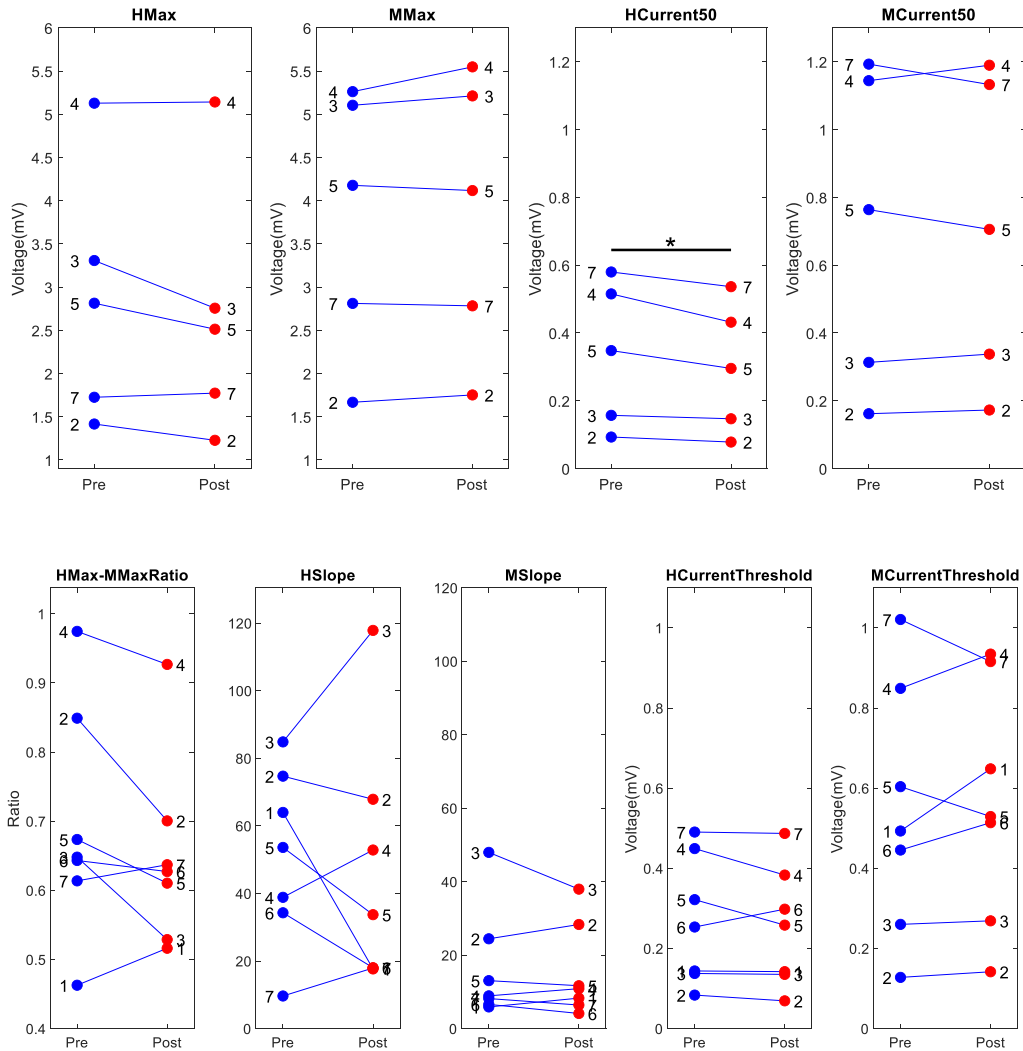


Figure 0-9: Graph showing individual changes in subjects for HMax, MMax, HCurrent50 and MCurrent50. None of the group changes were significant. Number in plots are subject ID numbers.

As explained in Chapter 3, MMax is thought to represent the maximum motor pool activation and therefore should not change from test to test. We observed a change greater than 5% in two

subjects (subjects 1 and 6 in Figure 4-9), eliminated them, and performed a paired t-test on the remaining subjects. There was now a significant decrease in HCurrent50 ( $t(4) = 3.053, p = .038$ ) indicating a left-shift of the recruitment curve. No significant changes were observed in the other variables. The results are shown in Figure 4-10; HMax ( $t(4) = 1.785, p = .149$ ), MMax ( $t(4) = -1.277, p = .271$ ), MCurrent50 ( $t(4) = 0.345, p = .747$ ), HSlope ( $t(4) = -0.631, p = .562$ ) and MSlope



**Figure 0-10: Individual subject changes between pre-test and post-test when subjects which had changes in MMax greater than 10% were eliminated. \* =  $p \leq .05$**

( $t(4) = 0.6122, p = .574$ ), HCurrentThreshold ( $t(4) = 2.080, p = .106$ ), MCurrentThreshold ( $t(4) = 0.418, p = .698$ ), HCurrentMax ( $t(4) = 2.992, p = .403$ ), and MCurrentMax ( $t(4) = 0.062, p = .953$ )

**H-Reflex Recovery Cycle:** Statistically significant increases were observed in the t-tests at all ISIs of the H-reflex recovery cycle tested, indicating that there was stronger recovery after the intervention; 80ms ( $t(6)=-3.017, p = .023$ ), 150ms ( $t(6)=-3.206, p = .018$ ), 250 ( $t(6)=-2.821, p = .030$ ), 500ms ( $t(6)=-2.583, p = .042$ ), 1000ms ( $t(6)=-2.707, p = .035$ ), Figure 4-11. Subsequently, the magnitude of the second H-reflex response in the pre-test was compared to that in the post-test, and we observed a significant increase only at the 80ms ISI ( $t(6) = -3.014, p = .024$ ). Comparing the first H-reflex responses in the same way yielded no significant changes at any ISI.

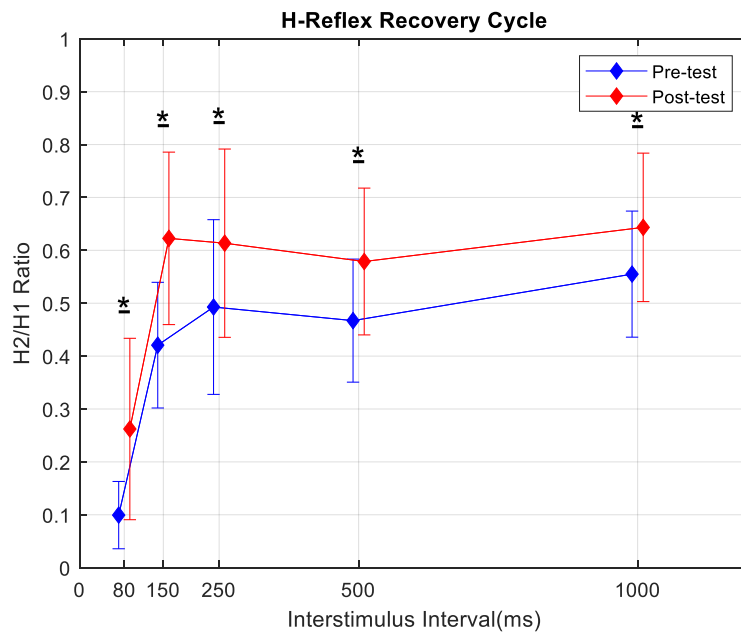


**Figure 0-11: H-reflex recovery cycle. Pre-test and post-test ratios of H2:H1 at 80, 150, 250, 500, 1000 ms interstimulus intervals. \* =  $p \leq .05$**

#### 4.4 Discussion

In this study, we set out to (i) investigate the effect of TSCS on balance and neurophysiological characteristics and (ii) explore the relationship between neurophysiological measures and balance measures in healthy individuals.

It was hypothesized that exposure to TSCS for a prolonged period would induce neuroplastic changes that would result in an increase in spinal excitability, which in turn would lead to increased muscle recruitment, activation, and, consequently, an improvement in perturbation success rate.

Three parts of this hypothesis that need to be supported are (i) the increase in spinal excitability, i.e., are larger spinal reflexes generated by the same stimulus, (ii) increased muscle activation, i.e., is there more muscle recruitment during the same functional task, and (iii) if the two previous events occur, do they lead to improvement in balance.

#### **4.4.1 Spinal Excitability**

Spinal excitability was measured by the neurophysiological variables – H-reflex recruitment curve characteristics, the H-reflex recovery cycle and the PRM threshold values.

A leftward shift of the H-reflex recruitment curve, indicated by significant decreases in HCurrent50 and HCurrentMax, was observed in a subgroup of subjects. This has to be interpreted in the context of the other changes or non-changes that occurred. In literature, changes in the HMax/MMax ratio indicate alterations in the excitability of the alpha-motoneuron pool by sensory afferent neurons or changes to presynaptic inhibition [124], [151]. No change was observed in this quantity. HSlope is said to measure the excitability of the motoneurons in terms of the amount of response generated for an amount of sensory afferent input [126], [152]. No change was observed in this term as well. The absence of changes to the HMax/MMax ratio, HSlope, as well as MMax, indicate the protocol did not change motoneuron excitability, the availability of motoneurons or the susceptibility of motoneurons to be excited by sensory input. This suggests that the decreases in HCurrent50 and HCurrentMax are the result of an increase in the efficacy of the sensory afferent – motoneuron synapse. Lamy et al. (in an experiment using TSDCS where stimulation was enacted at 0.33Hz) suggest that a similar leftward shift could be explained by reduced post-activation depression [153]. This explanation was supported by the changes observed in the H-reflex recovery cycle.

Significant increases in H-reflex recovery were observed at all ISIs (80, 150, 250, 500, 1000). Presynaptic inhibition and homosynaptic depression are two phenomena that affect the recovery

cycle, as explained in Sec. 3.4.3. The exact mechanisms governing these changes in H-reflex recovery are not well understood. Still, some speculation can be made about what caused the observed changes. Presynaptic inhibition is more dominant at smaller ISIs (below 250ms) and homosynaptic depression is dominant at the higher ISIs. The fact that recovery increased at all ISIs suggests that its source is a process that affects the H-reflex response across a broad range of ISIs. Other researchers have observed decreases in post-activation depression (increases in recovery), e.g., Winkler et al. [154] in a protocol using anodal TSDCS. Winkler hypothesized that electrical stimulation causes a lasting hypopolarisation in the sensory neurons' resting potential, which facilitates the release of neurotransmitters at the afferent – motoneuron synapse. Hypopolarisation makes the negative resting potential of neurons more positive and brings the neurons closer to depolarization and the discharge of EPSPs. They thus are easier to excite. The leftward shift of the recruitment curve supports hypopolarisation in that the H-reflex reached higher levels after being stimulated at lower currents in the post-test. Hypopolarisation would therefore increase the efficacy of the sensory afferent – motor neuron synapse.

It can be reasoned that this increased synaptic efficacy and the leftward shift of the recruitment curve should also cause an increase in the amplitude of the response to the conditioning stimuli, i.e., the H-reflex response to the first of the paired pulses. A t-test comparison of the pretest and posttest values of these amplitudes did not yield any significant differences. The absence of a change in amplitude of the conditioning stimulus response discounts the idea that hypopolarisation is the primary action phenomenon. On the other hand, it could imply that its effect is evident specifically in pulses applied in quick succession.

#### **4.4.2 Muscle Activation**

The trend in the muscle activation data is a general decrease in muscle activity, particularly in the L-RF and R-RF and in the coactivation of the LRF-LBF and RRF-RBF muscle pairs. Studies

have shown that this reduction is the natural course of change in muscle activity when reacting to repeated perturbations [2], [57], [155]. The muscle activity reduction phenomenon can be explained by the optimality principle of sensorimotor control [156]–[158]. The human musculoskeletal system is highly redundant and can execute a single task in multiple ways. In dealing with this redundancy, researchers have proposed minimizing metabolic and mechanical effort as an optimization principle in selecting sensorimotor patterns [159]. In addition to this minimization principle, a model for movement called the stochastic optimized-submovement model has been proposed in the literature. It claims that aimed movement involves a primary movement and a secondary corrective submovement. The submovements are progressively optimized so that total average movement is minimized, and this is achieved by optimally adjusting the average magnitudes and durations of force pulses that generate movement [157]. It can be concluded from these that in the course of repeating an action, more and more optimal solutions will be found, the magnitude and duration of force pulses will be reduced, and less effort will be applied. This process is manifested in the results of this dissertation. At the beginning of the trials, subjects may be unaware of the best way to coordinate an efficient response to perturbations and may adopt inefficient response modes. However, they evolve their responses with practice and converge on a stable and efficient solution [57], [155]. This explains the muscle activity reduction adaptations observed in this experiment. Horak et al. [2] also explain that muscle activity reductions improve performance as automatic responses become less vigorous and destabilizing and subjects reach stability quicker.

It should be noted that reductions in muscle activity were similarly observed in the experiments in Chapter 2. Thus, we can conclude that these reductions are part of the natural course of adaptation of the motor system when exposed to repeated perturbations. Hence the reductions

observed do not point to an effect of the intervention carried out in this study on muscle activation of the subjects.

#### **4.4.3 Balance Performance**

In the same vein, changes observed in the balance performance measures point to adaptations that suggest subjects became more adept at resisting perturbations. Reductions in the MOS in the backward, right, and left directions with no accompanying reduction in perturbation force or success rate at first glance may suggest that subjects' moved closer to instability. Nevertheless, it is important to consider that subjects need to make tradeoffs between energetics, safety, and achieving functional goals in coming to an optimal motor planning solution. These decreases can be seen as the motor system permitting a reduction in a "margin of safety" to reduce energy expenditure (reduction in muscle activity) without diminishing the perturbation success rate. The system is thus settling on some optimal mode of performance.

There was no change in the perturbation success rate, nor were there changes in any of the other kinematic measures, and so, the hypothesis that the increase in spinal excitability generated by the intervention would lead to improved performance was not supported.

#### **4.4.4 Conclusion**

The intervention described in this project successfully increased the excitability of spinal circuits, but this did not translate to muscle activation increases during balance tests nor an improvement in balance performance. It is possible that TSCS effects did not persist until the balance test session as it was carried out more than 30 mins after the end of the intervention but studies have shown that neural changes due to electrical stimulation have persisted for up to two hours [160]. It is also possible that the CNS of spinally intact subjects adjusts for the neural changes due to TSCS while conducting functional tasks. In this way, the sensorimotor system keeps performing optimally despite neural changes.

Nevertheless, this project has shown that TSCS can affect spinal excitability, particularly the activation of the motor neuron pool by sensory stimuli. Future work can focus on translating this increased excitability into functional task improvements. Studies have shown that the combination of plasticity-inducing factors and exercise increase the probability of functional improvements [161], and this can be trialed in future experiments.

## **Chapter 5: Effect of Transcutaneous Spinal Stimulation on Balance and Neurophysiological Characteristics**

### **5.1 Introduction**

In Chapter 4, we examined the effect of applying transcutaneous spinal cord stimulation (TSCS) on the neurophysiological and balance characteristics of a set of healthy, uninjured adults. We found that although the protocol caused an increase in spinal excitability, it did not lead to improved performance of the functional task. This reinforces a frequently encountered principle in the literature that functional training is essential in order for neurophysiological changes to manifest functional meaning and enable recovery [56], [161]–[163].

For example, it is well known that in the period immediately following SCI, the spinal cord is in a plastic state where motor learning can be achieved. In a study of cervically spinalized rats by Girgis et al. [164], rats were divided into two groups. One group was trained in a reaching task for six weeks immediately after injury, and the other was not. The results showed that the trained rats improved substantially in the task compared to the untrained ones. Garcia-Alias et al. [161] showed that even in the presence of the neuroplasticity boosting effects of Chondroitinase ABC, rats receiving this booster along with specific rehabilitation demonstrated a considerable improvement in the reaching task trained over rats that received only Chondroitinase. These studies demonstrate that activity-based training leads to greater motor improvement.

Megia-Garcia et al. also note that spinal stimulation interventions must be combined with activity-based rehabilitation to evoke adaptive neuroplasticity [117]. This includes movement, strength, coordination, assisted gait, transfer training, manual dexterity, and grip strength exercises.

The mechanism by which physical training benefits rehabilitation is not well understood [161], [165], [166], but there are abundant hypotheses in the literature. Lynskey et al. [166] suggest

that recovery after activity-based training relies on sensory feedback mechanisms. Fouad et al. [167] present a number of motor recovery mechanisms that have been observed with activity-based rehabilitation that include: the increased presence of growth chemicals like the brain-derived neurotrophic factor (BDNF), the ability of spinal circuitry to learn new movement patterns, changes to inhibition of spinal circuitry and spinal excitability, and changes to neuronal properties. They also note a strong relation between neuronal activity and plasticity. Since both training and electrical stimulation have the effect of generating neuronal activity, they both create the conditions for recovery.

Based on this knowledge, we hypothesize that training subjects while TSCS is applied will lead to gains in functional performance along with the increased spinal excitability observed in the previous experiment when the intervention only consisted of applying TSCS.

We have designed an experiment to assess how TSCS affects the balance performance of healthy subjects, first, once TSCS is turned on, and second, after going through a perturbation-based training intervention while TSCS is on. In an experiment, Meyer et al. [143] showed that TSCS immediately improved motor function once applied. Thus, we hypothesize that TSCS will increase motor performance both immediately after it is turned on and after the training intervention.

## **5.2 Methods**

### **5.2.1 Experimental Protocol – Study Design**

Study protocols and consent forms were approved by Columbia University (IRB-AAAR6780). The experimental structure in Figure 5-1 shows the method used to measure the immediate effect of TSCS and its effect after combining it with a training protocol. Neurophysiological tests bookended the experiment in order to measure the spinal excitability beginning and end states. Carrying out neurophysiological measurements at additional times

during the experiment would have made the protocol especially burdensome on the participants. The pre-test and post-test are referred to as P1 and P2, respectively. P1 was followed by the first balance test, T1, which was done without TSCS. TSCS was used during balance test 2, T2, the training intervention, and balance test 3, T3. TSCS was turned off for balance test 4, T4.

Eleven subjects were enrolled in this study: 7 male (age:  $25.8 \pm 4.8$  years; weight:  $75 \pm 6$  kg; height:  $1.79 \pm 0.08$  m) and 4 female (age:  $22.8 \pm 4.4$  years; weight:  $67.9 \pm 16.5$  kg; height:  $1.64 \pm 0.05$  m).

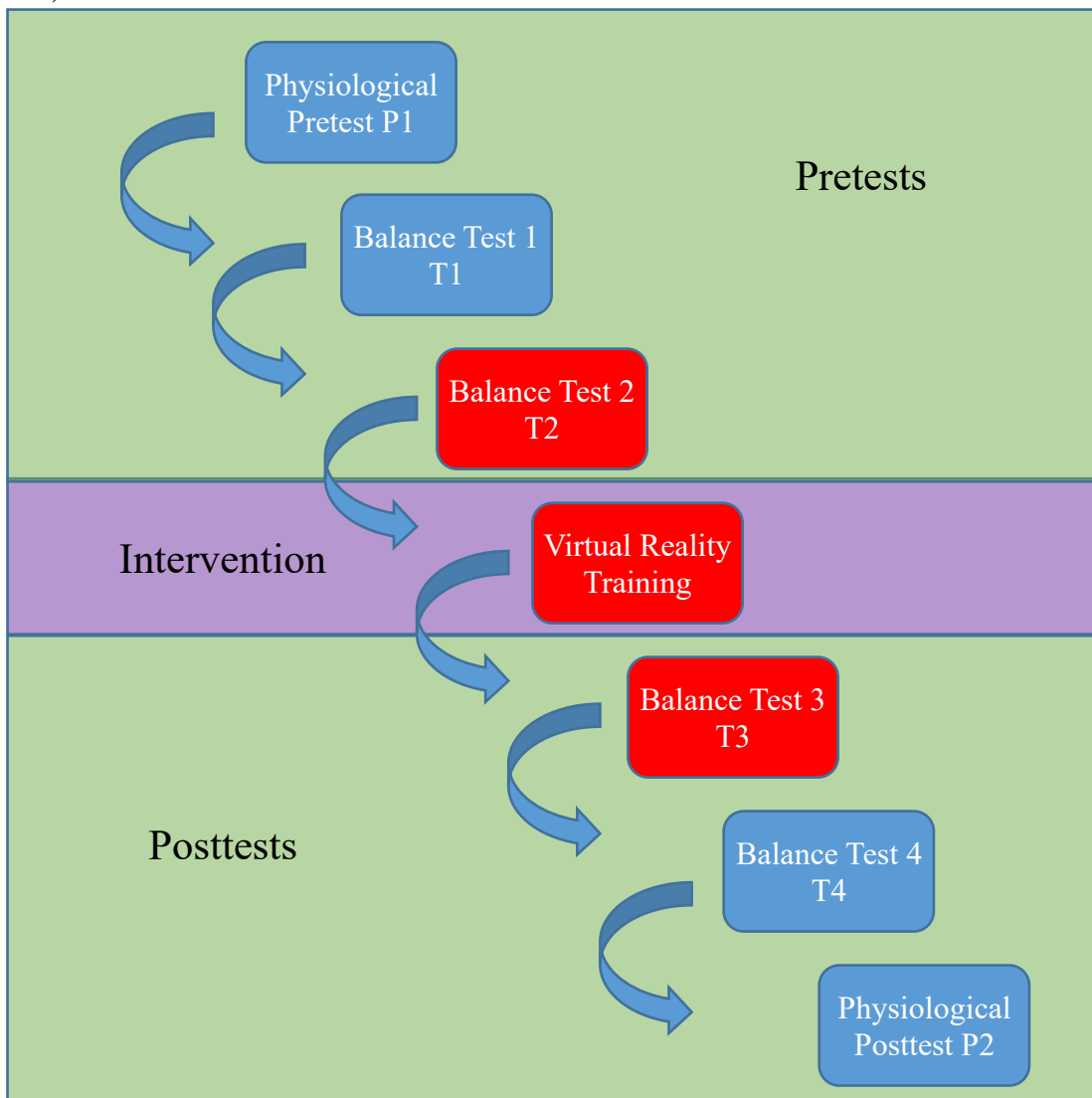


Figure 0-1: Flow chart of experimental procedure. Physiological tests were conducted at the beginning and end of the protocol. Balance tests T1 and T4 were conducted without TSCS (blue) and balance tests T2 and T2 (red) were conducted with TSCS

### 5.2.1.1 Neurophysiological Pretest

The experiment began with the collection of some neurophysiological metrics. The ascending limb of the H-reflex, the H-reflex recovery cycle, and the posterior root muscle (PRM) reflex threshold were measured. All neurophysiological tests were conducted while subjects lay supine.

**H-reflex:** In this experiment, only the ascending limb of the H-reflex was recorded. The data collected was used primarily to ascertain the appropriate current for assessing the H-reflex recovery cycle. The descending limb of the H-reflex and the corresponding section of the M-wave response were not collected, so our working assumption was that MMax did not change during this experiment. This was done to limit the time spent collecting data as well as the current intensity the subject was exposed to.

Section 4.2.6 provides details on the placement of electrodes. Subjects were stimulated at the tibial nerve starting at 5mA, and increased progressively by 5mA until HMax was reached.

**Recovery Cycle Procedure:** As described in Section 4.2.6, paired pulses were used to generate the H-reflex recovery cycle by varying the inter-stimulus interval (ISI). The paired-pulse current was determined from the H-reflex recruitment curve after sigmoid fitting as the current that generated a response approximately 30% of HMax. Paired pulses were enacted at least 15s apart and testing was done at 80ms, 150ms, 250ms, 500ms and 1000ms ISIs, with each ISI tested five times.

**Procedure for Posterior Root Muscle Reflexes:** Posterior root muscle (PRM) reflex thresholds were collected. Electrode placement was the same as in Section 4.2.6. The threshold was determined with the following procedure:

1. Start a single pulse stimulation at 30mA and progressively increase current by 5mA until a response in the LSL or RSL above 50 $\mu$ V is identified. The current at which this happens should be noted.

2. Reduce current by 1mA until the PRM responses generated are below 50 $\mu$ V.
3. At this point, increase current again by 1mA until the response again is above 50 $\mu$ V. This current is taken as the PRM threshold.

Once this threshold was found, the subjects were stimulated eight times at 120% of the threshold value. The response at this level was compared between pre-test and post-test.

#### 5.2.1.2 *Balance Test 1*

The progression of the perturbation forces was different in this experiment than in Chapter 4. Balance was assessed by perturbing subjects while they stood upright in RobUST. Once a participant was set up in the device, his perturbation threshold was found in each perturbation direction (forward, backward, right, and left). Subjects were perturbed twice at each perturbation force level starting at 25% body weight (BW) in each direction. If they did not lose balance both times, the force was increased by 5% BW. The perturbation force level 5% below that at which subjects failed to maintain balance twice a row was used as their threshold.

In each balance test, subjects were tested at the perturbation force threshold ten times in each direction and with a force 10% higher than the threshold, five times each. Hence, there were two force levels: low and high. The ten low force perturbations were first carried out, and then the five high force perturbations followed. The sequence of directions in which the subjects were perturbed was randomized in the four directions. Successful trials were defined as those in which the subject could stay in place without taking a step or reaching for external support after being perturbed. Perturbations had a trapezoidal profile in which a controller commanded cable force to rise from a base level to the target force level over 75ms, maintain that force for 400ms, and then decline to zero over 100ms, totaling 575ms.

### 5.2.1.3 *Setting up TSCS*

After the first balance test, subjects were connected to the stimulator while standing in RobUST, Figure 5-2. Subjects were stimulated at 5, 7.5, and 10mA and asked to choose the stimulating current at which they felt most comfortable. The current chosen was used for all subsequent TSCS stimulations for the subject.

### 5.2.1.4 *Balance Test 2*

Perturbations in T2 were carried out as in T1. Continuous TSCS was started at the beginning of this session and remained active throughout the test. While receiving TSCS, force perturbations were issued the same way as in T1.



Figure 0-2: Subject standing in RobUST

### 5.2.1.5 *Virtual Reality Training with TSCS*

After the two balance tests, the subjects played a catch-and-throw virtual reality game, the same as that described in Chapter 2. Again, an HTC Vive virtual reality system was used. The subjects went through two sessions of 50 catch-and-throw trials while still receiving TSCS.

Perturbations were consistently enacted 800ms after the ball was shot at the subject. This made it so that the perturbation arrived just when the subject was about to catch the ball as the ball was set to travel the distance to the subject in 1s. Subjects were asked to take a break for 5 mins before the VR games and for 5 mins afterward.

#### *5.2.1.6 Balance Test 3 – Balance Posttest with TSCS*

Subjects were put through the same perturbation regiment as in the previous balance tests while the subject received TSCS. Perturbation force levels were the same, but the sequence of directions was randomized. This test started after the 5 min pause at the end of VR training.

#### *5.2.1.7 Balance Test 4 – Balance Posttest without TSCS*

TSCS was turned off at the end of T3 and a final balance test was carried out without stimulation. The perturbation force levels were the same as in other balance tests but the sequence of directions was again randomized.

#### *5.2.1.8 Neurophysiological Posttest*

Neurophysiological tests to assess the H-reflex, H-reflex recovery cycle and PRM threshold were carried out as in the pretest. Subjects were moved from RobUST onto a bed and made to lie supine for this part of the experiment. The same neurophysiological tests as in P1 were carried out.

### **5.2.2 Measurement Variables**

#### *5.2.2.1 Measurement Variables Calculated from Balance Tests*

Motion capture data was collected during the balance tests with a nine camera Vicon motion capture system (Vicon, Denver) and retro-reflective markers placed bilaterally on the big toe, fifth metatarsal, lateral malleolus, heel, lateral femoral epicondyle, ASIS, PSIS, acromion, elbow and wrist. This marker set was used to generate the subject's center of mass (COM) based on the method in [146] and the anthropometric measurements of de Leva in [147]. Ground reaction forces were collected with two six-axis force plates (Bertec, Columbus, Ohio), one for each foot. The

data from these two force plates was used to compute the foot center of pressure location. Both marker position and center of pressure data were smoothed with a 0.1s moving average window. EMG data were collected bilaterally from 10 muscles, the soleus (SOL), lateral gastrocnemius (LG), tibialis anterior (TA), bicep femoris (BF), and rectus femoris (RF).

EMG data was band pass filtered between 20 and 300Hz, averaged with a 250ms moving window and used to calculate the area under the curve (iEMG) for each muscle, along with the maximum observed amplitude and its timing. All EMG amplitude measurements were normalized to each subject's observed maximum. The duration of EMG activity (Dur) was calculated using the Taiger-Kaiser energy operator method [79], [148] to determine muscle activity onset and cessation. Muscle coactivation was measured with TA/SOL, TA/LG, and RF/BF agonist-antagonist pairs. Coactivation index was defined using the formula:

$$Cidx = \frac{2 \times \sum \min[EMG_{agonist} + EMG_{antagonist}]}{\sum EMG_{agonist} + \sum EMG_{antagonist}}$$

$EMG_{agonist}$  is EMG voltage of the agonist muscle when the muscle is deemed to be activated,  $EMG_{antagonist}$  = EMG voltage of antagonist muscle when that muscle is deemed to be activated.  $\min()$  returns zero at time points when either  $EMG_{agonist}$  or  $EMG_{antagonist}$  is not activated.

Subjects' performance was assessed using variables calculated from these measurements over a four-second duration from the initiation of a perturbation. Extrapolated center of mass (COM) was calculated as in Hof et al. [39] and used to calculate the extrapolated margin of stability (MOS). The base of support (BOS) was bounded in the anterior-posterior direction by markers on the big toe and heel and in the lateral direction by markers on the right and left fifth metatarsals. The length of the vector from the COM to the COP (COP-COM) was assessed. The maximum (Max), root mean square (RMS) and timing relative to perturbation onset of the maximum (MaxIdx) of each of these variables and their first derivative (VelMax, VelRMS, VelMaxIdx) were calculated.

The distribution of balance strategy between ankle and hip strategies was assessed using the method described in Chapter 2. HipStrat is the percentage of time during the period of interest when upper body rotation and lower body rotation were significantly inversely correlated, and AnkStrat, the percentage of time they were positively correlated. Ground reaction force in the forward and backward directions were also recorded as GRF\_APmax and GRF\_APmin, respectively.

#### *5.2.2.2 Measurement Variables Calculated from Neurophysiological Tests*

Physiological tests yielded measurements of the H-reflex recruitment curve, the H-reflex recovery cycle, and the PRM threshold. Parameters generated from the H-reflex recruitment cycle include HMax, the maximum H-reflex response, HSlope, the maximum value of the slope of the sigmoid fit to the H-reflex response, and S50, the current that would generate half of HMax as determined from the fit sigmoid curve. Recovery cycle measurements produce the ratio of the conditioned H-reflex response to the non-conditioned response at 80, 150, 250, 500 and 1000 ms ISIs. Finally, PRM reflex measurements produce the current threshold needed to excite PRMs in either the LSL or RSL, PRM\_Threshold, and the PRM reflex response of each muscle to 120% of the pretest PRM\_Threshold.

### **5.2.3 Statistical Analysis**

Prior to statistical analysis, failed perturbation trials were discarded, and of the remaining trials, the low force level and the high force level trials were averaged separately for each perturbation direction. Paired t-tests were used to compare the performance variables measured in T1, T2, T3, and T4 to assess the effect of TSCS on balance. Paired t-tests were also used to determine what changes occurred in the neuro-physiological assessment variables between P1 and P2. No correction for multiple comparisons was made because of the small sample size. The significance level for all statistical tests was set to 0.05.

To assess the relationship between changes in the neurophysiological variables and the kinematic and EMG variables collected, Pearson correlation coefficients were computed between the percentage change in pairs of variables, and a Bonferroni correction was applied to adjust for multiple comparisons.

### **5.3 Results**

The balance performance of subjects with and without continuous TSCS was compared, and the effect of a training intervention on these two conditions was also assessed. The results point to an increase in muscle activity accompanied by a decrease in balance proficiency with TSCS. All subjects completed the protocol, but some muscle activity data was lost from one subject and motion capture data from two subjects due to failure of the recording equipment.

A large number of comparisons were run in this experiment to assess subjects' performance in the different conditions. This section will state the results, starting with the kinematic and EMG results from balance tests.

#### **5.3.1 Immediate Effects of Stimulation on Balance (T1 vs. T2)**

A number of statistically significant changes were observed in the transfemoral muscles in multiple directions, but very few were observed in the transtibial muscles, Figure 5-4 and 5-6. All changes observed pointed to increased muscle activity. There was increased muscle activity in the L-RF in the forward direction as evidenced by an increase in LRF\_iEMG ( $p = .030$ ) (Figure 5-3) while no statistical change was observed in the other directions (backward:  $p = .502$ , right:  $p = .074$  left:  $p = .284$ ). There was a similar increase in muscle activity in the R-RF for forward perturbations observed in both RRF\_iEMG (forward:  $p = .017$ ) and RRF\_Dur (forward:  $p = .045$ ).

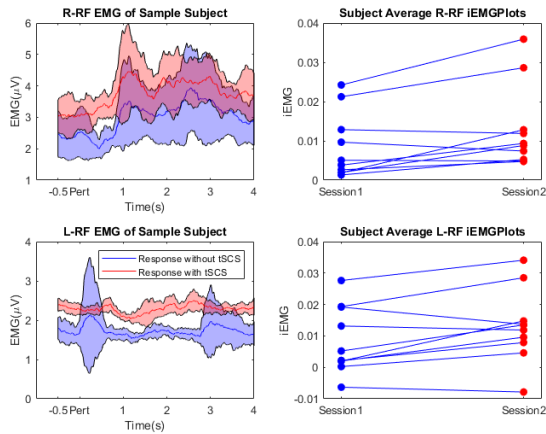


**Figure 0-3: Plots comparing integrated EMG (iEMG) without TSCS, T1, (blue) and with TSCS, T2, (red) during trunk force perturbation in the anterior direction. Top row plots are of the right rectus-femoris (R-RF) muscle and bottom row are of the left rectus femoris (L-LF). Left column plots are from individual subjects showing muscle activity from 0.5s before perturbation, through perturbation onset (pert on the graph), and for four seconds after. Right plots are average iEMG for individual subjects in session1 (without TSCS) and session 2 (with TSCS)**

display significant changes (right:  $p = .048$ ). There were no significant changes in RBF\_Dur.

LTA-LLG CIdx decreased significantly only for left perturbations (forward:  $p = .245$ , backward:  $p = .851$ , right:  $p = .300$ , left:  $p = .016$ ) and no significant change was observed in the other directions. There were also no significant changes observed in the L-TA/SOL, L-RF/BF, R-TA/LG, R-TA/SOL, and R-RF/BF CIdx's.

Among the kinematic measures (Figure 5-5), a small significant decrease in the normalized MOS was observed only for forward perturbations (forward:  $p = .045$ , backward:  $p = .197$ , right:  $p = .148$  left:  $p = .179$ ) accompanied by a decrease in perturbation success rate (forward:  $p = .039$ ,

An increase was also observed in RRF\_iEMG for left perturbations (left:  $p = .033$ ) but there were no significant changes in RRF\_iEMG for backward and right perturbations and in RRF\_Dur for backward, right and left perturbations.

In the L-BF muscle, LBF\_Dur showed increased muscle activity for forward and right perturbations (forward:  $p = .042$ , right:  $p = .032$ ) but not for backward and left perturbations. There was also an increase in LBF\_iEMG for right perturbations while perturbations in all other directions did not

backward:  $p = .802$ , right:  $p = .367$  left:  $p = .637$ ). There were no significant effects of TSCS in the backward, right and left directions.

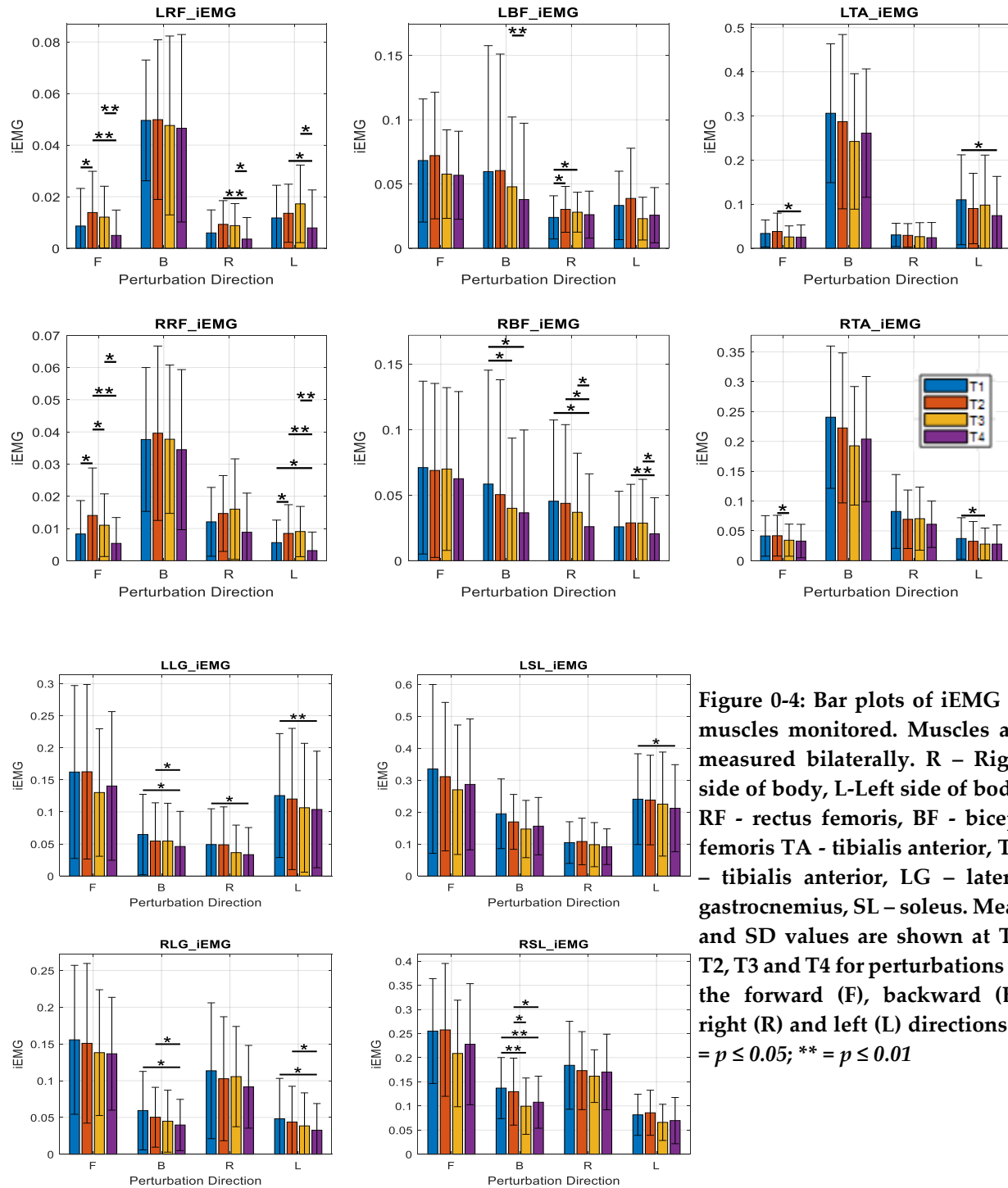


**Figure 0-4: Bar plots of iEMG of muscles monitored. Muscles are measured bilaterally. R – Right side of body, L-Left side of body. RF - rectus femoris, BF - biceps femoris TA - tibialis anterior, TA – tibialis anterior, LG – lateral gastrocnemius, SL – soleus. Mean and SD values are shown at T1, T2, T3 and T4 for perturbations in the forward (F), backward (B), right (R) and left (L) directions. \* =  $p \leq 0.05$ ; \*\* =  $p \leq 0.01$**

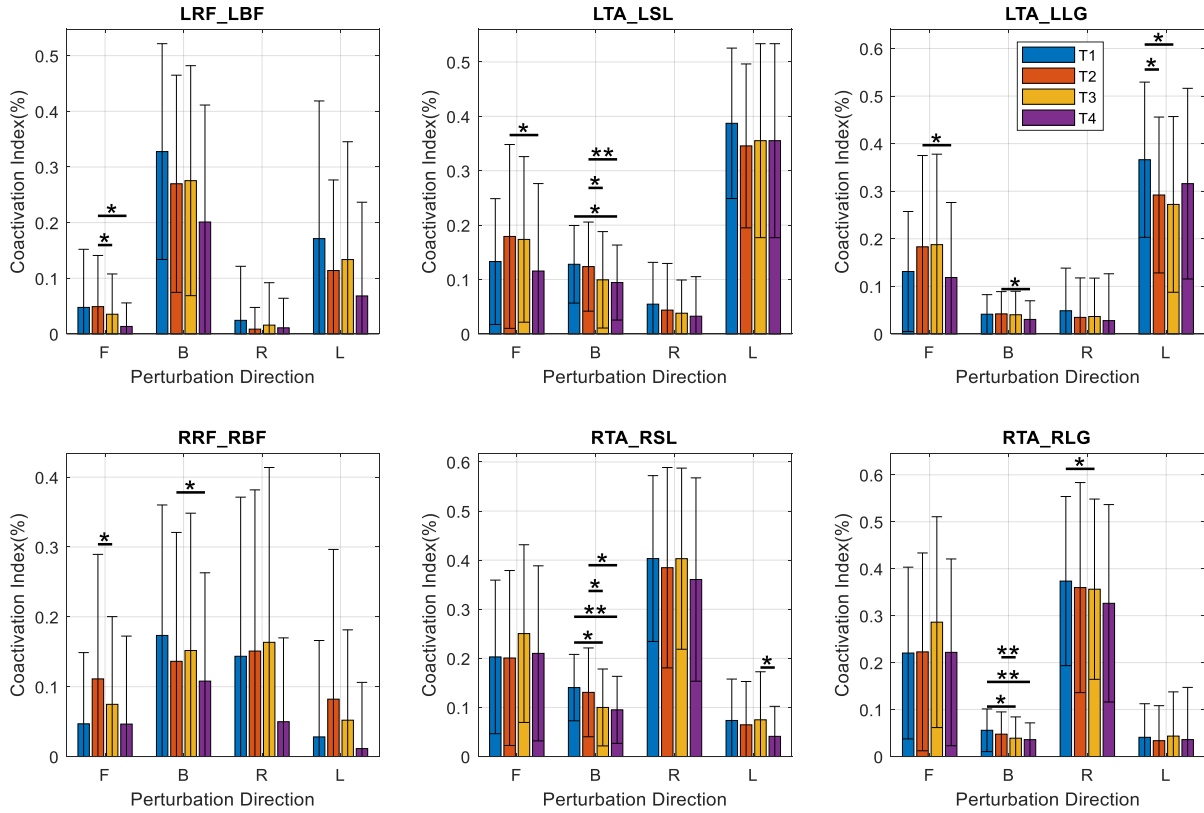


**Figure 0-6: Bar plots of coactivation indices for muscle pairs. Mean and SD values are shown at T1, T2, T3 and T4 for perturbations in the forward (F), backward (B), right (R) and left (L) directions. \* =  $p \leq 0.05$ ; \*\* =  $p \leq 0.01$**

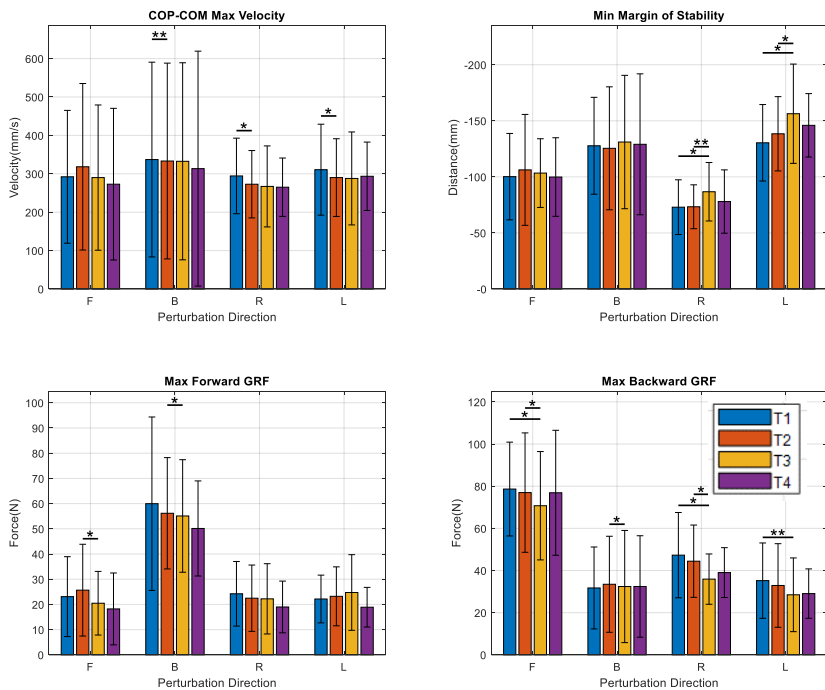


**Figure 0-5: Bar graphs of kinematic measures - COP-COM max velocity, margin of stability, max forward ground reaction force (GRF), and max backward GRF - showing mean and SD values at T1, T2, T3 and T4 for perturbations in the forward (F), backward (B), right (R) and left (L) directions. \* =  $p \leq 0.05$ ; \*\* =  $p \leq 0.01$**

CoPCoM VelMax which can be seen as a measure of how quickly the subject reacts to a perturbation decreased with significance in the backward, right and left directions (forward:  $p = .326$ , backward:  $p = .006$ , right:  $p = .021$  left:  $p = .024$ ) but not in the forward direction in which no significant change was observed

### **5.3.2 Effect of Training (T2 vs T3)**

In the comparison of T1 and T2 muscle activity increases were observed in the transfemoral muscles but between T2 and T3 no such increases were observed. There were significant decreases in muscle activity in the LRF and RRF observed by decreases in LRF\_iAEMG (forward:  $p = .028$ ), RRF\_iEMG (forward:  $p = .017$ ), RRF\_Dur (forward:  $p = .012$ ). Decreases were observed in LTA\_Dur (forward:  $p = .019$ ), and RTA\_iEMG (forward:  $p = .026$ ) for forward perturbations. In the backward direction, decreases were observed in RLG\_Dur (backward:  $p = .002$ ), and RSL\_iAEMG (backward:  $p = .031$ ). No significant changes were observed in the left and right directions.

Coactivation Indices (CI<sub>dx</sub>) had decreases. The LRF\_LBF (forward:  $p = .041$ ) and RRF\_RBF (forward:  $p = .028$ ) pairs in the forward direction and LTA\_LSL (backward:  $p = .015$ ), RTA\_RSL (backward:  $p = .016$ ) and RTA\_RLG (backward:  $p = .007$ ) pairs in the backward direction all decreased with significance.

A decrease was observed in the maximum forward ground reaction force, GRF-AP<sub>max</sub> for perturbations in both forward ( $p = .043$ ) and backward ( $p = .020$ ) directions. This was accompanied by decreases in the maximum backward ground reaction force, GRF-AP<sub>min</sub> for perturbations in the forward ( $p = .028$ ), backward ( $p = .039$ ) and right directions ( $p = .035$ ), suggesting a decrease in the magnitude in the antero-posterior forces used in balancing in both directions.

For both right and left perturbations there was an increase in COMExcursion (right:  $p = .020$ ; left:  $p = .014$ ) and in COPrms (right:  $p = .010$ ; left:  $p = .019$ ) which resulted in decreases in MeanMOS in the right direction ( $p = .049$ ) and in the MinMOS for both right and left perturbations (right:  $p = .008$ ; left:  $p = .035$ ).

### **5.3.3 Effect of Training and TSCS after TSCS is terminated (T1 vs T4)**

Between T1 and T4, the balance tests at the beginning and end, there were significant decreases in activity observed in multiple muscles. Significant decreases in LLG\_iEMG were observed in the backward ( $p = .013$ ), right ( $p = .028$ ) and left ( $p = .010$ ) directions. There were decreases in RBF\_iEMG, in the backward ( $p = .012$ ) and right ( $p = .038$ ) directions; in RLG\_iEMG in the backward ( $p = .034$ ) and left ( $p = .029$ ) directions; in RLG\_Dur in the backward ( $p = .002$ ) and left ( $p = .025$ ) directions; in the RRF\_iEMG, in the left ( $p = .026$ ) direction; in RSL\_iEMG (backward:  $p = .004$ ) and in RSL\_Dur (backward:  $p = .002$ ).

Decreases were observed in the LTA\_LSL CIdx (backward:  $p = .046$ ), RTA\_RSL CIdx (backward:  $p = .008$ ) and RTA\_RLG CIdx (backward:  $p = .004$ ).

Notably, no significant changes were observed in the kinematic and EMG measures for forward perturbations and that no notable changes in the kinematic variables were observed for all directions.

### **5.3.4 Effect of Training and TSCS while TSCS is present (T1 vs T3)**

Increases in muscle activity were observed in some muscles evidenced by an increase in LBF\_iEMG (right:  $p = .013$ ) and RRF\_Dur (backward:  $p = .042$ ). Other muscle activity changes were decreases in LSL\_Dur (backward:  $p = .008$ ), RLG\_Dur (backward:  $p = .006$ ), RSL\_Dur (backward:  $p < .001$ ), RSL\_iEMG (backward:  $p = .003$ ) and RTA\_iEMG (left:  $p = .037$ ).

There were decreases in LTA\_LLГ Cidx (left:  $p = .045$ ), RTA\_RLG (right:  $p = .028$ ) and RTA\_RSL (backward:  $p = .020$ ) and RTA\_RLG (backward:  $p = .026$ ).

A decrease was observed in MinMOS (backward:  $p = .020$ ) and MeanMOS (backward:  $p = .007$ ) for backward perturbations but was not observed for perturbations in other directions.

### **5.3.5 (T2 vs T4)**

There were no significant muscle activity increases between T2 and T4, all significant changes being decreases. Decreases were observed in the LBF\_Dur for forward ( $p = .041$ ) and backward ( $p = .014$ ) perturbations, in LRF\_Dur for backward ( $p = .018$ ) perturbations, for LLG\_iEMG for backward ( $p = .012$ ) perturbations, LRF\_iEMG for backward ( $p = .002$ ), forward ( $p = .014$ ), right ( $p = .005$ ) and left ( $p = .028$ ) perturbations, LTA\_Dur for forward ( $p = .005$ ) and right ( $p = .050$ ) perturbations, and in LTA\_iEMG for forward ( $p = .016$ ) perturbations. On the right leg, decreases were observed in RBF\_Dur for right ( $p = .018$ ) and left ( $p = .045$ ) perturbations, RBF\_iEMG for right ( $p = .022$ ) and left ( $p = .006$ ) perturbations, RLG\_Dur for backward ( $p = .002$ ), and left ( $p = .008$ ) perturbations, for RLG\_iEMG for backward ( $p = .013$ ), and left ( $p = .028$ ), for RRF\_iEMG for forward ( $p = .004$ ) and left ( $p = .005$ ) perturbations and RSL\_iEMG for backward ( $p = .013$ ) perturbations.

Cidxs' of the LTA\_LLГ decreased in the forward ( $p = .014$ ) and backward ( $p = .035$ ) directions, LTA\_LSL in the forward ( $p = .012$ ) and backward ( $p = .002$ ) directions, RRF\_RBF in the backward ( $p = .042$ ) direction and RTA\_RSL in the backward ( $p = .021$ ) direction.

### **5.3.6 H-Reflex Recruitment Curve Analysis**

The H-reflex recruitment curve was fit to 10 of the 11 subjects. Data points for one subject did not take the recognized shape of the recruitment curve. For the 20 sets of recruitment curve data points collected (ten subjects recorded at P1 and P2), the number of data points used to fit the recruitment curve ranged between 6 and 12. The  $R^2$  error measuring goodness of fit had a mean = 0.971, SD = 0.029. With the curves fit and the curve characteristics extracted paired t-tests were carried out between results in P1 and P2.

No significant changes between P1 and P2 were observed in HMax ( $p = .874$ ), HSlope ( $p = .198$ ) and HCurrent50 ( $p = .542$ )

### 5.3.7 PRM Results

A t-test comparison of the PRM reflex threshold at P1 and P2 yielded no significant change ( $p = .864$ ). There was no uniform effect of the protocol on the subjects as threshold increased by 3mA or more in two subjects, decreased by 3mA or more in four others and change by less than 3mA in 5 subjects. Figure 5-7 shows the changes in PRM\_Threshold of each subject.

Subjects' responses to 120% of the spinal stimulation threshold established in P1 were compared between P1 and P2 with T-tests. Since the protocol through which the threshold was determined only required the presence of a response in the RSL or LSL, low levels of muscle activation were observed in other muscles. Levels of activation below 50  $\mu\text{V}$  were registered as "0".

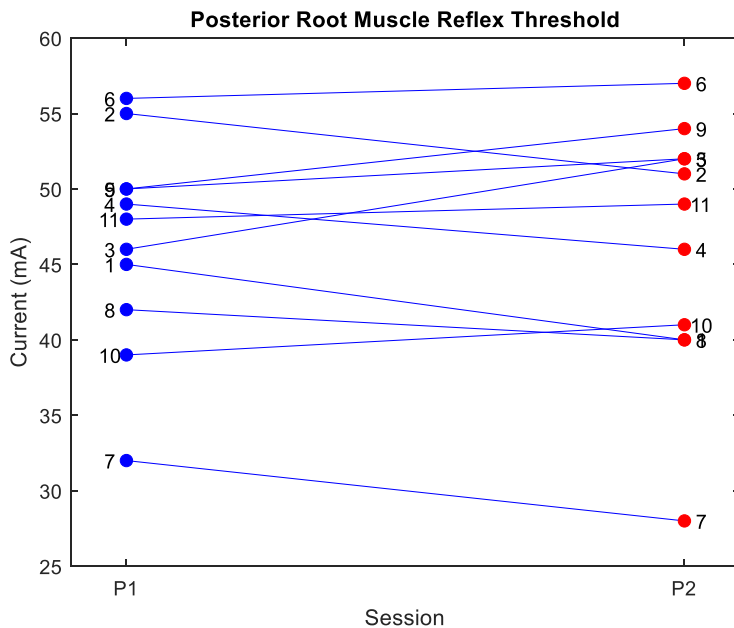


Figure 0-7: Pretest and posttest values of posterior root muscle reflex thresholds in the pretest (P1) and posttest (P2). Numbers on the side are for subject identification

### 5.3.8 H-Reflex Recovery Cycle

T-test comparisons between the magnitude of the pretest and posttest conditioned h-reflex at 80, 150, 250, 500 and 1000ms ISIs yielded a significant increase only at the 500ms ISI ( $p = .04$ ), Figure 5-8.

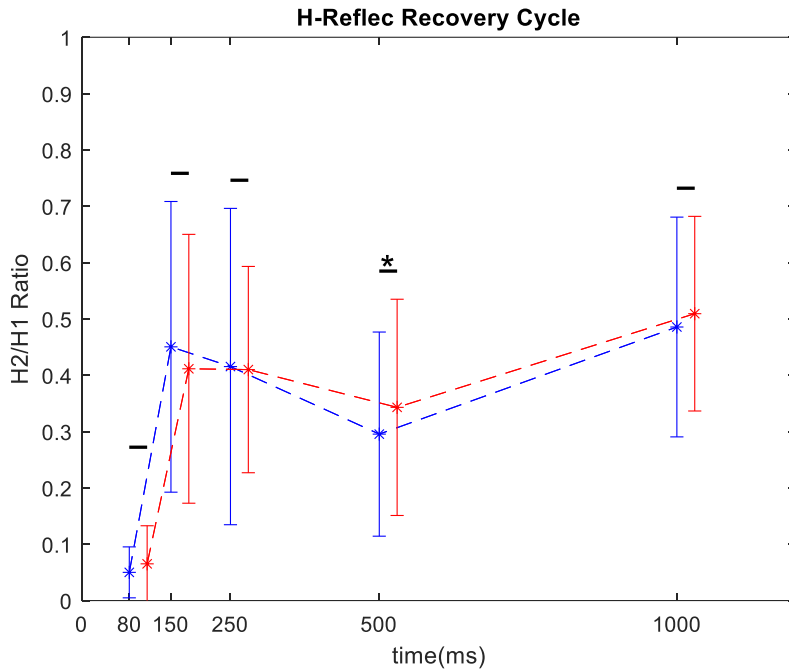


Figure 0-8: H-reflex recovery cycle. H2/H1 ratios at 80, 150, 250, 500 and 1000ms interstimulus intervals. \*:  $p \leq .05$

### 5.3.9 Correlation between Changes in Variables

Correlations between the change in the neurophysiological measures and that in the kinematic and EMG measures were examined in order to identify potential causal relationships between spinal excitability and functional performance.

Although significant changes were hardly observed in the neurophysiological measures correlations between them were examined. Pre-post changes in the PRM threshold correlated inversely and significantly with changes in the amplitude generated by 120% of the pretest PRM threshold in LSL ( $r(7) = -.846, p = .016$ ), LBF ( $r(7) = -.829, p = .021$ ), LLG ( $r(7) = -.750, p =$

.032) and RLG ( $r(7) = -.818, p = .013$ ). The change in PRM threshold also correlates inversely with the change in HMax ( $r(7) = -.724, p = .027$ ).

Changes in HMax were correlated with changes in LSL ( $r(7) = .799, p = .031$ ), LBF ( $r(7) = .949, p = .032$ ), LTA (coef:  $.957, p = .011$ ) and RBF ( $r(7) = .702, p = .035$ ).

Isi500 shankHipstrategy ( $r(7) = -.699, p = .036$ )

When we observed the strategies used by subjects, we noticed that the subjects react in two distinct ways. As we see in Figure 5-9, all subjects start out applying an ankle strategy but about 500ms after the start of the perturbation, subjects 3,6,10 and 11 turn to using the hip strategy. Subsequently subjects were divided into two groups and an ANOVA was carried out to examine the effect of two factors time, i.e. the effect of the protocol, and group on the balance strategy used. The ANOVA confirmed that the balance strategy employed by the two groups were significantly different ( $F(17.758, df = 1) = p < .001$ ): but there was no effect of time or an interaction effect between time and group. It was also found that the strategy had a strong correlation with the percentage change in HCurrent50 ( $r(7) = .7798, p = .013$ ) between pre and posttest and that group had positive percentage change and the other group was negative. They shall be called  $\Delta S50+$  and  $\Delta S50-$  respectively.

Along these lines, group differences were observed in other variables as well. COPExcursion ( $F(1,7) = 5.928, p = .022$ ) COPvelrms ( $F(1,7) = 5.703, p = .24$ ), CoPCoMrms ( $F(1,7) = 9.366, p = .005$ ), CoPCoMvelrms ( $F(1,7) = 6.886, p = .014$ ). Examining the difference in performance  $\Delta S50+$  and  $\Delta S50-$  groups during each balance test, it was observed that there were significant differences at in anterior perturbation HipStrat at T1 ( $53.36\% + 4.61\%$  vs  $44.83\% + 4.20\%$   $t(6.247) = -2.868, p = .027$ ), and T3 ( $54.64 + 4.33$  vs  $39.01\% + 4.52$   $t(6.699) = -5.28, p = .001$ ) between the two groups with the  $\Delta S50+$  group favoring the hip strategy. With respect to muscle activity,

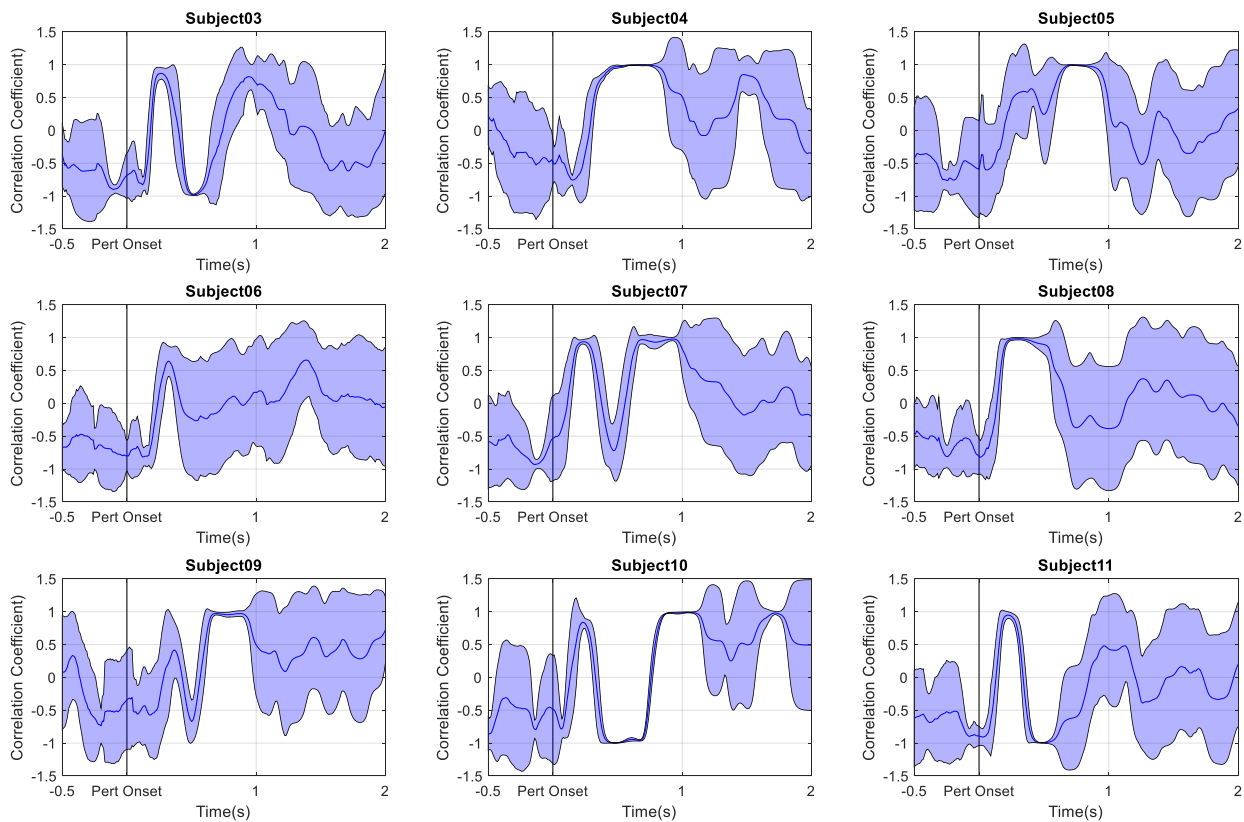


**Figure 0-9: Correlation coefficient of trunk rotation and shank rotation. Positive values above 0.3807 indicate Ankle strategy and negative values below -0.3807 indicate Hip strategy. Subjects 4, 5, 6, 8 and 9 have average correlation coefficient significantly lower than subjects 3,7,9,10 and 11 indicating that they use the hip strategy more often.**

there were no significant differences at T1 and T2 but significant differences were present in T3 for RRF\_Dur ( $1.96s + 1.31$  vs  $0.25 + 0.22$   $p = .042$ ), LRF\_Dur ( $1.55 + 0.20$  vs  $0.18 + 0.20$   $p = .012$ ) and LRF\_iEMG ( $p = .005$ ) and T4 for RRF\_Dur ( $1.39 + 0.69$  vs  $0.20 + 0.23$   $p = .020$ ), LRF\_Dur ( $0.88 + 0.46$  vs  $0.11 + 0.00$   $p = .020$ ), LRF\_iEMG ( $p = .027$ ) with the delta S50+ group having higher muscle activity.

## 5.4 Discussion

This experiment aimed to explore the effect of TSCS applied in tandem with the performance of a functional task. The experiment tested the impact of TSCS on performance in the immediate period after it was activated and its effects after a training intervention in which subjects

simultaneously received stimulation. It was hypothesized that exposure to TSCS would increase spinal excitability, which could have an incremental effect on reactive balance control. It was also hypothesized that TSCS would increase background muscle activation levels, facilitating higher muscle exertion during a task. Muscle activation increases were observed between some conditions (particularly in comparing T1 and T2), but a decrease in perturbation success rate accompanied these increases. The subsequent paragraphs will attempt to explain the changes that occurred between the different testing conditions.

The phenomenon of muscle activity reduction after multiple repetitions of a task is a common occurrence in motor control studies and one that is important in understanding the motor control changes observed in this study. It is a general rehabilitation principle that postural strategies improve with repeated exposure to a destabilizing stimulus [56], [168]. As people become more accustomed to a disturbance, the reaction involves less excessive muscle activation and improvement in performance [168]. Horak et al. noted that this improved performance emerges alongside a reduction in the torque response even if muscle onset latency does not change, further leading to the quicker attainment of a stable equilibrium position [169]. Babic et al and Welch et al [57], [155] provide the context that these changes result from the motor system optimizing for safety, energy expenditure, and the task requirement. Thus, as subjects become more comfortable and familiar with a task, they make a tradeoff between energy expenditure and safety while still fulfilling the task requirement. The effect was observed as muscle activity reductions in some conditions in the experiment, and it will be referred to here as the activity adaptation.

#### **5.4.1 Spinal Excitability**

Assessments of the H-reflex recruitment curve, its recovery cycle, PRM threshold, and PRM amplitude responses did not yield significant results except for an increase in the conditioned amplitude at 500ms ISI. The dominant process that causes attenuation of the H-reflex at this stage

of the recovery cycle is homosynaptic depression [120], [170] and is said to be caused by a reduced probability of neurotransmitter release after an initial activation at the synapse. The small increase observed could be explained as the priming of the spinal circuits after being stimulated for an amount of time and can be seen as the system being primed for activity.

The lack of significant changes in the other variables may be due to the timing of the assessments. Between the end of T3, when TSCS was deactivated, and the start of P2, the neurophysiological posttest, T4 was carried out. This took 30 mins on average. It is possible that the effects of TSCS had worn off before the start of P2, and spinal excitability changes could not be captured with our measurement protocol.

There is also an interaction between two effects. In Chapter 4 we demonstrated that TSCS reduces post-activation depression and increases the synaptic efficacy of the afferent – motoneuron connection. Therefore, we would have expected a similar increase in recovery in this experiment, but this was not the case. The difference in this experiment is the isochronous balance task which, as explained earlier, has the effect of reducing muscle activity. We suspect that this effect counteracts the effect of TSCS, which is why a significant increase in recovery was observed only at one ISI.

Hence, the lack of change in spinal excitability can be ascribed to the presence of two phenomena that have opposite effects on excitability.

Muscle activity and kinematic metrics were assessed during T1, T2, T3, and T4 balance tests. Subjects' responses varied by direction of perturbation as different muscle combinations were used in different directions, so responses were assessed directionally.

#### **5.4.2 Immediate Effects of TSCS (T1 vs. T2)**

The comparison between T1 and T2 best demonstrates the effect of TSCS on muscle activity in this experiment. Increases in muscle activity were observed in select muscles for perturbations in the forward, left, and right directions. These changes were accompanied by a deterioration in balance performance for forward perturbations and adaptations towards better coordination for lateral perturbations. No increases in muscle activity were observed for backward perturbations. It is important to note that these increases occurred despite the high probability that the activity reduction adaptation has an effect since T2 always comes after T1. Thus, our observation of increased muscle activity is unusual and suggests an effect of TSCS.

In each direction where these muscle activity increases were observed, the increases were in muscles that are not the primary support muscles for balance in that direction. For example, for left perturbations, subjects shifted their weight onto the left leg, but activity increase was observed in the RRF\_iEMG, while for right perturbations, activity increases were observed in the L-BF\_iEMG and LBF\_Dur. For forward perturbations, if we assume subjects used an ankle strategy, the R-RF and L-RF, muscles in which we observed increases, are expected to remain relatively inactive while the R-BF and L-BF are expected to be activated [30]. This suggests that the CNS prioritizes control over goal-critical muscles, making them conform to the activations required for the task at hand.

An improvement in balance performance did not accompany the observed muscle activity increases. In fact, the trial success rate and the average MOS for perturbations in the forward direction decreased with the use of TSCS. This suggests that increased muscle activity did not translate directly into improved performance in a task that required coordination.

According to Gerasimenko and colleagues, TSCS at increased intensities can have an occlusion effect on afferent pathways [101]. It is possible that this effect may result in reduced

sensory input and in turn, reduced efficacy of coordination as observed for forward perturbations. Deterioration of coordination could also result from a reduction in presynaptic inhibition. The CNS uses presynaptic inhibition to manage the sensory input it constantly receives from the environment in order to focus on the motor task that is a priority at the time [126]. It does this by suppressing the excitability of sensory afferents, thereby allowing the controlled execution of the priority task. Nielsen et al. [137] showed that ballet dancers, who regularly perform highly coordinated movements, have greater presynaptic inhibition than other athlete groups. On the other hand, TSCS acts to move sensory neurons closer to depolarization, causing an increase in the probability of triggering motor neurons [100], resulting in increased motor neuron excitability and reduced presynaptic inhibition [124], [171]. Increasing the excitability of sensory afferents could lead to a reduction of presynaptic inhibition, which leads to the body becoming more sensitive to sensory inputs. This causes unwanted motor activity in the muscles, making balance control more difficult. Thus, the increased motor activity observed in this experiment could deteriorate balance.

Deterioration of coordination could also result from TSCS disrupting spinal regulatory mechanisms, including alterations in presynaptic inhibition and recurrent inhibition. The central nervous system uses presynaptic inhibition to manage sensory input it constantly receives from the environment in order to facilitate an ongoing or planned motor task [126]. It does this by suppressing the excitability of sensory afferents, thereby allowing the controlled execution of the priority task. TSCS stimulates many sensory afferents at multiple spinal levels. Sensory afferent activity impacts various spinal regulatory pathways, including those of reciprocal inhibition, heteronymous monosynaptic Ia excitation, and presynaptic inhibition [126], [171]. These effects on spinal regulatory pathways could affect coordination of muscle activation.

The right, left, and backward responses show adaptations towards better-controlled reactions. There were decreases in COP-COM max velocity. COP-COM is a variable that correlates with the restoring torque applied to the COM [172], [173]. A reduction in its maximum velocity suggests an adaptation towards a less forceful, more stable reaction. Reductions in the L-TA/LG CIdx and the COP-COM max velocity for left perturbations also point to the same effect. Muscle activity increases were observed in the left and right perturbations, but those increases did not prevent this adaptation towards greater stability. This could be because, as stated earlier, the increases were observed in the non-critical side as in lateral perturbations almost all the weight is shifted to the leg on the side of the perturbation. In the backward direction, all the changes pointed to reductions in applied restorative force and more controlled reactions, which is the expected adaptation to repeated balance perturbations. It is important to note that adaptation in the COP-COM is absent from the forward perturbation responses in which the greatest increase in muscle activity and a reduction in perturbation balance success rate was observed.

In summary, turning on TSCS leads to increased muscle activity especially in muscles not directly implicated in the functional task and continued exposure to perturbations results in energy saving adjustments which include the decrease of muscle activity.

### **5.4.3 Effect of Training with TSCS (T2 vs. T3)**

The overarching change observed between T2 and T3 was a reduction in muscle activity and an adaptation towards the use of less force in reactive balance control. Subjects in both tests have TSCS on, but T3 occurs after the training intervention. The training intervention increased the subjects' comfort with perturbations, leading to decreased muscle activity. In the forward direction, decreases were observed in the L-RF and R-RF muscles, the same muscles in which increased activity was observed between T1 and T2. These reductions, accompanied by a non-significant increase in perturbation success rate (93% in T2 to 97.5% in T3), suggest that the neural system

of the subjects adjusted to TSCS input and reduced muscle activity to levels that allowed for the restoration of the initial level of balance performance. The increased success rate, decreases in ground reaction force and MOS, and an increase in COMExcursion suggest that after the training intervention, the subjects arrived at a more successful strategy for balance control that required less vigorous reactions and hence less energy expenditure. Therefore, the adaptive processes of the motor system were able to overcome the disruptive effect of TSCS, suppress the heightened muscle activity, and achieve a higher level of performance.

#### **5.4.4 Effect of Deactivating TSCS (T3 vs. T4)**

The forward direction was where the LRF and RRF experienced increases between T1 and T2 (TSCS effect) and decreases between T2 and T3 (adaptive effect). Along with other muscles, muscle activity reductions were observed in the RRF and LRF for forward and left perturbations between T3 and T4. This muscle, which most exhibited activity increasing effects of TSCS displayed a large fall in muscle activity once TSCS was deactivated, suggesting that TSCS increased muscle activity in previous balance tests. The activity reduction effect also contributed to the reduced activity observed in LRF and RRF.

The big drop in muscle activity in T4 is exemplified by the comparison between T2 and T4. Here, there is the double pressure of the activity reduction effect and the removal of TSCS. These results strongly point towards the counterbalancing of the effects of TSCS and the activity reduction effect.

#### **5.4.5 Effect of Training and TSCS (T1 vs T4)**

In comparing T1 and T4, we test whether there are any effects of TSCS and the training intervention after TSCS is deactivated. At this point the subject has been subjected to the opposing effects of the activity reduction adaptation and the activity augmenting effect of TSCS. Also, at this point TSCS is turned off reducing the excitatory input to the sensory neurons in the spine. In

the right, left and backward directions muscle activity decreases were observed in a large number of muscles which may have been caused by the doubly depressing effect of the removal of the increase caused by TSCS and the activity adaptive effect.

In the forward direction, there were no significant increases or decreases. In an experiment without TSCS it would be expected that the adaptive effect would have caused muscle activity reductions but its absence points towards a residual effect of TSCS. The presence of large reductions in other muscles assessed in the other directions would suggest that TSCS did not have an effect on muscle activity and an alternative explanation can be proposed that builds on our expectations of what the effect of TSCS should be. In lieu of the increase in excitatory stimuli introduced by TSCS, as observed between T1 and T2, it is thought that the motor system adapts to this by suppressing this new excitation. In healthy subjects it would seem increased excitation has a disadvantageous effect as we observed a decrease in perturbation success rate for perturbations in the forward direction. In order for the motor system to continue to perform optimally the excitation is suppressed. Both the inhibitory processes in the spine and descending supra-spinal commands are capable of causing this suppression. Hence it would seem that the adaptation induced by TSCS in the subjects is not the muscle activity increase hypothesized but a stronger suppression of muscle activity.

#### **5.4.6 Other Results**

One peculiar result worth investigating was the presence of a relationship between the percentage change of the S50 current of the H-reflex and the balance strategy utilized by the subjects. When subjects with a positive change in S50 between P1 and P2 were grouped together and those that experienced a negative change are made into another group, it was found that the first group displayed a propensity to use the hip strategy while the other the ankle strategy. This propensity was not the result of TSCS as the subjects already demonstrated this bifurcation at T1.

It is suggested here that there is a relationship between the subjects' tendency to select the ankle or hip strategy and his neurophysiological reaction to stimulation.

Looking at the difference in performance of these two groups during each balance test, it was observed that there were significant differences at T1, T3 and T4 between the two groups with the delta S50+ group favored the hip strategy. With respect to muscle activity, there were no significant differences at T1 and T2 but significant differences were present in the RRF and LRF between T3 and T4 with the delta S50+ group having higher muscle activity.

An increase in S50 would imply a shift of the H-reflex recruitment curve to the right and hence is termed a right-shift in literature. A right-shift also implies that more current is needed to generate a certain voltage of the H-reflex response which means that the reflex becomes less excitable. The reverse holds so that a negative change implies a left-shift and more excitability. Therefore subjects who favored the hip strategy which involves greater coordination [106] and who displayed greater muscle activity, at the end of the training adapted towards suppression of the H-reflex, a right shift of the recruitment curve. Vice versa, subjects who favored the ankle strategy adapted towards greater excitability of the H-reflex. At this point of our research, we can only speculate about the cause of this relationship but future experiments can be setup to determine whether this finding is just a result of chance or a real effect of balance strategy on spinal excitability.

#### **5.4.7 Conclusion**

In this study, we have shown the effect of applying TSCS during a training exercise in healthy subjects. Most significantly we have observed the interaction of the muscle activity reduction effect of caused by continuous repetition of an activity and the muscle activity augmentation effect of TSCS. Once TSCS is turned on there is an initial increase in muscle activity in select muscles which leads to worse perturbation performance in the forward direction. Subsequently, with more exposure to the perturbations and after training, the motor system adjusts and returns muscle

activation levels lower and coordination improves. With the removal of stimulation, muscle activity gets even lower, suggesting that the body has adapted towards suppression of muscle activity. The mechanism of this suppression could be the result of greater presynaptic inhibition, hyperpolarization of the sensory afferents, or a number of other neural processes and it needs to be further investigated.

These results provide some insight into the complex interactions of the different parts elements in the CNS and what triggers could be used to get a desired behavior. In future studies, the activity combined with TSCS should be in which greater muscle exertion leads to better performance in order to take advantage of the effect of TSCS. Alternatively changing the parameters for TSCS could generate different adaptations that could lead to improvements in task performance. For example, 60 Hz stimulation has been used to reduce spasticity. This could generate increased inhibition in healthy subjects as well which could possibly lead to greater control and better performance. Nevertheless, the observed spinal plasticity and increases in muscle activity suggests that 30 Hz simple pulsed current could be beneficial for people with SCI.

## Conclusion

This study aimed to explore exercise and electrical stimulation as methods of improving postural balance control by taking advantage of the neuroplasticity of the CNS so as to project its uses in the rehabilitation of spinal cord injury (SCI) patients.

### 6.1 Summary of Contributions

In RobUST, we developed a device that is effective at executing perturbation-based balance training (PBT) in healthy subjects. Training with RobUST led to the improvement of postural balance control. Attaching to subjects via cables and harnesses, it avoids the drawbacks of most other exoskeletons by permitting full actuation of the subjects' joints, and full loading of the limbs, while still being able to control the movement of subjects. With this setup, subjects could explore the balance strategies that occurred naturally to them without much encumbrance. We hypothesize that this makes the strategies learned more transferable to real-world situations. In addition, we integrated virtual reality (VR) and PBT in RobUST, so that the subject's position and the occurrence of training events were synchronized in RobUST and the VR game. The results of this experiment indicate that subjects trained in RobUST with and without assistance improved their ability to withstand perturbations. They make changes to their balance control strategies that optimize the mechanical and metabolic cost of movement. This shows up as increases in perturbation force threshold and reductions in muscle activity in most of the muscles assessed. RobUST-assisted training was found to have slightly different adaptations than non-assisted training. Non-assisted subjects reacted faster and adapted towards more use of the hip strategy. This indicates that although both groups improved postural balance, subjects in the assisted group learned to rely on RobUST, so the non-assisted group had more robust responses. In impaired populations, it can thus be used as a way of scaling the balance training so that subjects who cannot

stand without assistance use it until they can support themselves and receive training without support. This was done recently in a study with SCI patients at the University of Louisville [174].

In the second study discussed in this work we tested the effect of transcutaneous spinal cord stimulation (TSCS) on the neurophysiological and balance characteristics of healthy subjects. A MATLAB-based app for the collection of muscle activity during physiological tests was developed. The app can collect data for H-reflex recruitment curve, H-reflex recovery cycle, and posterior root muscle reflexes. It can be easily modified to include more operating modes. Protocols for the collection of these assessments were also developed.

Experimental results found that TSCS caused a leftward shift of the H-reflex recruitment curve and increased H-reflex recovery. It was postulated that this resulted from hypopolarisation of sensory afferents due to prolonged exposure to TSCS. Hypopolarisation of neurons reduces their resting potential, so they are more easily excited to release excitatory postsynaptic potentials (EPSPs), increasing synaptic efficacy. This change was not reflected in kinematic and electromyographic (EMG) measures taken during balance tests carried out without TSCS. It was concluded that TSCS modulates the excitability of spinal circuits by hypopolarisation of the synapse.

TSCS was combined with exercise to assess the effect of these two sources of neuroplasticity on subjects' neurophysiological and balance characteristics. It was found that these two intervention modes have opposing effects on muscle activity. Repeated exercise reduced muscle activity and TSCS led to elevated muscle activity. The concurrent interaction of these two interventions was such that an initial increase in muscle activity accompanied by a reduction in trial success rate was followed by a reduction in muscle activity with continued practice. This suggests that the elevation of muscle activity in healthy subjects is detrimental to coordination,

and the CNS suppresses this increase to institute control. These results show that, although detrimental, TSCS does have an effect on the balance performance in subjects. The elevated levels of TSCS would be beneficial for SCI subjects in whom it could augment the release of EPSPs from sensory afferents by the residual weak cortical signals available.

## **6.2 Challenges and Limitations**

The primary challenge in this work was identifying a balance exercise that was challenging enough for healthy subjects and in which sizeable improvement could be observed in a single-day training session. There were limitations on motor response speed as well as motor current limits that limited the quickness and amplitude of the perturbing forces. For assessment of reactive balance control, the perturbing force should ideally be instantaneous, but we were unable to produce quick-acting forces with enough power to destabilize the subjects. Therefore the perturbing force continued for a few hundred milliseconds after the subjects became conscious that they were being perturbed. It was thus difficult to separate reaction movements from movements forced by the device. Future versions of RobUST should have more compliant, quicker reacting motors capable of applying large forces quickly.

In the first study described, there was a limited number of valid trials for statistical comparison. This affected our statistical tests' power and ability to draw conclusions.

Concerning TSCS, our primary limitation was our inability to carry out the neurophysiological tests during the balance tests. In the literature, it has been suggested that the neurophysiological measures tested vary with the muscle contraction and the body's posture. Therefore, collecting these measures during balance tests would have supplied information about the state of spinal circuits during the activity which would have been a better measure of the intervention.

The fact that the effects of TSCS and those of exercise were in opposition to each other meant that it was difficult to assess whether TSCS may have been beneficial in other ways e.g., in learning rate of the subjects.

Lastly, there is no certainty that the results gained from experimentation with healthy subjects will be transferable to SCI subjects or subjects with other pathologies. Still, we can rely on the commonalities in the CNS of the systems to predict what results will hold true. Taccola et al. suggest as much [100]. In SCI, the lesion disrupts the normal operation of the nervous system so that supraspinal signals do not reach below the lesion. This precludes the normal operation of reflexes and other processes like presynaptic inhibition. We can predict that with TSCS, SCI subjects will also experience elevated muscle activity if stimulation is done below the lesion, but it is unlikely that the activity would be suppressed as quickly as in uninjured subjects. This is because we hypothesize that the suppression is mediated cortically, and as there is minimal supraspinal control in SCI subjects there is unlikely to be suppression. Therefore we hypothesize that TSCS would yield increased muscle activity that would be beneficial the SCI population.

### **6.3 Future Work**

In this dissertation, We have attempted to study how effective TSCS is as a replacement for epidural stimulation. TSCS was used because it offers a more accessible method for delivering electrical stimulation to subjects so that they do not need to undergo risky, expensive surgeries to implant electrodes. The task we undertook was to show that TSCS has the potential to generate positive neural changes in the nervous system that could improve postural balance control. Unfortunately, we could not make this conclusion from our results but there are several opportunities for research that we think can be carried out to achieve this goal.

There is some uncertainty as to which intervertebral position permits the best penetration of electric charge to the most relevant neurons for postural balance control improvement. The factors to consider are the directions in which the electric field disperses, the strength of the signal in the different directions, and the impact of signal strength on the generation of plasticity. Research into the relationship between these factors can provide needed guidance on where to place electrodes in order to get a desired effect.

In this experiment TSCS led to an increase in muscle activation accompanied by a decrease in functional performance. One reason for this disadvantageous relationship, we think, is that, especially with the hip strategy, coordination of muscles was also very important and TSCS disrupted this coordination. We postulate that choosing a task in which greater muscle activation invariably leads to better performance would harness the power of TSCS to increase muscle activation and thus benefit functional task goals. Exercises like loaded knee extensions, push-ups, squats, and deadlifts may show performance improvements with TSCS. Additionally, although challenging to implement, the subjects could be restricted to using only the ankle strategy during the task. For example, the ankle strategy in forward sway involves strong contractions of the soleus, gastrocnemius, and bicep femoris muscles. The limit of this contraction for standing upright can easily be reached; hence, improvements in this would more easily be identified if TSCS can increase the strength of the contraction.

We can attempt to overcome the disruptive effect of electrical stimulation by using pulses timed to coincide with bursts of activity in specific muscles. Coordinated pulses can be achieved by identifying the muscle synergy organization for the movement of interest and then passing an electrical pulse during the phase in which the muscles of interest are active.

In Chapter 5, we postulated that the destabilizing effect of electrical stimulation on functional performance resulted in the nervous system of healthy subjects moving to suppress muscle activity. We think this suppression was achieved by some neuro-inhibitory processes. The response in patients with pathologies affecting the nervous system will be different, especially in spinal cord injury patients, as the inhibitory processes, which are mediated by supraspinal signals, are abrogated. SCI patients have a lesion in the spinal cord that interrupts spinal signals, so the amount of supraspinal signals arriving below the lesion is significantly reduced. Thus, the suppression observed in healthy subjects will not be present because of the lack of mediation from the cortical centers, and therefore increased muscle activation will be sustained. Thus, we postulate that there is a greater potential for TSCS to be beneficial for subjects with neurological pathologies than healthy patients, as their neuropathies will not get in the way of its effects. This theory should be explored in future studies primarily as it can provide a greater understanding of the nature of spinal cord injury and other pathologies.

There is still a tremendous amount left to understand about the effects of TSCS and the influence of the different parameter settings. Research is already going on using high-voltage power sources with carrier frequencies. Also, literature suggests that the frequency of stimulation can change its motor effect on the nervous system; for example, 30 Hz pulses are prescribed for improving functional task performance, and 60 Hz pulses for reducing spasticity. In addition, the polarity of the pulses has been shown to modulate the effect of electrical stimulation. Future studies can combine these parameters in various ways to come to an understanding of the optimal setting to achieve a desired result.

Lastly, the experiments presented in this dissertation put subjects through only a one-day training session. Longitudinal studies with TSCS should be carried out to allow for the potential

compounding of TSCS effects to be more measurable. In addition, the persistence of the effects should be investigated.

## References

- [1] F. B. M. J. Horak, “Postural orientation and equilibrium,” in *Handbook of physiology*, 1996.
- [2] F. B. Horak and J. M. Macpherson, “Postural Orientation and Equilibrium,” in *Comprehensive Physiology*, 2011. doi: 10.1002/cphy.cp120107.
- [3] A. Shumway-Cook and M. H. Woollacott, *Motor control: Translating research into clinical practice: Fourth edition*. 2014.
- [4] H. W. Wallmann, “The basics of balance and falls,” *Home Heal. Care Manag. Pract.*, vol. 21, no. 6, pp. 436–439, 2009, doi: 10.1177/1084822309337189.
- [5] L. H. Ting, “Dimensional reduction in sensorimotor systems: a framework for understanding muscle coordination of posture,” *Progress in Brain Research*. 2007. doi: 10.1016/S0079-6123(06)65019-X.
- [6] “Important Facts about Falls | Home and Recreational Safety | CDC Injury Center.” <https://www.cdc.gov/homeandrecreationalafety/falls/adultfalls.html> (accessed Nov. 22, 2020).
- [7] J. Tresilian, *Sensorimotor Control and Learning*. 2012. doi: 10.1007/978-1-137-00511-3.
- [8] P. Kroker, “The problem of remaining upright,” *BMJ Br. Med. J.*, vol. 319, no. 7220, p. 1300, Nov. 1999, doi: 10.1136/BMJ.319.7220.1300.
- [9] B. G. Rasman, P. A. Forbes, R. Tisserand, and J. S. Blouin, “Sensorimotor manipulations of the balance control loop-beyond imposed external perturbations,” *Front. Neurol.*, vol. 9, no. OCT, pp. 1–17, 2018, doi: 10.3389/fneur.2018.00899.
- [10] “The Somatosensory System | Boundless Anatomy and Physiology.” <https://courses.lumenlearning.com/boundless-ap/chapter/the-somatosensory-system/> (accessed Dec. 17, 2021).

- [11] J. Cole, “Large-fiber Sensory Neuropathy: Effect On Proprioception,” *Encycl. Neurosci.*, pp. 2105–2107, Nov. 2009, doi: 10.1007/978-3-540-29678-2\_2696.
- [12] “Neuropathy (Peripheral Neuropathy).” <https://my.clevelandclinic.org/health/diseases/14737-neuropathy> (accessed Dec. 18, 2021).
- [13] U. Misra, J. Kalita, and P. Nair, “Diagnostic approach to peripheral neuropathy,” *Ann. Indian Acad. Neurol.*, vol. 11, no. 2, p. 89, Apr. 2008, doi: 10.4103/0972-2327.41875.
- [14] D. M. Stramel, R. M. Carrera, S. A. Rahok, J. Stein, and S. K. Agrawal, “Effects of a Person-Following Light-Touch Device During Overground Walking With Visual Perturbations in a Virtual Reality Environment,” *IEEE Robot. Autom. Lett.*, vol. 4, no. 4, pp. 4139–4146, Jul. 2019, doi: 10.1109/LRA.2019.2931267.
- [15] J. R. Lackner, E. Rabin, and P. DiZio, “Stabilization of posture by precision touch of the index finger with rigid and flexible filaments,” *Exp. Brain Res.*, vol. 139, no. 4, pp. 454–464, 2001, doi: 10.1007/s002210100775.
- [16] P. A. Forbes, A. Chen, and J. S. Blouin, “Sensorimotor control of standing balance,” *Handb. Clin. Neurol.*, vol. 159, pp. 61–83, Jan. 2018, doi: 10.1016/B978-0-444-63916-5.00004-5.
- [17] H. Aoki, S. Demura, H. Kawabata, H. Sugiura, Y. Uchida, N. Xu, and H. Murase, “Evaluating the effects of open/closed eyes and age-related differences on center of foot pressure sway during stepping at a set tempo,” *Adv. Aging Res.*, vol. 2012, no. 03, pp. 72–77, Nov. 2012, doi: 10.4236/AAR.2012.13009.
- [18] T. Nagata, Y. Fukuoka, A. Ishida, and H. Minamitani, “Analysis of role of vision in human upright posture control,” *Annu. Int. Conf. IEEE Eng. Med. Biol. - Proc.*, vol. 2, pp. 1155–1158, 2001, doi: 10.1109/IEMBS.2001.1020396.
- [19] F. Horak and J. Macpherson, “Postural orientation and equilibrium. En: Shepard J, Rowell

- I, eds. *Handbook of Physiology.*,” vol. Section 12, no. Chapter 7. pp. 255–292, 1996.
- [20] F. Horak and A. Kuo, “Postural Adaptation for Altered Environments, Tasks, and Intentions,” *Biomech. Neural Control Posture Mov.*, pp. 267–281, 2000, doi: 10.1007/978-1-4612-2104-3\_19.
- [21] L. M. Nashner, C. L. Shupert, F. B. Horak, and F. O. Black, “Chapter 33 Organization of posture controls: an analysis of sensory and mechanical constraints,” *Prog. Brain Res.*, vol. 80, no. C, pp. 411–418, Jan. 1989, doi: 10.1016/S0079-6123(08)62237-2.
- [22] F. B. Horak, “Clinical Measurement of Postural Control in Adults,” *Phys. Ther.*, vol. 67, no. 12, pp. 1881–1885, Dec. 1987, doi: 10.1093/PTJ/67.12.1881.
- [23] S. M. Henry, J. Fung, and F. B. Horak, “Control of stance during lateral and anterior/posterior surface translations,” *IEEE Trans. Rehabil. Eng.*, vol. 6, no. 1, pp. 32–42, 1998, doi: 10.1109/86.662618.
- [24] G. M. Blenkinsop, M. T. G. Pain, and M. J. Hiley, “Balance control strategies during perturbed and unperturbed balance in standing and handstand,” *R. Soc. Open Sci.*, vol. 4, no. 7, 2017, doi: 10.1098/rsos.161018.
- [25] M. Bruton and X. Nicholas O’dwyer, “Synergies in coordination: a comprehensive overview of neural, computational, and behavioral approaches,” *J Neurophysiol*, vol. 120, pp. 2761–2774, 2018, doi: 10.1152/jn.00052.2018.-At.
- [26] “Motor units.” <https://ouhsc.edu/bserdac/dthompsoweb/namics/mu.htm> (accessed Dec. 23, 2021).
- [27] “What Is a Motor Unit? Motor Units and Strength Training.” <https://www.verywellfit.com/motor-unit-part-of-muscles-1231223> (accessed Dec. 23, 2021).

- [28] D. Purves, G. J. Augustine, D. Fitzpatrick, L. C. Katz, A.-S. LaMantia, J. O. McNamara, and S. M. Williams, “The Motor Unit,” 2001, Accessed: Dec. 23, 2021. [Online]. Available: <https://www.ncbi.nlm.nih.gov/books/NBK10874/>
- [29] N. A. Bernshteĭn, *The co-ordination and regulation of movements*, [1st English ed.]. Oxford,: Pergamon Press, 1967.
- [30] A. d’Avella, “Muscle Synergies,” *Encycl. Neurosci.*, pp. 2509–2512, Nov. 2009, doi: 10.1007/978-3-540-29678-2\_3678.
- [31] B. J. Benda, P. O. Riley, and D. E. Krebs, “Biomechanical Relationship Between Center of Gravity and Center of Pressure During Standing,” *IEEE Trans. Rehabil. Eng.*, vol. 2, no. 1, pp. 3–10, 1994, doi: 10.1109/86.296348.
- [32] S. J. Harkema, J. Hillyer, M. Schmidt-Read, E. Ardolino, S. A. Sisto, and A. L. Behrman, “Locomotor Training: As a treatment of spinal cord injury and in the progression of neurologic rehabilitation,” *Archives of Physical Medicine and Rehabilitation*. 2012. doi: 10.1016/j.apmr.2012.04.032.
- [33] D. A. Winter, “Human balance and posture control during standing and walking,” *Gait and Posture*. 1995. doi: 10.1016/0966-6362(96)82849-9.
- [34] J. Massion, “Movement, posture and equilibrium: Interaction and coordination,” *Prog. Neurobiol.*, vol. 38, no. 1, pp. 35–56, 1992, doi: 10.1016/0301-0082(92)90034-C.
- [35] V. Dietz, “Interaction between central programs and afferent input in the control of posture and locomotion,” *J. Biomech.*, vol. 29, no. 7, pp. 841–844, Jul. 1996, doi: 10.1016/0021-9290(95)00175-1.
- [36] R. Jacobs, A. Burleigh-Jacobs, and D. A. Winter, “Neuromuscular Control Strategies in Postural Coordination,” *Biomech. Neural Control Posture Mov.*, pp. 300–311, 2000, doi:

10.1007/978-1-4612-2104-3\_22.

- [37] P. Morasso, A. Cherif, and J. Zenzeriid, “Quiet standing: The Single Inverted Pendulum model is not so bad after all,” 2019, doi: 10.1371/journal.pone.0213870.
- [38] W. H. Gage, D. A. Winter, J. S. Frank, and A. L. Adkin, “Kinematic and kinetic validity of the inverted pendulum model in quiet standing,” *Gait Posture*, vol. 19, no. 2, pp. 124–132, Apr. 2004, doi: 10.1016/S0966-6362(03)00037-7.
- [39] A. L. Hof, M. G. J. Gazendam, and W. E. Sinke, “The condition for dynamic stability,” *J. Biomech.*, 2005, doi: 10.1016/j.jbiomech.2004.03.025.
- [40] L. Alizadehsaravi, R. A. J. Koster, W. Muijres, H. Maas, S. M. Bruijn, and J. H. van Dieën, “The underlying mechanisms of improved balance after one and ten sessions of balance training in older adults,” *Hum. Mov. Sci.*, vol. 81, p. 102910, Feb. 2022, doi: 10.1016/J.HUMOV.2021.102910.
- [41] N. E. Allen, C. Sherrington, S. S. Paul, and C. G. Canning, “Balance and falls in Parkinson’s disease: A meta-analysis of the effect of exercise and motor training,” *Mov. Disord.*, vol. 26, no. 9, pp. 1605–1615, Aug. 2011, doi: 10.1002/MDS.23790.
- [42] F. L. Tung, Y. R. Yang, C. C. Lee, and R. Y. Wang, “Balance outcomes after additional sit-to-stand training in subjects with stroke: A randomized controlled trial,” *Clin. Rehabil.*, vol. 24, no. 6, pp. 533–542, Jun. 2010, doi: 10.1177/0269215509360751.
- [43] T. Cronin, Q. Arshad, and B. M. Seemungal, “Vestibular deficits in neurodegenerative disorders: Balance, dizziness, and spatial disorientation,” *Front. Neurol.*, vol. 8, no. OCT, p. 538, Oct. 2017, doi: 10.3389/FNEUR.2017.00538/BIBTEX.
- [44] P. Mateos-Aparicio and A. Rodríguez-Moreno, “The Impact of Studying Brain Plasticity,” *Front. Cell. Neurosci.*, vol. 13, p. 66, Feb. 2019, doi: 10.3389/fncel.2019.00066.

- [45] Pascual-Leone, A. ; Amedi, A. ; Fregni, F. ; Merabet, and Lotfi, “The Plastic Human Brain Cortex,” vol. 28, 2005.
- [46] M. Hallett, “Neuroplasticity and rehabilitation,” *Journal of Rehabilitation Research and Development*. 2005. doi: 10.1682/JRRD.2005.07.0126.
- [47] R. J. Nudo and G. W. Milliken, “Reorganization of movement representations in primary motor cortex following focal ischemic infarcts in adult squirrel monkeys,” <https://doi-org.ezproxy.cul.columbia.edu/10.1152/jn.1996.75.5.2144>, vol. 75, no. 5, pp. 2144–2149, 1996, doi: 10.1152/JN.1996.75.5.2144.
- [48] M. S. Remple, R. M. Bruneau, P. M. VandenBerg, C. Goertzen, and J. A. Kleim, “Sensitivity of cortical movement representations to motor experience: evidence that skill learning but not strength training induces cortical reorganization,” *Behav. Brain Res.*, vol. 123, no. 2, pp. 133–141, Sep. 2001, doi: 10.1016/S0166-4328(01)00199-1.
- [49] V. Santamaria, M. Khan, T. Luna, J. Kang, J. Dutkowsky, A. M. Gordon, and S. K. Agrawal, “Promoting Functional and Independent Sitting in Children with Cerebral Palsy Using the Robotic Trunk Support Trainer,” *IEEE Trans. Neural Syst. Rehabil. Eng.*, vol. 28, no. 12, pp. 2995–3004, Dec. 2020, doi: 10.1109/TNSRE.2020.3031580.
- [50] A. Mansfield, A. L. Peters, B. A. Liu, and B. E. Maki, “Effect of a perturbation-based balance training program on compensatory stepping and grasping reactions in older adults: a randomized controlled trial,” *Phys. Ther.*, vol. 90, no. 4, pp. 476–491, Apr. 2010, doi: 10.2522/PTJ.20090070.
- [51] K. Nagai, M. Yamada, B. Tanaka, K. Uemura, S. Mori, T. Aoyama, N. Ichihashi, and T. Tsuboyama, “Effects of balance training on muscle coactivation during postural control in older adults: a randomized controlled trial,” *J. Gerontol. A. Biol. Sci. Med. Sci.*, vol. 67, no.

- 8, pp. 882–889, Aug. 2012, doi: 10.1093/GERONA/GLR252.
- [52] P. O. Mckeon, C. D. Ingersoll, D. Casey Kerrigan, E. Saliba, B. C. Bennett, J. Hertel, C. D. Ingersoll, D. C. Kerrigan, E. Saliba, B. C. Bennett, and J. Hertel, “Balance Training Improves Function and Postural Control in Those with Chronic Ankle Instability,” *Med. Sci. Sport. Exerc.*, vol. 40, no. 10, pp. 1810–1819, 2008, doi: 10.1249/MSS.0b013e31817e0f92.
- [53] C. A. Emery, J. D. Cassidy, T. P. Klassen, R. J. Rosychuk, and B. H. Rowe, “Effectiveness of a home-based balance-training program in reducing sports-related injuries among healthy adolescents: a cluster randomized controlled trial,” *CMAJ*, vol. 172, no. 6, pp. 749–754, Mar. 2005, doi: 10.1503/CMAJ.1040805.
- [54] U. Granacher, A. Gollhofer, and D. Strass, “Training induced adaptations in characteristics of postural reflexes in elderly men,” *Gait Posture*, vol. 24, no. 4, pp. 459–466, Dec. 2006, doi: 10.1016/j.gaitpost.2005.12.007.
- [55] A. S. C. Oliveira, P. Brito Silva, D. Farina, and U. G. Kersting, “Unilateral balance training enhances neuromuscular reactions to perturbations in the trained and contralateral limb,” *Gait Posture*, vol. 38, no. 4, pp. 894–899, Sep. 2013, doi: 10.1016/J.GAITPOST.2013.04.015.
- [56] J. A. Kleim and T. A. Jones, “Principles of experience-dependent neural plasticity: Implications for rehabilitation after brain damage,” *Journal of Speech, Language, and Hearing Research*. 2008. doi: 10.1044/1092-4388(2008/018).
- [57] T. D. J. Welch and L. H. Ting, “Mechanisms of motor adaptation in reactive balance control,” *PLoS One*, vol. 9, no. 5, 2014, doi: 10.1371/journal.pone.0096440.
- [58] M. H. G. Gerards, C. McCrum, A. Mansfield, and K. Meijer, “Perturbation-based balance

- training for falls reduction among older adults: Current evidence and implications for clinical practice,” *Geriatrics and Gerontology International*, vol. 17, no. 12. Blackwell Publishing, pp. 2294–2303, Dec. 01, 2017. doi: 10.1111/ggi.13082.
- [59] A. Mansfield, A. L. Peters, B. A. Liu, and B. E. Maki, “A perturbation-based balance training program for older adults: study protocol for a randomised controlled trial,” 2007, doi: 10.1186/1471-2318-7-12.
- [60] B. W. Dijkstra, F. B. Horak, Y. P. T. Kamsma, and D. S. Peterson, “Older adults can improve compensatory stepping with repeated postural perturbations,” *Front. Aging Neurosci.*, vol. 7, no. OCT, p. 201, 2015, doi: 10.3389/FNAGI.2015.00201/BIBTEX.
- [61] H. C. Heitkamp, T. Horstmann, F. Mayer, J. Weller, and H. H. Dickhuth, “Gain in strength and muscular balance after balance training,” *Int. J. Sports Med.*, 2001, doi: 10.1055/s-2001-13819.
- [62] F. B. Horak, S. M. Henry, and A. Shumway-Cook, “Postural perturbations: New insights for treatment of balance disorders,” *Physical Therapy*. 1997. doi: 10.1093/ptj/77.5.517.
- [63] T. Kajrolkar, F. Yang, Y. C. Pai, and T. Bhatt, “Dynamic stability and compensatory stepping responses during anterior gait-slip perturbations in people with chronic hemiparetic stroke,” *J. Biomech.*, 2014, doi: 10.1016/j.jbiomech.2014.04.051.
- [64] A. Mansfield, J. S. Wong, J. Bryce, S. Knorr, and K. K. Patterson, “Does Perturbation-Based Balance Training Prevent Falls? Systematic Review and Meta-Analysis of Preliminary Randomized Controlled Trials,” *Phys. Ther.*, 2015, doi: 10.2522/ptj.20140090.
- [65] F. Aprigliano, D. Martelli, J. Kang, S. H. Kuo, U. J. Kang, V. Monaco, S. Micera, and S. K. Agrawal, “Effects of repeated waist-pull perturbations on gait stability in subjects with cerebellar ataxia,” *J. Neuroeng. Rehabil.*, vol. 16, no. 1, 2019, doi: 10.1186/s12984-019-

0522-z.

- [66] D. L. Sturnieks, J. Menant, K. Delbaere, J. Vanrenterghem, M. W. Rogers, R. C. Fitzpatrick, and S. R. Lord, “Force-Controlled Balance Perturbations Associated with Falls in Older People: A Prospective Cohort Study,” *PLoS One*, vol. 8, no. 8, Aug. 2013, doi: 10.1371/journal.pone.0070981.
- [67] A. L. Hof, S. M. Vermerris, and W. A. Gjaltema, “Balance responses to lateral perturbations in human treadmill walking,” *J. Exp. Biol.*, vol. 213, no. 15, pp. 2655–2664, Aug. 2010, doi: 10.1242/jeb.042572.
- [68] M. Peshkin, D. A. Brown, J. J. Santos-Munné, A. Makhlin, E. Lewis, J. E. Colgate, J. Patton, and D. Schwandt, “KineAssist: A robotic overground gait and balance training device,” 2005. doi: 10.1109/ICORR.2005.1501094.
- [69] C. Shirota, E. Van Asseldonk, Z. Matjačić, H. Vallery, P. Barralon, S. Maggioni, J. H. Buurke, and J. F. Veneman, “Robot-supported assessment of balance in standing and walking,” *J. Neuroeng. Rehabil.*, vol. 14, no. 1, pp. 1–19, 2017, doi: 10.1186/s12984-017-0273-7.
- [70] “PROPRIO - Vereen Rehabilitation Center.” <http://www.vereecenter.com/facility/proprio/> (accessed May 09, 2020).
- [71] J. D. Collins, A. Markham, K. Service, S. Reini, E. Wolf, and P. Sessoms, “A systematic literature review of the use and effectiveness of the Computer Assisted Rehabilitation Environment for research and rehabilitation as it relates to the wounded warrior,” *Work*, vol. 50, no. 1, pp. 121–129, Jan. 2015, doi: 10.3233/WOR-141927.
- [72] E. Ionescu, T. Morlet, P. Froehlich, and C. Ferber-Viart, “Vestibular assessment with Balance Quest. Normative data for children and young adults,” *Int. J. Pediatr.*

- Otorhinolaryngol.*, vol. 70, no. 8, pp. 1457–1465, Aug. 2006, doi: 10.1016/j.ijporl.2006.03.012.
- [73] M. Khan, T. Luna, V. Santamaria, I. Omofuma, D. Martelli, E. Rejc, J. Stein, S. Harkema, and S. Agrawal, “Stand Trainer with Applied Forces at the Pelvis and Trunk: Response to Perturbations and Assist-As-Needed Support,” *IEEE Trans. Neural Syst. Rehabil. Eng.*, 2019, doi: 10.1109/tnsre.2019.2933381.
- [74] T. D. Luna, V. Santamaria, I. Omofumal, M. I. Khan, and S. K. Agrawal, “Control Mechanisms in Standing while Simultaneously Receiving Perturbations and Active Assistance from the Robotic Upright Stand Trainer (RobUST),” 2020. doi: 10.1109/BioRob49111.2020.9224445.
- [75] D. A. Winter, F. Prince, and A. Patla, “Validity of the inverted pendulum model of balance in quiet standing,” *Gait Posture*, vol. 5, no. 2, pp. 153–154, Apr. 1997, doi: 10.1016/S0966-6362(97)83376-0.
- [76] A. L. Hof, “The equations of motion for a standing human reveal three mechanisms for balance,” *J. Biomech.*, vol. 40, no. 2, pp. 451–457, 2007, doi: 10.1016/J.JBIOMECH.2005.12.016.
- [77] R. J. Peterka, “Sensorimotor integration in human postural control,” *J. Neurophysiol.*, vol. 88, no. 3, pp. 1097–1118, 2002, doi: 10.1152/jn.2002.88.3.1097.
- [78] G. M. Blenkinsop, M. T. G. Pain, and M. J. Hiley, “Balance control strategies during perturbed and unperturbed balance in standing and handstand,” *R. Soc. Open Sci.*, vol. 4, no. 7, 2017, doi: 10.1098/RSOS.161018.
- [79] S. Solnik, P. Rider, K. Steinweg, P. Devita, and T. Hortobágyi, “Teager-Kaiser energy operator signal conditioning improves EMG onset detection,” *Eur. J. Appl. Physiol.*, 2010,

doi: 10.1007/s00421-010-1521-8.

- [80] L. Pizzigalli, M. Micheletti Cremasco, A. Mulasso, and A. Rainoldi, “The contribution of postural balance analysis in older adult fallers: A narrative review,” *J. Bodyw. Mov. Ther.*, vol. 20, no. 2, pp. 409–417, Apr. 2016, doi: 10.1016/j.jbmt.2015.12.008.
- [81] B. E. Maki, K. C. C. Cheng, A. Mansfield, C. Y. Scovil, S. D. Perry, A. L. Peters, S. McKay, T. Lee, A. Marquis, P. Corbeil, G. R. Fernie, B. Liu, and W. E. McIlroy, “Preventing falls in older adults: New interventions to promote more effective change-in-support balance reactions,” *J. Electromyogr. Kinesiol.*, vol. 18, no. 2, pp. 243–254, 2008, doi: 10.1016/j.jelekin.2007.06.005.
- [82] A. K. Topper, B. E. Maki, and P. J. Holliday, “Are Activity-Based Assessments of Balance and Gait in the Elderly Predictive of Risk of Falling and/or Type of Fall?,” *J. Am. Geriatr. Soc.*, vol. 41, no. 5, pp. 479–487, 1993, doi: 10.1111/j.1532-5415.1993.tb01881.x.
- [83] B. E. Maki, P. J. Holliday, and A. K. Topper, “A Prospective Study of Postural Balance and Risk of Falling in An Ambulatory and Independent Elderly Population,” *J. Gerontol.*, vol. 49, no. 2, pp. M72–M84, Mar. 1994, doi: 10.1093/geronj/49.2.M72.
- [84] M. Billot, E. M. Simoneau, J. Van Hoecke, and A. Martin, “Age-related relative increases in electromyography activity and torque according to the maximal capacity during upright standing”, doi: 10.1007/s00421-010-1397-7.
- [85] M. Salavati, M. Moghadam, I. Ebrahimi, and A. M. Arab, “Changes in postural stability with fatigue of lower extremity frontal and sagittal plane movers,” *Gait Posture*, vol. 26, no. 2, pp. 214–218, Jul. 2007, doi: 10.1016/j.gaitpost.2006.09.001.
- [86] N. Benjuya, I. Melzer, and J. Kaplanski, “Aging-Induced Shifts From a Reliance on Sensory Input to Muscle Cocontraction During Balanced Standing,” 2004. [Online]. Available:

<https://academic.oup.com/biomedgerontology/article/59/2/M166/610294>

- [87] C. A. Laughton, M. Slavin, K. Katdare, L. Nolan, J. F. Bean, D. C. Kerrigan, E. Phillips, L. A. Lipsitz, and J. J. Collins, “Aging, muscle activity, and balance control: Physiologic changes associated with balance impairment,” *Gait Posture*, vol. 18, no. 2, pp. 101–108, Oct. 2003, doi: 10.1016/S0966-6362(02)00200-X.
- [88] E. Nagy, A. Feher-Kiss, M. Barnai, A. Domján-Preszner, L. Angyan, and G. Horvath, “Postural control in elderly subjects participating in balance training,” *Eur. J. Appl. Physiol.*, 2007, doi: 10.1007/s00421-007-0407-x.
- [89] F. B. Horak, S. M. Henry, and A. Shumway-Cook, “Postural perturbations: New insights for treatment of balance disorders,” *Physical Therapy*. 1997. doi: 10.1093/ptj/77.5.517.
- [90] A. Shumway-Cook and M. H. Woollacott, *Motor control: Translating research into clinical practice: Fourth edition*. 2014.
- [91] D. Purves, G. J. Augustine, D. Fitzpatrick, L. C. Katz, A.-S. LaMantia, J. O. McNamara, and S. M. Williams, “Electrical Signals of Nerve Cells,” 2001, Accessed: Jan. 10, 2022. [Online]. Available: <https://www.ncbi.nlm.nih.gov/books/NBK11053/>
- [92] “The Principles of Nerve Cell Communication,” *Alcohol Health Res. World*, vol. 21, no. 2, p. 107, 1997, Accessed: Jan. 10, 2022. [Online]. Available: </pmc/articles/PMC6826821/>
- [93] “Neuroanatomy: Text and Atlas, 5e | AccessMedicine | McGraw Hill Medical.” <https://accessmedicine-mhmedical-com.ezproxy.cul.columbia.edu/book.aspx?bookid=2945#248248940> (accessed Jan. 10, 2022).
- [94] “Spinal Reflexes and Descending Motor Pathways (Section 3, Chapter 2) Neuroscience Online: An Electronic Textbook for the Neurosciences | Department of Neurobiology and

- Anatomy - The University of Texas Medical School at Houston.”  
<https://nba.uth.tmc.edu/neuroscience/m/s3/chapter02.html> (accessed Jan. 11, 2022).
- [95] R. C. Miall, “Cortical Motor Control,” *Neurosci. 21st Century From Basic to Clin. Second Ed.*, pp. 1315–1336, Jan. 2016, doi: 10.1007/978-1-4939-3474-4\_128.
- [96] “Reflexes | Boundless Anatomy and Physiology.”  
<https://courses.lumenlearning.com/boundless-ap/chapter/reflexes/> (accessed Jan. 11, 2022).
- [97] I. L. Kurtzer, “Long-latency reflexes account for limb biomechanics through several supraspinal pathways,” *Front. Integr. Neurosci.*, vol. 8, no. JAN, p. 99, Jan. 2015, doi: 10.3389/FNINT.2014.00099/BIBTEX.
- [98] M. MacKay-Lyons, “Central Pattern Generation of Locomotion: A Review of the Evidence,” *Phys. Ther.*, vol. 82, no. 1, pp. 69–83, Jan. 2002, doi: 10.1093/PTJ/82.1.69.
- [99] D. Bucher, “Central Pattern Generators,” in *Encyclopedia of Neuroscience*, Elsevier Ltd, 2009, pp. 691–700. doi: 10.1016/B978-008045046-9.01944-6.
- [100] G. Taccola, D. Sayenko, P. Gad, Y. Gerasimenko, and V. R. Edgerton, “And yet it moves: Recovery of volitional control after spinal cord injury,” *Prog. Neurobiol.*, vol. 160, pp. 64–81, Jan. 2018, doi: 10.1016/J.PNEUROBIO.2017.10.004.
- [101] Y. Gerasimenko, R. Gorodnichev, T. Moshonkina, D. Sayenko, P. Gad, and V. Reggie Edgerton, “Transcutaneous electrical spinal-cord stimulation in humans,” *Annals of Physical and Rehabilitation Medicine*, vol. 58, no. 4. Elsevier Masson SAS, pp. 225–231, Sep. 01, 2015. doi: 10.1016/j.rehab.2015.05.003.
- [102] “Brain Basics: The Life and Death of a Neuron | National Institute of Neurological Disorders and Stroke.” <https://www.ninds.nih.gov/Disorders/Patient-Caregiver-Education/Life-and-Death-Neuron> (accessed Jan. 12, 2022).

- [103] J. H. Byrne, D. Ph, and T. Ut, “Introduction to Neurons and Neuronal Networks,” *Cellular and Molecular Neurobiology*, 2012.  
<https://nba.uth.tmc.edu/neuroscience/m/s1/introduction.html>
- [104] “Action potentials and synapses - Queensland Brain Institute - University of Queensland.”  
<https://qbi.uq.edu.au/brain-basics/brain/brain-physiology/action-potentials-and-synapses>  
(accessed May 07, 2022).
- [105] J. H. Byrne, “Ionic Mechanisms and Action Potentials,” *Neuroscience Online*, 2021.  
<https://nba.uth.tmc.edu/neuroscience/m/s1/chapter02.html>
- [106] A. S.-C. M. H. Woollacott, *Motor Control. Translating Research into Clinical Practice*, vol. 53, no. 9. Wolters Kluwer -- Medknow Publications, 2013.
- [107] James Knierim, “Motor Units and Muscle Receptors (Section 3, Chapter 1) Neuroscience Online: An Electronic Textbook for the Neurosciences | Department of Neurobiology and Anatomy - The University of Texas Medical School at Houston,” 2000.  
<https://nba.uth.tmc.edu/neuroscience/m/s3/chapter01.html> (accessed May 10, 2020).
- [108] M. Hu, L. Hong, C. Liu, S. Hong, S. He, M. Zhou, G. Huang, and Q. Chen, “Electrical stimulation enhances neuronal cell activity mediated by Schwann cell derived exosomes,” *Sci. Reports 2019 91*, vol. 9, no. 1, pp. 1–12, Mar. 2019, doi: 10.1038/s41598-019-41007-5.
- [109] U. S. Hofstoetter, B. Freundl, P. Lackner, and H. Binder, “Transcutaneous Spinal Cord Stimulation Enhances Walking Performance and Reduces Spasticity in Individuals with Multiple Sclerosis,” *Brain Sci.*, vol. 11, no. 4, 2021, doi: 10.3390/BRAINSCI11040472.
- [110] E. Rejc, C. A. Angeli, D. Atkinson, and S. J. Harkema, “Motor recovery after activity-based training with spinal cord epidural stimulation in a chronic motor complete paraplegic,” *Sci.*

- Rep.*, 2017, doi: 10.1038/s41598-017-14003-w.
- [111] J. T. Eisdorfer, R. D. Smit, K. M. Keefe, M. A. Lemay, G. M. Smith, and A. J. Spence, “Epidural Electrical Stimulation: A Review of Plasticity Mechanisms That Are Hypothesized to Underlie Enhanced Recovery From Spinal Cord Injury With Stimulation,” *Front. Mol. Neurosci.*, vol. 13, p. 163, Sep. 2020, doi: 10.3389/FNMOL.2020.00163/BIBTEX.
- [112] C. A. Angeli, M. Boakye, R. A. Morton, J. Vogt, K. Benton, Y. Chen, C. K. Ferreira, and S. J. Harkema, “Recovery of over-ground walking after chronic motor complete spinal cord injury,” *N. Engl. J. Med.*, 2018, doi: 10.1056/NEJMoa1803588.
- [113] U. S. Hofstoetter, B. Freundl, H. Binder, and K. Minassian, “Common neural structures activated by epidural and transcutaneous lumbar spinal cord stimulation: Elicitation of posterior root-muscle reflexes,” *PLoS One*, vol. 13, no. 1, Jan. 2018, doi: 10.1371/JOURNAL.PONE.0192013.
- [114] Y. Chen, L. Chen, R. Liu, Y. Wang, X. Y. Chen, and J. R. Wolpaw, “Locomotor impact of beneficial or nonbeneficial H-reflex conditioning after spinal cord injury,” *J. Neurophysiol.*, vol. 111, no. 6, pp. 1249–1258, Mar. 2014, doi: 10.1152/JN.00756.2013.
- [115] L. V. Zholudeva, V. E. Abaira, K. Satkunendrarajah, T. C. McDevitt, M. D. Goulding, D. S. K. Magnuson, and M. A. Lane, “Spinal Interneurons as Gatekeepers to Neuroplasticity after Injury or Disease,” *J. Neurosci.*, vol. 41, no. 5, pp. 845–854, Feb. 2021, doi: 10.1523/JNEUROSCI.1654-20.2020.
- [116] K. Minassian, U. Hofstoetter, and F. Rattay, “Transcutaneous Lumbar Posterior Root Stimulation for Motor Control Studies and Modification of Motor Activity after Spinal Cord Injury,” in *Restorative Neurology of Spinal Cord Injury*, 2012. doi:

10.1093/acprof:oso/9780199746507.003.0010.

- [117] A. Megía García, D. Serrano-Muñoz, J. Taylor, J. Avendaño-Coy, and J. Gómez-Soriano, “Transcutaneous Spinal Cord Stimulation and Motor Rehabilitation in Spinal Cord Injury: A Systematic Review,” *Neurorehabilitation and Neural Repair*. 2020. doi: 10.1177/1545968319893298.
- [118] O. Bican, A. Minagar, and A. A. Pruitt, “The Spinal Cord: A Review of Functional Neuroanatomy,” *Neurol. Clin.*, vol. 31, no. 1, pp. 1–18, Feb. 2013, doi: 10.1016/J.NCL.2012.09.009.
- [119] “Anatomy of the Spinal Cord (Section 2, Chapter 3) Neuroscience Online: An Electronic Textbook for the Neurosciences | Department of Neurobiology and Anatomy - The University of Texas Medical School at Houston.” <https://nba.uth.tmc.edu/neuroscience/m/s2/chapter03.html> (accessed Oct. 11, 2022).
- [120] U. S. Hofstoetter, B. Freundl, H. Binder, and K. Minassian, “Recovery cycles of posterior root-muscle reflexes evoked by transcutaneous spinal cord stimulation and of the H reflex in individuals with intact and injured spinal cord,” *PLoS One*, vol. 14, no. 12, p. e0227057, Dec. 2019, doi: 10.1371/JOURNAL.PONE.0227057.
- [121] K. Minassian, B. Freundl, and U. S. Hofstoetter, “The posterior root-muscle reflex,” *Neurophysiol. Neurosurg.*, pp. 239–253, 2020, doi: 10.1016/B978-0-12-815000-9.00018-6.
- [122] J. E. Misiaszek, “The H-reflex as a tool in neurophysiology: Its limitations and uses in understanding nervous system function,” *Muscle Nerve*, vol. 28, no. 2, pp. 144–160, Aug. 2003, doi: 10.1002/MUS.10372.
- [123] R. M. Palmieri, C. D. Ingersoll, and M. A. Hoffman, “The Hoffmann reflex: Methodologic considerations and applications for use in sports medicine and athletic training research,”

- Journal of Athletic Training*, vol. 39, no. 3. National Athletic Trainers Association, pp. 268–277, Jul. 2004.
- [124] W. Taube, M. Gruber, and A. Gollhofer, “Spinal and supraspinal adaptations associated with balance training and their functional relevance,” *Acta Physiol.*, vol. 193, no. 2, pp. 101–116, Jun. 2008, doi: 10.1111/J.1748-1716.2008.01850.X.
- [125] M. Schieppati, “The Hoffmann reflex: A means of assessing spinal reflex excitability and its descending control in man,” *Prog. Neurobiol.*, vol. 28, no. 4, pp. 345–376, Jan. 1987, doi: 10.1016/0301-0082(87)90007-4.
- [126] M. Knikou, “The H-reflex as a probe: pathways and pitfalls,” *J. Neurosci. Methods*, vol. 171, no. 1, pp. 1–12, Jun. 2008, doi: 10.1016/J.JNEUMETH.2008.02.012.
- [127] S. Grosprêtre and A. Martin, “H reflex and spinal excitability: Methodological considerations,” *J. Neurophysiol.*, vol. 107, no. 6, pp. 1649–1654, Mar. 2012, doi: 10.1152/JN.00611.2011/ASSET/IMAGES/LARGE/Z9K0051212450004.JPEG.
- [128] M. Knikou and L. M. Murray, “Repeated transspinal stimulation decreases soleus H-reflex excitability and restores spinal inhibition in human spinal cord injury,” *PLoS One*, vol. 14, no. 9, Sep. 2019, doi: 10.1371/JOURNAL.PONE.0223135.
- [129] M. Klimstra and E. P. Zehr, “A sigmoid function is the best fit for the ascending limb of the Hoffmann reflex recruitment curve,” *Exp. Brain Res. 2007 1861*, vol. 186, no. 1, pp. 93–105, Nov. 2007, doi: 10.1007/S00221-007-1207-6.
- [130] S. J. Spaulding, K. C. Hayes, and K. L. Harburn, “Periodicity in the hoffmann reflex recovery curve,” *Exp. Neurol.*, vol. 98, no. 1, pp. 13–25, Oct. 1987, doi: 10.1016/0014-4886(87)90067-7.
- [131] H. M. Straßburg, G. Oepen, and U. Thoden, “The late facilitation in H-reflex recovery

- cycles in different pyramidal lesions,” *Arch. für Psychiatr. und Nervenkrankheiten* 1980 2283, vol. 228, no. 3, pp. 197–204, Jun. 1980, doi: 10.1007/BF00342345.
- [132] A. F. Kohn, M. K. Floeter, and M. Hallett, “Presynaptic inhibition compared with homosynaptic depression as an explanation for soleus H-reflex depression in humans,” *Exp. Brain Res.* 1997 1162, vol. 116, no. 2, pp. 375–380, 1997, doi: 10.1007/PL00005765.
- [133] K. L. Robinson, J. S. McIlwain, and K. C. Hayes, “Effects of H-reflex conditioning upon the contralateral alpha motoneuron pool,” *Electroencephalogr. Clin. Neurophysiol.*, vol. 46, no. 1, pp. 65–71, 1979, doi: 10.1016/0013-4694(79)90050-6.
- [134] P. Rudomin and R. F. Schmidt, “Presynaptic inhibition in the vertebrate spinal cord revisited,” *Exp. Brain Res.* 1999 1291, vol. 129, no. 1, pp. 1–37, 1999, doi: 10.1007/S002210050933.
- [135] J. M. Clair, J. M. Anderson-Reid, C. M. Graham, and D. F. Collins, “Postactivation depression and recovery of reflex transmission during repetitive electrical stimulation of the human tibial nerve,” *J. Neurophysiol.*, vol. 106, no. 1, pp. 184–192, Jul. 2011, doi: 10.1152/JN.00932.2010.
- [136] Y. Kawaishi, N. Matsumoto, T. Nishiwaki, and T. Hirano, “Postactivation depression of soleus H-reflex increase with recovery of lowerextremities motor functions in patients with subacute stroke,” *J. Phys. Ther. Sci.*, vol. 29, no. 9, p. 1539, 2017, doi: 10.1589/JPTS.29.1539.
- [137] J. Nielsen, C. Crone, and H. Hultborn, “H-reflexes are smaller in dancers from The Royal Danish Ballet than in well-trained athletes,” *Eur. J. Appl. Physiol. Occup. Physiol.*, vol. 66, no. 2, pp. 116–121, Mar. 1993, doi: 10.1007/BF01427051.
- [138] B. A. Karamian, N. Siegel, B. Nourie, M. D. Serruya, R. F. Heary, J. S. Harrop, and A. R.

- Vaccaro, “The role of electrical stimulation for rehabilitation and regeneration after spinal cord injury,” *J. Orthop. Traumatol.* 2022 231, vol. 23, no. 1, pp. 1–17, Jan. 2022, doi: 10.1186/S10195-021-00623-6.
- [139] B. Ellenbroek *et al.*, “EPSPs and IPSPs,” *Encycl. Psychopharmacol.*, pp. 489–489, 2010, doi: 10.1007/978-3-540-68706-1\_618.
- [140] L. H. Grecco, S. Li, S. Michel, L. Castillo-Saavedra, A. Mourdoukoutas, M. Bikson, and F. Fregni, “Transcutaneous spinal stimulation as a therapeutic strategy for spinal cord injury: state of the art,” *J. Neurorestoratology*, vol. 3, pp. 73–82, Mar. 2015, doi: 10.2147/JN.S77813.
- [141] E. Y. Shapkova, E. V. Pismennaya, D. V. Emelyannikov, and Y. Ivanenko, “Exoskeleton Walk Training in Paralyzed Individuals Benefits From Transcutaneous Lumbar Cord Tonic Electrical Stimulation,” *Front. Neurosci.*, vol. 14, p. 416, May 2020, doi: 10.3389/FNINS.2020.00416/BIBTEX.
- [142] F. Inanici, S. Samejima, P. Gad, V. R. Edgerton, C. P. Hofstetter, and C. T. Moritz, “Transcutaneous electrical spinal stimulation promotes long-term recovery of upper extremity function in chronic tetraplegia,” *IEEE Trans. Neural Syst. Rehabil. Eng.*, vol. 26, no. 6, pp. 1272–1278, Jun. 2018, doi: 10.1109/TNSRE.2018.2834339.
- [143] C. Meyer, U. S. Hofstoetter, M. Hubli, R. H. Hassani, C. Rinaldo, A. Curt, and M. Bolliger, “Immediate Effects of Transcutaneous Spinal Cord Stimulation on Motor Function in Chronic, Sensorimotor Incomplete Spinal Cord Injury,” *J. Clin. Med.*, vol. 9, no. 11, p. 3541, Nov. 2020, doi: 10.3390/jcm9113541.
- [144] O. O. Awosika, M. Sandrini, R. Volochayev, R. M. Thompson, N. Fishman, T. Wu, M. K. Floeter, M. Hallett, and L. G. Cohen, “Transcutaneous spinal direct current stimulation

- improves locomotor learning in healthy humans,” *Brain Stimul.*, 2019, doi: 10.1016/j.brs.2019.01.017.
- [145] J. S. Calvert, G. A. Manson, P. J. Grahn, and D. G. Sayenko, “Preferential activation of spinal sensorimotor networks via lateralized transcutaneous spinal stimulation in neurologically intact humans,” *J. Neurophysiol.*, vol. 122, no. 5, pp. 2111–2118, 2019, doi: 10.1152/JN.00454.2019/ASSET/IMAGES/LARGE/Z9K0111952630004.JPEG.
- [146] R. Tisserand, T. Robert, R. Dumas, and L. Chèze, “A simplified marker set to define the center of mass for stability analysis in dynamic situations,” *Gait Posture*, vol. 48, pp. 64–67, Jul. 2016, doi: 10.1016/J.GAITPOST.2016.04.032.
- [147] P. De Leva, “Adjustments to Zatsiorsky-Seluyanov’s segment inertia parameters,” *J. Biomech.*, vol. 29, no. 9, pp. 1223–1230, 1996, doi: 10.1016/0021-9290(95)00178-6.
- [148] X. Li, P. Zhou, and A. S. Aruin, “Teager-kaiser energy operation of surface EMG improves muscle activity onset detection,” *Ann. Biomed. Eng.*, 2007, doi: 10.1007/s10439-007-9320-z.
- [149] H. Devanne, B. A. Lavoie, and C. Capaday, “Input-output properties and gain changes in the human corticospinal pathway,” *Exp. Brain Res.*, vol. 114, no. 2, pp. 329–338, 1997, doi: 10.1007/PL00005641.
- [150] F. Campfens, M. Papaiordanidou, D. Guiraud, M. Hayashibe, and A. Varray, “An activation model of motor response and H-reflex under {FES},” *13th Int. FES Soc. Conf.*, pp. 356–358, 2008.
- [151] E. P. Zehr, “Considerations for use of the Hoffmann reflex in exercise studies,” *Eur. J. Appl. Physiol.* 2002 866, vol. 86, no. 6, pp. 455–468, Apr. 2002, doi: 10.1007/S00421-002-0577-5.

- [152] K. Funase, K. Imanaka, and Y. Nishihira, “Excitability of the soleus motoneuron pool revealed by the developmental slope of the H-reflex as reflex gain,” *Electromyogr. Clin. Neurophysiol.*, vol. 34, no. 8, pp. 477–489, Dec. 1994, Accessed: Jun. 29, 2022. [Online]. Available: <https://europepmc.org/article/med/7882891>
- [153] J.-C. Lamy, C. Ho, A. Badel, R. T. Arrigo, and M. Boakye, “Modulation of soleus H reflex by spinal DC stimulation in humans,” *J. Neurophysiol.*, vol. 108, no. 3, pp. 906–914, Aug. 2012, doi: 10.1152/jn.10898.2011.
- [154] T. Winkler, P. Hering, and A. Straube, “Spinal DC stimulation in humans modulates post-activation depression of the H-reflex depending on current polarity,” *Clin. Neurophysiol.*, vol. 121, no. 6, pp. 957–961, Jun. 2010, doi: 10.1016/j.clinph.2010.01.014.
- [155] J. Babic, E. Oztop, and M. Kawato, “Human motor adaptation in whole body motion,” *Sci. Reports 2016 61*, vol. 6, no. 1, pp. 1–12, Sep. 2016, doi: 10.1038/srep32868.
- [156] E. Todorov, “Optimality principles in sensorimotor control (review),” *Nat. Neurosci.*, vol. 7, no. 9, p. 907, Sep. 2004, doi: 10.1038/NN1309.
- [157] D. E. Meyer, R. A. Abrams, S. Kornblum, C. E. Wright, and J. E. K. Smith, “Optimality in Human Motor Performance: Ideal Control of Rapid Aimed Movements,” *Psychol. Rev.*, vol. 95, no. 3, pp. 340–370, 1988, doi: 10.1037/0033-295X.95.3.340.
- [158] I. Wochner, D. Driess, H. Zimmermann, D. F. B. Haeufle, M. Toussaint, and S. Schmitt, “Optimality Principles in Human Point-to-Manifold Reaching Accounting for Muscle Dynamics,” *Front. Comput. Neurosci.*, vol. 14, p. 38, May 2020, doi: 10.3389/FNCOM.2020.00038/BIBTEX.
- [159] S. Hagler, “Patterns of Selection of Human Movements I: Movement Utility, Metabolic Energy, and Normal Walking Gaits,” Aug. 2016, doi: 10.13140/RG.2.2.29167.02720.

- [160] M. E. Stoykov and S. Madhavan, “Motor priming in neurorehabilitation,” *J. Neurol. Phys. Ther.*, vol. 39, no. 1, pp. 33–42, Jan. 2015, doi: 10.1097/NPT.0000000000000065.
- [161] Á. Flores, D. López-Santos, and G. García-Álías, “When Spinal Neuromodulation Meets Sensorimotor Rehabilitation: Lessons Learned From Animal Models to Regain Manual Dexterity After a Spinal Cord Injury,” *Front. Rehabil. Sci.*, vol. 0, p. 94, Dec. 2021, doi: 10.3389/FRESC.2021.755963.
- [162] W. Taube, M. Gruber, S. Beck, M. Faist, A. Gollhofer, and M. Schubert, “Cortical and spinal adaptations induced by balance training: correlation between stance stability and corticospinal activation,” *Acta Physiol.*, vol. 189, no. 4, pp. 347–358, Apr. 2007, doi: 10.1111/J.1748-1716.2007.01665.X.
- [163] M. Nahum, H. Lee, and M. M. Merzenich, *Principles of neuroplasticity-based rehabilitation*, 1st ed., vol. 207. Elsevier B.V., 2013. doi: 10.1016/B978-0-444-63327-9.00009-6.
- [164] J. Girgis, D. Merrett, S. Kirkland, G. A. S. Metz, V. Verge, and K. Fouad, “Reaching training in rats with spinal cord injury promotes plasticity and task specific recovery,” *Brain*, vol. 130, no. 11, pp. 2993–3003, Nov. 2007, doi: 10.1093/BRAIN/AWM245.
- [165] F. D. Benavides, H. J. Jo, H. Lundell, V. R. Edgerton, Y. Gerasimenko, and M. A. Perez, “Cortical and Subcortical Effects of Transcutaneous Spinal Cord Stimulation in Humans with Tetraplegia,” *J. Neurosci.*, vol. 40, no. 13, pp. 2633–2643, Mar. 2020, doi: 10.1523/JNEUROSCI.2374-19.2020.
- [166] J. V. Lynskey, A. Belanger, and R. Jung, “Activity-dependent plasticity in spinal cord injury,” *J. Rehabil. Res. Dev.*, vol. 45, no. 2, p. 229, 2008, doi: 10.1682/JRRD.2007.03.0047.

- [167] K. Fouad and W. Tetzlaff, “Rehabilitative training and plasticity following spinal cord injury,” *Exp. Neurol.*, vol. 235, no. 1, pp. 91–99, May 2012, doi: 10.1016/J.EXPNEUROL.2011.02.009.
- [168] F. B. Horak, S. M. Henry, and A. Shumway-Cook, “Postural perturbations: New insights for treatment of balance disorders,” *Phys. Ther.*, vol. 77, no. 5, pp. 517–533, 1997, doi: 10.1093/ptj/77.5.517.
- [169] C. F. Runge, C. L. Shupert, F. B. Horak, and F. E. Zajac, “Ankle and hip postural strategies defined by joint torques,” *Gait Posture*, vol. 10, no. 2, pp. 161–170, Oct. 1999, doi: 10.1016/S0966-6362(99)00032-6.
- [170] J. M. Clair, J. M. Anderson-Reid, C. M. Graham, and D. F. Collins, “Postactivation depression and recovery of reflex transmission during repetitive electrical stimulation of the human tibial nerve,” *J. Neurophysiol.*, vol. 106, no. 1, pp. 184–192, Jul. 2011, doi: 10.1152/JN.00932.2010.
- [171] C. Taylor, C. McHugh, D. Mockler, C. Minogue, R. B. Reilly, and N. Fleming, “Transcutaneous spinal cord stimulation and motor responses in individuals with spinal cord injury: A methodological review,” *PLoS One*, vol. 16, no. 11, p. e0260166, Nov. 2021, doi: 10.1371/JOURNAL.PONE.0260166.
- [172] D. A. Winter, A. E. Patla, F. Prince, M. Ishac, and K. Gielo-perczak, “Stiffness control of balance in quiet standing,” *J. Neurophysiol.*, vol. 80, no. 3, pp. 1211–1221, 1998, doi: 10.1152/jn.1998.80.3.1211.
- [173] H. S. Choi and Y. H. Kim, “The relationship between the COP-COM variable and the horizontal acceleration of the body in postural sway, falling and walking,” 2009. doi: 10.1007/978-3-642-03882-2-74.

[174] C. D. Bowersock, T. Pisolkar, I. Omofuma, T. Luna, M. Khan, V. Santamaria, J. Stein, S. Agrawal, S. J. Harkema, and E. Rejc, “Robotic upright stand trainer (RobUST) and postural control in individuals with spinal cord injury,” <https://doi.org/10.1080/10790268.2022.2069532>, 2022, doi: 10.1080/10790268.2022.2069532.